SOLAR PHOTO VOLTAIC WATER PUMPING SYSTEM

Thesis

Submitted in partial fulfilment of the requirements for the degree of

DOCTOR OF PHILOSOPHY

by

MRITYUNJAYA KAPPALI

DEPARTMENT OF ELECTRICAL AND ELECTRONICS ENGINEERING
NATIONAL INSTITUTE OF TECHNOLOGY KARNATAKA
SURATHKAL, MANGALORE - 575025

June, 2014

NATIONAL INSTITUTE OF TECHNOLOGY KARNATAKA, SURATHKAL

D E C L A R A T I O N

by the Ph.D. Research Scholar

I hereby *declare* that the Research Thesis entitled "**Solar Photo Voltaic Water Pumping System**" which is being submitted to the **National Institute of Technology Karnataka, Surathkal** in partial fulfillment of the requirements for the award of the Degree of Doctor of Philosophy in Electrical and Electronics Engineering is a *bonafide report of the research work carried out by me*. The material contained in this Research Thesis has not been submitted to any University or Institution for the award of any degree.

050587EE05P01 Mrityunjaya Kappali

(Register Number, Name & Signature of the Research Scholar)
Department of Electrical and Electronics Engineering

Place: NITK-Surathkal

Date:

Note: Declaration to be signed by the Scholar and incorporated as part of the Ph.D. Research Thesis

NATIONAL INSTITUTE OF TECHNOLOGY KARNATAKA, SURATHKAL

C E R T I F I C A T E

This is to *certify* that the Research Thesis entitled "**Solar Photo Voltaic Water Pumping System**" submitted by **Mrityunjaya Kappali** (Register Number: 050587EE05P01) as the record of the research work carried out by him, is *accepted as the Research Thesis submission* in partial fulfillment of the requirements for the award of degree of **Doctor of Philosophy**.

Dr. Udaykumar R. Y.
Research Guide
(Name and Signature
with Date and Seal)

Chairman - DRPC
(Signature with Date and Seal)

ACKNOWLEDGEMENT

A task accomplished has many a hands supporting the cause and the process. Blessed am I, to have the encouragement and guidance from several corners in the course of my present research work and it's my pleasure to acknowledge all of them.

Prof. Udaykumar R. Y., research guide, has been a source of strength and motivation all through this research work. He has rendered moral support, guidance and facilitation to navigate through the doctoral program and complete my thesis. My heartfelt thanks to him for his concern, timely inputs and well wishes.

I take this opportunity to thank the Director, National Institute of Technology Karnataka, Surathkal and Head of the Department of Electrical and Electronics Engineering for their support and encouragement. My thanks are due to all the Faculty members and staff of the Electrical Engineering Department at NITK for their cooperation.

My sincere thanks to the respective Chairman and members of Doctoral Research Program Committee (DRPC), Research Progress Assessment Committee (RPAC) and Doctoral Thesis Assessment Committee (DTAC) for their timely guidance and suggestions. It has helped me in refining my research work and following more appropriate path.

I thank sincerely the Management, Principal and Head of Department (Electrical and Electronics Engineering) of Sri Dharmasthala Manjunatheshwara College of Engineering and Technology, Dharwad for encouraging and supporting my research work.

I would like to convey thanks to the administrators of all those journals and conferences who have given me an opportunity to publish and present my papers and to the reviewers for their constructive comments and suggestions.

I am thankful to all my dear colleagues and staff at SDMCET for their support and encouragement. I thank profusely all the research scholars for rendering helping hand and inspiring company during the course of my stay at NITK.

My heartfelt thanks to my Father, Mother and all other elders of my family for bestowing on me their everlasting blessings for all my ventures. My appreciation and thanks to my wife, son, daughter and all other family members for their patience and understanding all through my doctoral program.

I extend sincere thanks to all others who have rendered a helping hand directly or indirectly in pursuing and completing my PhD program.

-- Mrityunjaya Kappali

ABSTRACT

Water pumping is an important application of solar photo voltaic (PV) power. However growth in the number of solar pumps is not promising mainly due to higher cost per litre of water pumped and complex technology. These issues can be addressed by harnessing more power per unit installed capacity of solar panel and making the system simple.

Present research work has dealt with the aspect of harnessing more power from PV panel using maximum power point tracking (MPPT) for a standalone water pumping system. Literature review indicates the need for MPPT method which is simple, accurate as well as non-interruptive in nature. This thesis has proposed a novel method for accomplishing MPPT wherein only load voltage is to be used as control parameter for MPPT converter ($MPPT_{lv}$). This method is simpler than the present more commonly employed method of monitoring panel power ($MPPT_{pp}$) which requires measurement of two parameters (panel voltage & current) and then multiplying them to obtain power. The proposal is substantiated by theoretical explanation and results from simulation & experimental testing. In addition to its simplicity, the new proposal is also found to give higher power output and enhance water yield. An algorithm is developed to show simulation implementation of the proposal made.

Another outcome of the present research work is the development of a new strategy "Individual Floor Storage Method (IFSM)" for solar pumping in multi-floored buildings where over head (OH) tanks act as storage elements. Present practice is "Top Floor Storage Method (TFSM)" wherein one single large OH tank is placed on topmost floor. IFSM proposes to employ small tanks at each floor height supplying water to corresponding floor. Water is pumped to the required optimum heights only, avoiding wastage of energy. For a particular power capacity of solar panel, the amount of water lifted will be more. Effective total cost per litre of water lifted is appreciably reduced. In other words, for a particular amount of water to be lifted per day, the PV panel size needs to be less.

The two new proposals made in this research work, giving increased water yield from the solar pump for a particular capacity of solar panel, are expected increase the acceptability of solar water pumps and thus contribute to their growth.

Key Words:

Solar PV Water Pumping; Maximum Power Point Tracking; Maximum Load Voltage Tracking; Water Pumping in Multi-floored Buildings; Individual Floor Storage Method.

CONTENTS

CONTENTS **Page No.**

CONTENTS **Page No.**

FIGURES

TABLES

NOTATIONS & UNITS

Symbol/ Abbreviation	Significance	Unit
a.c.	Alternating Current	
C	Capacitance	F
d.c.	Direct Current	
D	Switching duty cycle of the converter	
D_{ref}	Previous duty cycle	
E or W_e	Energy or work done	J
E_b	Motor back EMF constant	V/r/s
EMF	Electro Motive Force	V
Exp.	Experimental	
FF	First floor	
f	Frequency	Hz
	Hour (time)	h
GF	Ground Floor	
H_d	Delivery head	m
H_s	Suction head	m
I_a	Load current	A
I_a'	I_a referred to panel side	A
I_m	Panel current for maximum rated power	A
I_p	Panel side current	A
I_{ph} or I_{sc}	Panel short circuit current	A
IFSM	Individual Floor Storage Method	
J	Moment of inertia	Kg m^2
L	Inductance	H
m	Mass	kg
MI	Moment of Inertia	kg m^2
MPPT	Maximum Power Point Tracking	
OH	Over Head	

Symbol/ Abbreviation	Significance	Unit
P_a	Load side power	W
P_{adir}	Load side power without MPPT converter	
P_g	Air gap power developed in motor	W
P_m	Panel side rated maximum power	W
P_p	Panel side power	W
P_{pm}	Panel side maximum power at a particular radiation	W
P_{pmcon}	Panel side maximum power at a particular radiation with MPPT converter	
PV	Photo Voltaic	
PVC	Poly Vinyl Chloride	
Q	Water flow rate	L/s
R	Resistive load	Ω
R'	R referred to panel side	Ω
R_a	Motor armature resistance	Ω
R_s	Series equivalent resistance of PV panel	Ω
R_{sh}	Shunt equivalent resistance of PV panel	Ω
SF	Second Floor	
SWP	Solar Water Pump	
Sim.	Simulation	
t	Time (second)	s
T	Motor torque	N m
TF	Third floor	
TFSM	Top Floor Storage Method	
V_a	Load side voltage	V
V_a'	V_a referred to panel side	V
V_{c1}	Voltage across capacitor C_1 in MPPT converter	V
V_{ds}	MOSFET drain to source voltage	V
V_g	MOSFET Gate Voltage	V

Symbol/ Abbreviation	Significance	Unit
V_{oc}	Panel open circuit voltage	V
V_m	Panel voltage for maximum rated power	V
V_p	Panel side voltage	V
	Volume (litre)	L
V_{ref}	Previous load voltage	V
ω	Motor/Pump speed (radians/second)	rad/s
W_p	Peak Watt	W
	Watt hour (energy)	W h
y	Transformation ratio of the converter (y = D/(1-D))	

CHAPTER 1

INTRODUCTION

This chapter tries to provide a broad background to the present thesis. To begin with, it brings out the significance of energy, the problem of energy scarcity being faced now and hence the need for renewable energy sources. Then solar photo voltaic source is presented as a promising renewable source and a brief idea about its basic features is given. Finally the composition of the thesis is narrated.

1.1 NEED FOR RENEWABLE ENERGY SOURCES

Energy is the reason for all our activities. Very life on this earth is the manifestation of energy. Life style of man has changed drastically over the centuries and presently it is characterized by larger use of energy. Our Industry, Business, Communication, Transportation, Teaching, Learning, - - - all are energy driven. Such being the significance of energy, usually per capita energy consumption is taken as index of living standard and prosperity or development of a nation. Per capita energy consumption in developed countries like USA is more than that in developing countries like India (IEA 2013) (Table 1.1). It can also be observed that USA with 4.5% of world population consume 16.7% of total energy whereas India with 17.8% of world population consume only 5.7% of total energy.

Different energy sources like fossil fuels (coal, oil, natural gas etc.), hydel, animal energy are employed for different applications e.g. transportation, household, industrial etc. The vast bulk (to the extent of 82%) of the energy used in the world today is obtained from fossil fuels (IEA 2013) (Table 1.2). The situation is no different in India. About 68% of the total electricity produced in India is from fossil fuels (CEA 2014) (Table 1.3). The fossil fuels, being non-renewable, are getting depleted fast. We are heading towards “Energy Crisis”, an acute shortage of energy, posing a possibility of economic disaster. Hence opting for alternate energy sources is not only essential but inevitable.

Table1.1 Per Capita Energy Consumption.

Country	**Population**		**Total Energy Consumed**		**Annual Per Capita Total Energy Consumption**	**Total Electric Energy Consumed**	**Annual Per Capita Electric Energy Consumption**
	million	%	(1000 x TWh)	%	kWh/capita	(1000 x TWh)	kWh/ capita
USA	312.04	4.5	25.48	16.7	81640	4.127	13227
China	1351	19.4	31.9	20.9	23609	4.475	3312
India	1241.49	17.8	8.7	5.7	6978	0.835	673
World	6958	100	152.5	100	21864	20.407	2933

Table1.2 Global Energy Consumption Scenario.

Fuel	**TWh**	**%**	
Oil	49073.5	31.9	**82 % Fossil Fuels**
Coal	43915.5	28.6	
Gas	32412.2	21.1	
Nuclear	7838.7	5.1	**18 % Alternate Sources**
Hydro	3490.1	2.2	
Biofuels, Waste, etc.	15260.3	9.9	
Others	1489.2	0.97	
Total	153479.5	100	

Table 1.3 Electric Power Generation (India).

Fuel	**Power (MW)**	**%**	
Coal	145408.4	59	Fossil Fuels: 68%
Gas	21781.8	8.9	
Oil	1199.7	0.005	
Hydro	40531	17	Alternate Sources: 32%
Nuclear	4780	2	
Other RES	31693.1	13	
Total	245394	100	

1.2 SOLAR PHOTO VOLTAIC ENERGY

While exploring alternate sources, focus is to be on the ones which are renewable in nature so that in future there will not be again the problem of sources getting depleted. Different renewable energy sources being explored are Solar, Wind, Ocean (Wave, Tidal & Thermal), Geothermal, Biomass, etc. Among these, solar Photo Voltaic (PV) source is emerging as a promising source due to its many advantages like:

- It's available abundantly.
- It’s renewable. No carbon pollution, noise generation and moving parts.
- Small independent units can be set up meeting local demands. It’s flexible in size. Due to modular design, an existing solar PV system can be easily expanded to meet the evolving needs. Installation and maintenance can be performed by semiskilled personnel of the locality. It has low lead time.

- It does not need cooling. Hence can be installed far away from water supply which is an important advantage in arid lands.
- It is appropriate and better for situations where grid connection or fuel transport is difficult, costly or impossible as in the case of Satellites, Island communities, Remote locations, Ocean vessels, etc.

However there are some demerits also for solar PV like:

- Solar PV suffers from uncertainty as it depends on sun shine, season etc. The energy density is less. It is available during day time only. Hence energy storage arrangement is required.
- Energy conversion efficiency of solar PV cells is very low.
- Solar cells produce d.c. which needs to be converted to a.c. when used in existing distribution grids or for a.c. loads.
- Energy cost for solar PV is high (Table 1.4) (Renewable 2014).

Table 1.4. Cost Comparison.

Sl. No.	**Source**	**Cost (Rs/kW h)**
1	Coal	5.9
2	Natural Gas	4.1
3	Hydro	4.7
4	Nuclear	5.9
5	Wind	4.7
6	Solar PV	7.6
7	Biomass	5.9

Solar Photo Voltaic Effect

- It's the direct conversion of solar radiation into electro motive force. The output is d.c. electricity. Basic unit of solar PV power is the PV cell. It's a pn junction generating a voltage of approximately 0.45 V per cell and a current of 270 A/sq m of the cell area.

- To get higher voltages and currents, the cells are connected in series and parallel manner leading to solar panel. In a similar fashion multiple connection of panels leads to module and that of modules leads to array.
- Material used for PV cell is either monocrystaline or polycrystaline silicon (Si). Nowadays the trend is towards thin film technology using amorphous Si or microcrystalline Si. The cost of the solar panel is approximately Rs 110 per W_p.
- The efficiency of PV conversion from solar radiation to electricity is very less and is of the order of 10-15%. Such a low efficiency is due to the wide spectral distribution of sun's radiation. Energy band gap of absorber material of the PV cell being a specific value, some radiation has energy less than required hence not absorbed at all. Whereas some radiation has energy more than required resulting in creation of heat. Lesser efficiency results in the need for a bigger panel.

Applications:

Solar PV is finding applications widely like domestic electrification, satellites, grid connected micro systems, rural electrification, solar water pumps (SWP), solar lantern, street lighting, calculators, cathodic protection of pipe lines, parking meters, emergency telephones, trash compactors, temporary traffic signs, remote guard posts & signals, etc. Of these, water pumping is an important application.

The present research work deals with the methodology for harnessing maximum power of PV source for solar water pumping application.

1.3 CONTENTS OF THE THESIS

The thesis is structured into six chapters (Table 1.5). Chapter 1 provides broad introduction to the domain of energy in general and solar energy in particular. Chapter 2 deals with the different aspects of solar water pumping. Problem of harnessing maximum power is analyzed and literature survey is provided. With the idea of state of art, the problem for the research work is defined spelling out the objectives.

Table 1.5. Organisation of thesis.

Chapter No.	Title of Chapter
1.	Introduction
2.	Solar Water Pumping and Harnessing Maximum Power
3.	Simulation of Solar Water Pumping System
4.	New Method Proposed For Solar Pumping: MPPT by Load Voltage Tracking ($MPPT_{lv}$)
5.	Individual Floor Storage Method : A Novel Strategy Proposed for Solar Pumping in Multi floored Buildings
6.	Discussions and Conclusion
Appendixes	Special observations made during the course of work

Chapter 3 treats the simulation of the solar PV system. To start with, simulation models for individual components of the system are developed. Using them, the system as a whole is simulated incorporating maximum power point tracking (MPPT). Contribution of MPPT is shown. Chapter 4 proposes the method "MPPT by load voltage tracking ($MPPT_{lv}$)". This proposal is worked out first with resistive load and then with pump load. Theoretical background for the proposal is given followed by simulation as well as experimental testing to validate the proposal. Chapter 5 deals with the solar water lifting in multi floored buildings. It proposes a unique strategy "Individual Floor Storage Method" which is typically suitable for solar water pumping application. The proposal is worked out taking the example of a two floored building. Chapter 6 is the concluding one giving discussions, scope for future work, etc. Some of the special/ allied observations made are added as appendixes.

CHAPTER 2

SOLAR WATER PUMPING AND HARNESSING MAXIMUM POWER

Present chapter deals with the aspect of optimizing the harnessing of power. Different approaches are presented and the one with MPPT converter is explained. Then the configuration of solar water pumping systems are given. Comprehensive literature survey is provided and critical remarks are made. With this as the background, the problem for the present research work is defined and the objectives are set.

One paper is published covering some of the aspects of this chapter (Sl. No. 11 in the list of publications, page 156).

2.1 PRECIOUS WATT AND OPTIMIZING THE OUTPUT

Main drawback of solar PV is its higher cost compared to other sources. Hence solar watt can be referred to as precious watt. Effective cost of the solar PV system can be reduced by enhancing useful output. Methods of optimizing the output power fall under three categories:

- Improving cell efficiency: This approach attempts at identifying less costly and more efficient materials for solar PV cells.
- Using the harnessed power more efficiently: This approach calls for improving efficiency of the load apparatus (e.g.: solar pump) or overall energy conversion strategy of the load (e.g.: water pumping strategy).
- Optimizing the harnessing of the available power from the solar insolation and PV panel: This approach relates to the working of PV panel itself & is explained below.

2.1.1 Optimizing the Harnessing of the Available Energy

This can be accomplished by:

- Trapping maximum insolation by employing sun tracking: This is also called mechanical tracking or sun tracking. Instead of keeping the PV panel in a fixed position, it is physically tilted (manually or automatically) so that it always faces the sun. By this, the amount of insolation incident on the panel at right angle will increase thereby giving a higher electric power output.
- Controlling operating point of solar PV panel employing Maximum Power Point Tracking (MPPT): This is referred to as electrical tracking and is discussed in the following section.

2.1.2 Operating point of solar panel

The electrical characteristic of a solar PV panel is a function of solar insolation and temperature of panel. Typical "panel voltage (V_p) vs. panel current (I_p)" and "V_p vs. panel power (P_p)" characteristics of a solar panel, as a function of insolation level, are shown in Fig.2.1 and 2.2 respectively (Vongmanee et al. 2002). The short circuit current I_{ph} is proportional to insolation and hence is used as a measure of insolation.

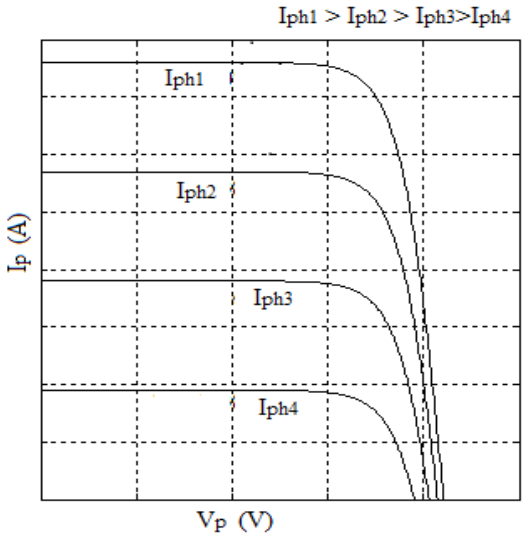

Fig.2.1 Typical "V_p vs. I_p" for PV panel.

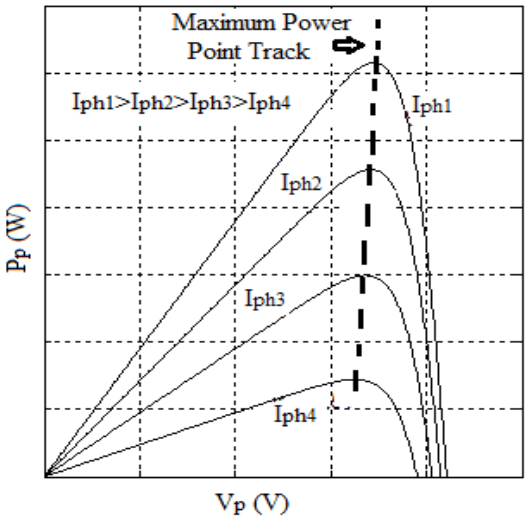

Fig.2.2 Typical "V_p vs. P_p" for PV panel.

To drive home the significance of operating points, a solar pump is considered connected to solar PV source without MPPT converter (Fig. 2.3). Typical V-I and V-P characteristics of the PV source at different insolations are considered and load characteristics is superimposed on the panel curves (Fig. 2.4 & 2.5). It is observed that with a decrease in insolation, the load power also decreases. However at each insolation there exists a maximum power (P_{max}) point. Points AA, BB, CC correspond to maximum powers. The load will operate at different points A, B, & C depending on the insolation. However these points do not correspond to maximum power. Hence the load will get less power though there is possibility of getting more power. It becomes clear that location of the operating point on the PV source characteristics is very critical in deciding the power output to the load.

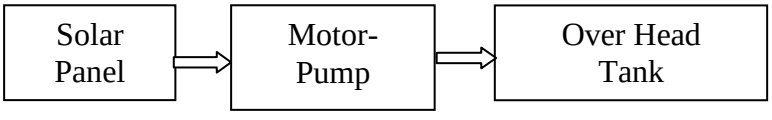

Fig.2.3 Solar pump without MPPT.

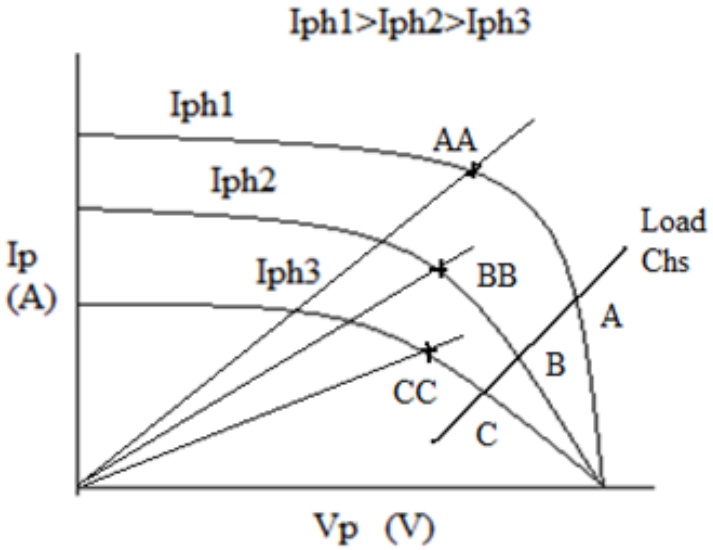

Fig. 2.4 'V-I' plot for PV panel & Load characteristics.

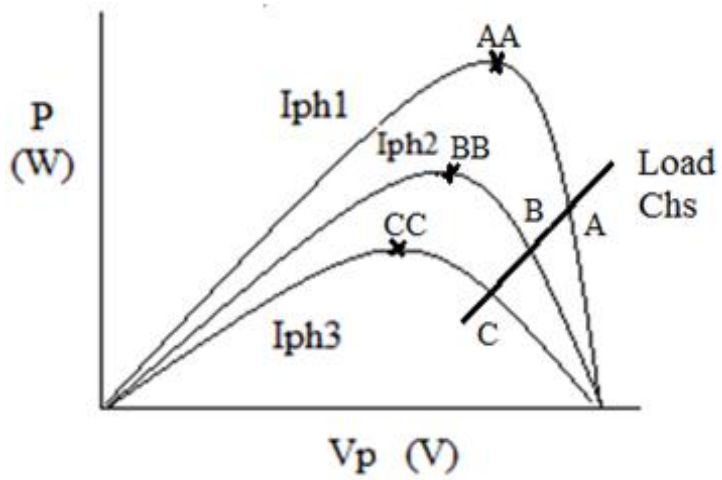

Fig. 2.5 'V-P' plot for PV panel & Load characteristics.

Maximum Power Point Tracking (MPPT)

From the above it is observed that in order to obtain maximum power from solar PV, it's necessary that the load is operated at corresponding P_{max} point. Realizing this i.e. operating the load always along the maximum power trajectory is referred to as Maximum Power Point Tracking (MPPT). Here the load is matched with the panel such that the operating voltage & current correspond to maximum power point. MPPT can be accomplished in two ways:

a) **Source side matching:** Here PV source consists of multiple panels. The series–parallel configuration of these panels is adjusted to correspond to required V-I combination yielding maximum power (Bogdan et al. 1994).

b) **Load side matching:** Here a power electronic converter is incorporated between PV panel and the pump load. Typical solar pump with load side matching (Silveira et al. 2004) is shown in Fig 2.6. By varying switching duty cycle (D) of converter, the load impedance and hence the operating point is altered to match with the corresponding P_{max} point (Van et al. 1998).

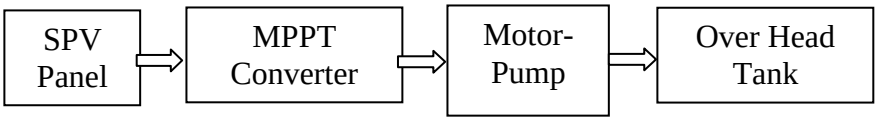

Fig. 2.6 Solar pumping system with MPPT converter.

Shifting of Operating Point

The process of shifting operating point to realise MPPT is demonstrated in Fig. 2.7. Two load curves, A & B are considered. At a typical insolation with load A, the effective load impedance is R_A. Maximum power point corresponds to an impedance of R_{MP}. R_A is more than RMP. Hence load A operates at a point which is away from the maximum power point. By decreasing the effective load impedance from R_A to R_{MP}, the load operating point can be shifted to correspond to maximum power. Similarly, with load B, the effective load impedance is R_B. Maximum power point corresponds to an impedance of R_{MP}. R_B is less than R_{MP}. Hence load B operates at a point which is away from the maximum power point. By increasing the effective load impedance from R_B to R_{MP}, the load operating point can be shifted to correspond to maximum power. The job of changing the effective impedance is accomplished by MPPT converter. It acts like a resistance emulator. By varying the switching duty cycle (D) of the converter, the effective impedance can be changed and hence the operating point can be shifted as needed to realise maximum power harnessing.

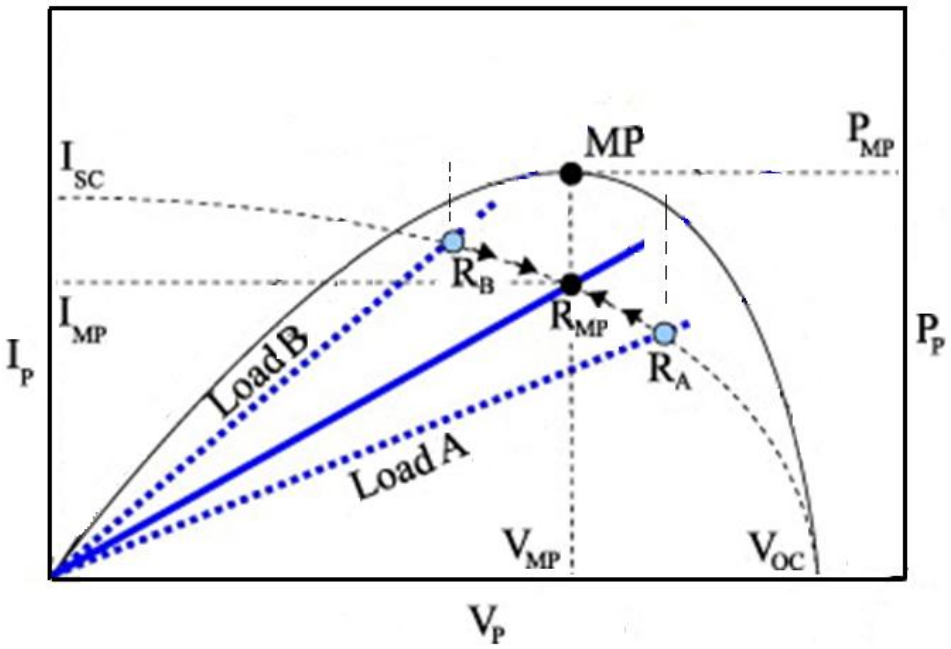

Fig.2.7 'V-I' characteristics of solar pump with MPPT converter.

2.1.3 Different strategies to control MPPT converter:

There exist different strategies to vary D (Cristinel et al. 2010). These can be broadly categorised as:

a) Interruptive Type:

This method is based on the observation that for maximum power, the panel voltage is a fixed percentage of corresponding open circuit voltage (V_{oc}) or the panel current is a fixed percentage of the short circuit current (I_{sc}). Hence there are mainly two approaches.

Monitoring of V_{oc}: Here periodically the panel is disconnected from the load and V_{oc} is measured. The panel voltage (V_p) is continuously sensed and value of MPPT converter duty cycle is adjusted till this V_p becomes the expected percentage (usually 71%) of the V_{oc}. This approximately corresponds to maximum power point.

Monitoring of I_{sc}: Here periodically the panel is disconnected from the load and I_{sc} is measured. The panel current (I_p) is continuously sensed and value of D is adjusted till this I_p becomes the expected percentage (usually 85%) of the I_{sc}. This approximately corresponds to maximum power point.

The above methods are simple as only one parameter is to be monitored (either voltage or current) and no multiplication process is involved. But the disadvantage is the periodic interruption from the load leading to loss of power that otherwise could have been tapped. Also in their basic form, these methods are not accurate in tracking the maximum power as the relation between V_p (I_p) and V_{oc} (I_{sc}) depends on the ambient temperature. To achieve higher accuracy, temperature compensation is to be incorporated which makes these methods also complicated.

b) Non Interruptive Type:

Here there is no need to delink panel from load. Important approaches are:

Constant Voltage: Panel voltage is monitored and maintained constant at a fixed value which approximately corresponds to maximum power. This method is quite simple and cheap. But the accuracy is less.

Monitoring Panel Power: Here the PV panel power (P_p) is monitored continuously. D is varied till P_p becomes maximum. Perturb and Observe (P&O) approach is employed to continue to ascertain the maximum power availability. This method is direct in nature, more accurate and hence is more commonly employed. No prior information of the PV characteristics is required. It is versatile with respect to the load profile. But for computing power ($P_p = V_p \times I_p$), two parameters (V_p & I_p) are to be measured and then multiplication operation is to be performed. That makes the controller comparatively complicated. The algorithm and additional details are given in Appendix I.

Monitoring Conductance: This method makes use of the fact that at maximum power point, the slope of the V-P curve is zero (Fig.2.2). Using this feature an expression for incremental conductance can be obtained as shown in equation (2.1).

$$(dI/dV)_{MPP} = - I/V \qquad (2.1)$$

Here V_p & I_p are monitored. D is varied to satisfy the condition in equation (2.1) which automatically ensures maximum power. This method is also direct in nature. No prior information of the PV characteristics is required. It is versatile with respect to the load profile. It is more accurate than the P&O approach but requires monitoring of more parameters. Hence is more complex and the cost of implementation is more. The algorithm and additional details are given in Appendix I.

From the above discussion it's found that interruptive methods are simple but yield less power whereas non-interruptive methods yield more power but are more complicated. **Hence there is need for a method which is non interruptive as well as simple.**

2.2 SOLAR WATER PUMPING

Water pumping is a basic and critical need for urban as well as rural dwellings for drinking, small irrigation and livestock watering applications (Dunlop 1988). These are being powered by mostly fossil fuels (diesel, petrol etc) or fossil fuel based electric grids. Of late solar photo voltaic driven water pumping systems are receiving considerable attention due to the developments in the field of power electronics and solar cell materials.

Solar pumping system can be with or without battery backup. Battery is not a must for solar pumping as compared to other solar PV applications. Whenever the PV power is available, water is transferred to an overhead tank (OH) which itself acts as a storage element. However the position of OH tank is very critical. Solar pumping system can also be with (Fig.2.6) or without (Fig.2.3) MPPT converter. In the former, the converter is employed to realise maximum power point tracking. The latter type is the most basic and simple configuration wherein motor is directly connected to the PV panel.

2.3 STATE OF ART:

Considerable work is accomplished by the researchers in the field of solar water pumping. A brief account of the same is given below.

Solar PV Basics and Simulation

- Gilbert (2004), Mohammad et al. (2002), Mukherjee (1997) and Vongmanee et al. (2002) have deliberated on the basic aspects of energy conversion, characteristics, modelling and simulation of solar PV panel. Cristinel et al. (2010), Hairul et al. (2010), Hohm et al, (2003), Hussein et al. (1995) and Nikhil et al. (2011) have given review and comparative study of different MPPT methods. The MPPT converter acts as "resistance emulator".
- Kim et al. (1996) have dealt with perturb & observe (P&O) method for MPPT. Calavia et al. (2010) and Hussein (1995) have dealt with incremental conductance (IC) method and compared with P&O method. They claim IC method is better regarding efficiency.
- Kiranmayi et al. (2008) have dealt with constant voltage control method for MPPT. Tafticht et al. (2008) have considered V_{oc} and proposed non linear expression for the optimal operating voltage. MPPT is accomplished using P&O approach. The proposal claims reduction in oscillations around maximum power point and increase in average efficiency of MPPT.
- Casey et al. (2009) have proposed an efficient voltage based MPPT using V_{oc} information from a reference cell.
- Toshihiko et al. (2000) have proposed short current pulse based adaptive MPPT. Eduardo (2008) has proposed MPPT using the optimal duty ratio for DC-DC converters and load matching in terms of effective resistance.
- Bogdam et al. (2002) have discussed different methods like P&O and IC. Fuzzy system based MPPT is proposed. Kim et al. (1997) and Mummadi et al. (2000) have proposed neural network based approach for MPPT. They have claimed that this approach allows less accurate sensors to be used.

- Jantsch et al. (1997) have given details of methodology for measurement of MPPT performance. Clin (1988) has discussed system testing techniques.
- Francisco (2005) and Mohammad et al. (2002) have presented simulation of PV module in Matlab. Armando et al. (2009) have proposed a method for getting mathematical model for PV module using parameters provided by manufacturers' data sheets. Katan et al. (1996) have proposed two diode model considering R_{sh} using PSPICE software.
- Swiegers et al. (1998), Lyon et al. (1998) and Wernher et al. (1998) propose the idea that MPPT converter can be integrated with individual panel itself. This improves the overall efficiency. Increase in energy transfer is 26%. Provision of integrated panel converter costs 2.8% of that of PV panels. Integrated MPPT ensures right size of MPPT. Overrating or underrating of MPPT which are possible with a single high power MPPT will be avoided.

Basic Solar Water Pumping

- Battery is not a must for solar water pumping. OH tank itself acts as a storage element. (Alghuwainum 1996, Anis et al. 1994, Chandrasekaran et al. 2011, Kagarakis et al. 1989, Short et al. 2002 and Viorel 2003).
- Dunlop (1988) and Silveira et al. (2004) have given basic analysis of solar water pumping system. Kirk et al. (1993) have given the outcome of a survey of utilities regarding reliability, cost, performance of PV powered water pumping system. Mahmoud (1990) has given comparison between diesel motor as against using PV power for water pumping.
- Sangal et al. (1988) have given general field experience in India regarding shallow head pumps. Necessity of solar PV for rural India is emphasised. Bhargava (1994) has given overall idea about radiation potential in India. Daily average solar energy incident in the country is 4 to 7 kWh/m^2 with about 250 to 300 sunny days/year. Hence there is good opportunity for several solar PV applications in general and water pumping in particular.

Why No Progress?

- Short et al. (2002) have discussed about poor growth of solar water pumping as an application. Solar pumping was portrayed as being able to revolutionize water provision in rural and developing communities. But the reality is different in terms of levels of penetration. Only 60000 units were installed across the globe as against the aim of 10 million units installation. Even among whatever installed, half of them ceased to function within 10 years of installation. It is observed that as the converters and regulators become complex, the reliability in service decreases. Converters, regulators and batteries are the weak links and 77% of failures are due to them (Anderson 2000). This poses reservations regarding the very provision of complicated MPPT and controllers anticipating high performance. Direct coupling between the solar panel and the pump is the most reliable pumping technique. But requirement of matching between panel and pump compels introduction of a converter.

- Even in India, the growth in the installation of solar pumps has not been promising. In the whole country, total number of pumps is 21 million. Of these 12 million are grid connected and 9 million are diesel driven. There exists a big opportunity for solar pumps to replace the diesel pumps (Subha et al. 2010). But the increase in the number of solar pumps is just 2334 over a span of 10 years, from 5000 in the year 2000 to 7334 in the year 2010 (Subha et al. 2010 and Surendra et al. 2002).

- Why poor response from the people? Why these systems are not performing reliably? Major reasons for the poor growth are higher "cost per watt" and poor reliability due to complex technology. Hence it is necessary to reduce the cost and keep the technology as simple as possible. Cost reduction can be achieved by harnessing more power per unit installed capacity of the solar panel (Short et al. 2002). One method of realising this is by MPPT. Here a power electronic converter is used to match pump with the PV panel so that harnessed power is maximum. There are different approaches for MPPT. Some of them are more accurate but complicated, whereas others are simple but less accurate. There is need for a simple as well as more accurate method.

Pump Drive

Various options exist regarding the drive for the pump.

- Liebenberg et al. (1993) and Short et al. (2002) have proposed linear electromagnetic actuator in place of conventional motor. By this they claim higher reliability, less cost and ease of maintenance. Hamid et al. (1997) have discussed the performance of PV pump using switched reluctance motor. Swamy et al. (1996) have proposed BLDC motors highlighting their advantages like no brushes, less maintenance, high efficiency etc. However a power electronic converter is needed to condition the input to the motor. This makes the system more complicated.

- Squirrel cage induction motor (IM) can also be used as the drive. It has the advantages like rugged construction, almost nil maintenance, compactness, etc. However it calls for introducing a power electronic converter to convert d.c. to a.c. Clinton et al. (1998) have discussed different MPPT strategies for induction motor pump. Enslin et al. (1991) and Muljadi (1997) have proposed different inverter configurations. Neway (1994) has dealt with determination of matching factors between PV panel and motor-pump load. Nayar et al. (1993) have presented simulation using electromagnetic transient program for IM driven pump. Singh et al. (1996) have presented modelling of IM driven solar pump and current controlled voltage source inverter for optimal matching. Vongmanee et al. (2002) have proposed vector control of 3-phase IM for driving centrifugal pump. Varin (2004) has discussed about field oriented principle for controlling 1-phase IM driving centrifugal pump. The speed is varied to obtain maximum output power.

- Considerable work is done in the area of solar water pumping with dc motor as the drive. Mohamed (1998) has discussed about matching dc motor - pump load to PV panel for realising maximum gross mechanical energy by controlling magnetic flux. This requires motor to be separately excited. Hamid et al. (1996), Kolhe et al. (2004) and Mohamed (1998) have narrated merits of the system having PMDC (brushed) motor coupled to centrifugal pump. Abdelmalek et al. (2007) have presented the results of tests carried out on directly coupled dc motor-centrifugal pump system. They have opined that such a system is clearly

suitable for low head application in remote areas not covered by the national electricity grid and where access to water comes as first priority issue than access to technology. Brushed PMDC motor is simple. It needs plain d.c. which is readily available from the PV panels. No need of conversion from d.c. to a.c. However it suffers by the disadvantage that the presence of brushes calls for maintenance. Centrifugal pump is suitable for moderate heads and flow rates.

Sun Tracking

- Sun tracking is the process of orienting the PV panel physically so as to face the sun making the solar radiation fall on the panel at right angle (Dunlop 1988, Hadj et al. 2006, Katan et al. 1996, Kolhe et al. 2004, Sangal et al. 1998 and Vilela et al. 2003). It can be done either manually or automatically using an external drive. Sun tracking results in enhancement of radiation captured. It improves performance of direct coupled systems by making motor to start earlier in the day and then operating the pump closer to the optimal design point over a great portion of the day. Water yield increases by 20-30%. However the mechanism of providing the tracking is to be carefully looked into. If the tracking is manual, it can be done only at few intervals. It can happen continuously, if it is automatic, making the gain more. However the tracking drive itself requires energy. Also taking into consideration the expenditure on the tracking drive, the sun tracking proposal will be suitable for large systems.

Efficiency of Components

- Performance of individual components of the solar pumping system decides the efficiency of the overall system. Lujara et al. (1999), Mahmoud (1990) and Reshef et al. (1995) have analysed the efficiency aspects. Simulation as well as field tests are done. Average efficiency values (Reshef et al. 1995) for different components of a typical solar pumping system are shown in Table 2.1. Overall efficiency, from solar insolation on panel to water output from pump, referred to as 'light to water efficiency' is of the order of 2-3%. Very poor value really!! PV

panel and pump turn out to be the bottlenecks as their individual efficiencies are poor .

Table 2.1 Solar pumping system:

Component efficiency.

Component	**Efficiency**
PV panel	11.5%
MPPT Converter	93.3%
DC Motor	56.8%
Pump	48.2%

PMDC Motor Driven Solar Pump

- Eugenio et al. (1991), Hadj et al. (2006), Meirios et al. (1991) and Viorel (2003) have dealt with modelling, simulation and performance evaluation of direct coupled solar pumping system with PV panel, PMDC motor, centrifugal pump. Kou (1998) has proposed a method for estimating long term performance of direct coupled solar pumping systems using information available from PV panel & pump manufacturers' data.
- Appelbaum et al. (1989) have compared the operation of two PMDC motor pumps powered by a common PV source. They have shown that the net performance of the two sets improves as compared to their performance when powered by individual sources.

MPPT by PV Source Side Matching

- Bogdan et al. (1994), Dunlop (1988), Eugenio et al. (1991), Salameh et al. (1990) and have proposed that dc motor pumps directly coupled to PV arrays perform optimally at specific "array series parallel configuration" leading to MPPT. However this approach has the disadvantage that the available steps are discrete and limited in number. Smooth variation is not possible.

MPPT by Load Side Matching

- Different strategies for MPPT with load side matching are proposed for solar PMDC motor solar pump application. Different parameters on the input side like panel voltage, current & power are taken as control parameters for realising MPPT. Swamy et al. (1996) have discussed different MPPT approaches. Enslin et al. (1991) and Van et al. (1998) have opined that fixed voltage with temperature compensation gives performance comparable to true power tracking strategy. The advantages are simple hardware, lower noise etc. Alghuwainem (1994) has proposed the method of keeping current proportional to the insolation levels (ie I_{ph}) using a converter. I_{mp}=0.85 I_{ph} is taken for dc shunt motor driven centrifugal pump. Katan et al (1996) propose MPPT by keeping voltage equal to ref voltage using a converter. Panel voltage is made proportional to the open circuit voltage. Typically, V_{mp} is taken equal to 0.71 times V_{oc}. Mohammad et al. (2002) have analysed both voltage and current based MPPT approaches. It's opined that voltage based technique results in simple hardware, higher efficiency and lower noise & cost.

- Kolhe et al. (2004) give details of experimental test done on PMDC motor centrifugal pump direct connected system. The relation between the water flow rate and the head is given. As the head increases the flow decreases and the power taken will increase. Odeh et al. (2006) have analysed influence of pumping head, insolation and PV array size on performance of solar water pumping system .

- Veerachary (2000) has analysed steady state & transient performance of PV powered dc motor centrifugal pump. Buck boost converter is taken for MPPT. Here they deal with both a) extracting max power from PV source and b) yielding maximum gross mechanical energy output. The latter is realised by controlling the motor flux. Singer et al. (1993) have dealt with dynamic performance of DC shunt motor & centrifugal pump system. Hamid et al. (1996) have given analysis of directly coupled solar pumping system using DC shunt motor. Fam et al. (1988) have analysed starting characteristics of DC motors powered by solar cells. The advantage of MPPT is that starting torque will increase at lower insolation levels. Hence water pumping duration will increase.

- Arrouf et al. (2007), Hamidat et al. (2008) and Taufik et al. (2009) have presented modelling and simulation of pumping system fed from PV source. Abidin et al. (2004) and Ghoneim (2006) have discussed optimization of solar solar pumping systems.
- Davies et al. (1992), Moussi et al. (2005), Muljadi (1997) and Varin (2002 & 2002) have taken speed as reference for controlling MPPT for maximising output of water in solar pumping application.

Critical observations from literature survey:

- The growth in the installation of solar pumps has not been promising.
- It is necessary to reduce the effective cost. The technology is to be simple and easily maintainable so that it can be installed in remote areas where technical knowhow of the system maintenance and operation are very much limited.
- Solar pump with overhead tank and without battery backup is simple and reliable. Load side matching provides simpler and more effective approach to realising MPPT. Brushed PMDC motor is economic and quite commonly employed. Centrifugal pump is better for moderate head and flow applications.
- Control parameters employed for MPPT converter till now are panel side voltage, current, power and pump speed.
- There is need for simple yet accurate and non interruptive approach for MPPT.
- The aspect of position of overhead tanks for water pumping in multi-storeyed buildings is not found in literature and hence can be explored for possible benefits.
- Specifically, papers by Anderson (2000), Cristinel et al. (2010) and Short et al. (2002) were found to be motivating as well as more informative. They have made deep impression on this research scholar.

With the above as the background, present research work is taken up.

2.4 PROBLEM DEFINITION & OBJECTIVES:

Present research work "Solar Photo Voltaic Water Pumping System" deals with the methodology for harnessing maximum power of PV source for water pumping application. The problem identified for research is: "To develop simple and effective method or strategy to improve solar pump performance in terms of the daily power harnessed leading to an increase in the quantity of water lifted per day for a particular installed capacity of PV panel". The objectives of the research work are:

- Development of a method or strategy to improve solar pump performance requires an understanding of the operation of the system as well as the work done in this field till now. Comprehensive literature review is necessary. With the state of the art in mind, the attempt is to be towards a conceptual reorientation.
- Simulation models are to be developed for solar pump. The system to be considered is PV source feeding PMDC (brushed) motor coupled to centrifugal motor. This motor-pump combination is more common and suitable for solar PV applications.
- Opportunity for realising MPPT in a different way is to be explored. New simple approach is to be evolved for harnessing maximum power, yielding more water per watt of installed solar power capacity. The proposed method is to be supported by suitable theoretical explanation.
- The proposal is to be validated by simulation and experimental test results performed on the system considered.
- The aspect of position of overhead tanks for solar water pumping in multi-floored buildings is to be explored for possible benefits.

Research Justification:

Present research work aims at developing simple strategy to harness more power per unit installed capacity of PV panels. It leads to decrease in effective cost per rated watt of solar panel. The acceptability of solar pumps increases. More number of people will opt for solar PV applications in general and solar pumps in particular,

accelerating the growth in the number of solar pumps. Thus the results of this research work are expected to contribute in improving the water supply at remote and rural areas. With easy water supply assured for drinking, small farming and live stock watering, the quality of life of these people will improve. Hence the research work is of societal relevance. It is also of scientific relevance as it attempts to propose new methodology which complements existing literature.

CHAPTER 3

SIMULATION OF SOLAR WATER PUMPING SYSTEM

This chapter details the solar pumping system considered in the present work. Individual components of the system are explained giving specifications. Simulation model for each component is developed using MATLAB-SIMULINK (Version 7.5) (Appendix II) and validated. Then the simulation model for the entire system is developed. With the help of this system model, simulation tests are conducted for the cases of with and without MPPT converter. For MPPT, panel power is considered as the reference ($MPPT_{pp}$) which, at present, is more commonly employed method. The results are presented to demonstrate the role of MPPT in enhancing the power delivered to the load.

One paper is published covering some of the aspects of this chapter (Sl. No. 8 in the list of publications, page 155).

3.1 SYSTEM CONSIDERED

In the present work, a standalone solar PV pumping system is considered (Fig.3.1). Different components of the system are: a) Solar PV source b) MPPT converter c) PMDC brushed motor - centrifugal pump unit.

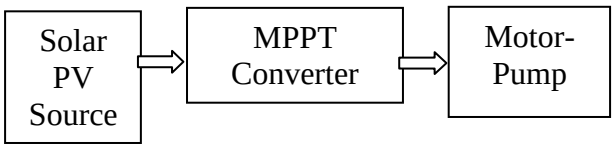

Fig.3.1 Solar pumping system considered.

3.2 PV SOURCE

Parallel combination of two panels is used as PV source. Specifications of each panel are: Tata BP Solar make; P_m = 74 W_p; V_{mp} = 17 V; I_{mp} = 4.4 A; V_{oc} = 21.8 V; I_{sc} = 4.9 A; Effective series resistance of panel, R_s = 2.13 Ω (found experimentally).

SIMULATION

The PV panel can be simulated either by equation based approach or circuit based approach.

3.2.1 Equation based approach:

Here equation for PV cell output current (or voltage) is obtained using the equivalent circuit of the cell. With this background the equation for PV panel output current (or voltage) is developed and simulated. This simulation model represents the panel.

Simulation of PV Cell

PV cell can be represented by a simple equivalent circuit (Ghoneim 2006, Hadj et al. 2006 and Mohammad et al. 2002) with a current source having a diode in parallel and resistance in series (Fig.3.2) neglecting the shunt branch.

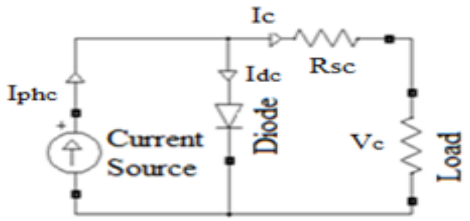

Fig.3.2 Equivalent Circuit of PV Cell.

Output current I_c is given by,

$$I_c = I_{phc} - I_{dc} \qquad (3.1)$$

$$= I_{phc} - I_{oc}\{ \exp(q[V_c + I_c R_{sc}]/AKT) - 1\} \qquad (3.2)$$

$$= I_{phc} - I_{oc}\{ exp([V_c + I_c R_{sc}]/D - 1\} \qquad (3.3)$$

where:

I_{phc}= Photon current proportional to the insolation.

I_{oc}= cell reverse saturation current = 10^{-7} A/m^2 (for silicon) = 0.0005 A.

I_c = Cell output current; R_{sc} = Series resistance of the cell;

q = Electric charge of electron = 11.6 x 10^{-19} C

A = Compilation factor or ideality factor;

K = Boltzinan constant = 1.38 x 10^{-23} ; T = Temperature (^{0}K);

$D = AKT/q$.

Simulation of PV Panel

A PV panel is made up of solar cells connected in series and parallel, in order to get the desired level of voltage and power. Fig.3.3 represents the equivalent circuit of a PV panel neglecting shunt current.

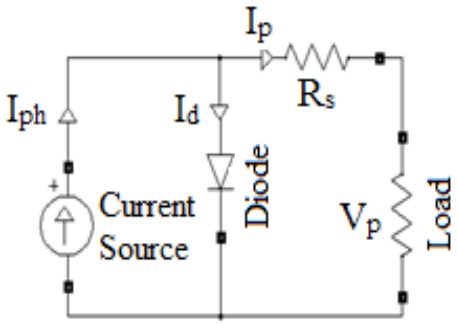

Fig.3.3 Equivalent circuit of PV source.

For the panel equivalent circuit, the output current I_p is given by the equation (3.4).

$$I_p = I_{ph} - I_d \qquad (3.4)$$

$$I_p = b\, I_{phc} - b\, I_{dc} \qquad (3.5)$$

Using the equations (3.1 to 3.3) written for PV cell, V_p can be expressed as

$$V_p = D_p\, ln\{(I_{scp} - I_p + b\, I_o) / b\, I_o\} - R_s\, I_p \qquad (3.6)$$

D_p is found using open circuit (OC) conditions for the solar panel and is obtained as equal to 2.565. Substituting other values for the panel in equation (3.6), equation for panel voltage is obtained as in equation (3.7).

$$V_p = 2.565\ ln\{1000(4.901 - I_p)\} - 2.13\ I_p \qquad (3.7)$$

where:

I_{ph}: short circuit current of the PV panel (A). This is directly proportional to the radiation and hence used as a measure of radiation.;

I_p = panel current; I_o= Equivalent reverse saturation current for panel;

I_d: Diode Current (A); V_p = panel voltage; R_{sp} : Series resistances of panel;

b = Number of parallel paths = 2; a = Number of series cells = 44;

$R_{sp}=(a/b)R_{sc}$ = 2.13 Ω (measured);

T =273+25 = 298 ^{0}K (taking ambient temperature as 25^{0}C).

Equation (3.7) is simulated and that model represents PV panel. However this approach of using equation to represent PV panel is more mathematical in nature and lacks the circuit touch required for electrical performance analysis.

3.2.2 Circuit Based Approach:

PV panel can be represented by actual circuit components instead of representing by an equation. Modelling like this is called circuit based approach. Circuit based model is more useful in analysing the performance features compared to equation based model. Hence this approach is employed in the present work.

Photo current, I_{ph} is represented by a current source. A single diode is connected in parallel to current source to account for the current I_d. The specification of the diode i.e., voltage drop across it is so taken as to represent the open circuit voltage V_{oc}. Each panel has 44 cells in series. Effect of diodes of all these cells is represented by an equivalent diode giving the equivalent open circuit voltage. Voltage per diode is taken as 0.42 so that open circuit voltage will be 44 x 0.42 = 18.5 V which is the rated value for the panel considered.

PV source is taken as parallel combination of two panels. The simulation model developed for individual panel is extended to represent the PV source by taking the total photo current I_{ph} = 2 x Photo current per panel. The series resistance is taken as Rs/m = Rs/2 where m = number of panels connected in parallel. With these features, PV source model is developed (Fig.3.4). The power (P_p) is given by the equation (3.8).

$$P_p = I_p \, x \, V_p \quad \text{(W)} \qquad (3.8)$$

The simulation results of "V_p-I_p" and "V_p-P_p" characteristics are given in Fig. 3.6 & 3.7. These characteristics are in tune with the normal nature of curves for PV panel.

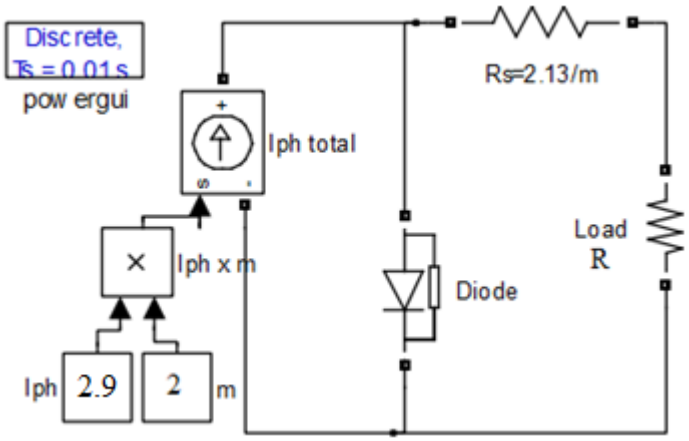

Fig.3.4 Simulation setup for PV source (Two panels).

"V_p vs. I_p" characteristics are also obtained experimentally. The experimental setup is shown in Fig 3.5. Keeping S_1 off & S_2 on, I_{sc} is found. Keeping S_1 & S_2 off, V_{oc} is found. Keeping S_1 on, S_2 off and varying load resistance, other operating points are found.

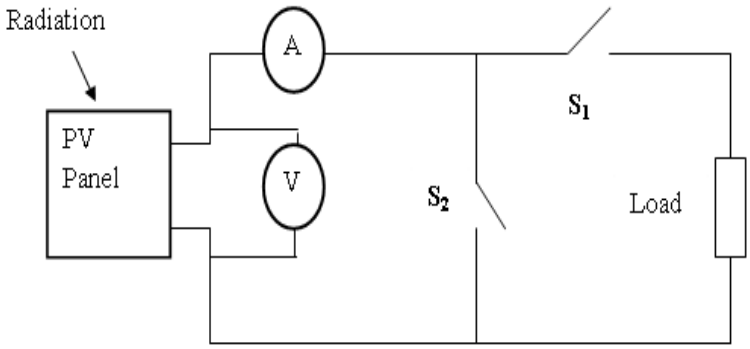

Fig.3.5 Experimental setup to get "V_p vs. I_p" plot of PV source.

Using the experimental results, "V_p-I_p" and "V_p-P_p" characteristics are plotted. It is observed that simulation results are in close match with the experimental results (Fig.3.6 & 3.7) thus validating the simulation model developed for the solar PV source.

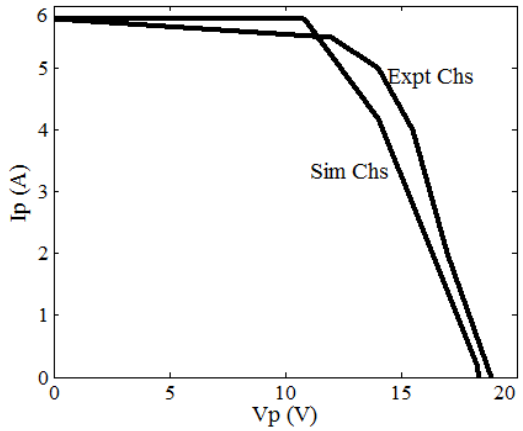

Fig.3.6 "V_p vs. I_p" for 148 W_p PV source
(Experimental & Simulation)

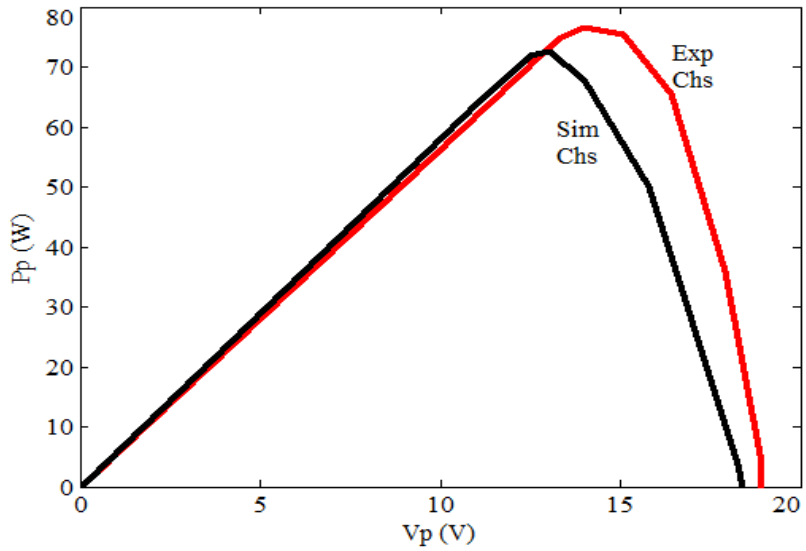

Fig.3.7 "V_p vs. P_p" for 148 W_p PV source

(Experimental & Simulation**)**

3.3 SOLAR PV PUMP

3.3.1 Motor-Pump Unit:

It is a mono-block of PMDC brushed motor and centrifugal pump with the following specifications: 'Lotus', Tata BP Solar make, 12 V, 70-100 W, Total Head: 9 m. The equivalent circuit of PMDC motor is as shown in Fig.3.8.

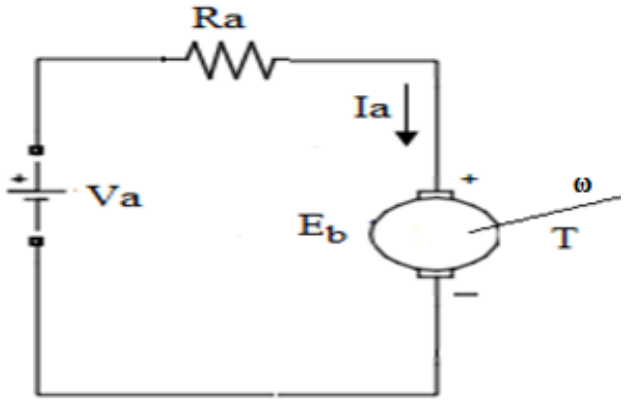

Fig.3.8 Equivalent circuit of PMDC (brushed) motor.

where R_a: Armature winding resistance (Ω); E_b: Back EMF (V); T: torque (N m); ω: rotational speed (rad/s); P_g: air gap power (W); I_a : Armature Current (A).

The steady state performance equations for dc motor can be obtained as shown in equations (3.9) to (3.14).

$$E_b = K_b \omega \quad (3.9)$$

$$E_b = V_a - I_a R_a \quad (3.10)$$

$$T = K_b I_a \quad (3.11)$$

$$V \, x \, I_a = E_b \, x \, I_a + R_a \, x \, (I_a)^2 \quad (3.12)$$

$$P_g = \omega \, x \, T = E_b \, x \, I_a \quad (3.13)$$

$$T = (E_b \, x \, I_a) / \omega \quad (3.14)$$

3.3.2 Basic parameters of DC Motor

Different parameters of the motor are determined experimentally as detailed below.

a) Motor Inertia is determined measuring the mass and geometric parameters of the stator & rotor parts of motor. Mass of rotor = 3.375 kg; Length of rotor= 0.09 m; Radius of rotor = 0.045 m;

Moment of Inertia (MI) = Mass x $(\text{Radius})^2$

$= 3.375 \text{ x } (0.045)^2$

$= 6.83 \text{ x } 10^{-3} \text{ kg m}^2$

b) Armature resistance (R_a) and inductance (L_a) are measured directly with digital multimeter. $R_a = 0.7\ \Omega$; $L_a = 0.12 \text{ x } 10^{-3}$ H.

c) Back EMF constant (K_b): It is determined by conducting no-load test on motor. The motor is supplied with varying input voltage (Fig.3.9). At each voltage the speed and current are observed (Table 3.1). Value of back EMF is calculated using equation (3.10) and plot of "ω vs. E_b" is obtained (Fig. 3.10). From this K_b is obtained as K_b = 0.033V/rad/s.

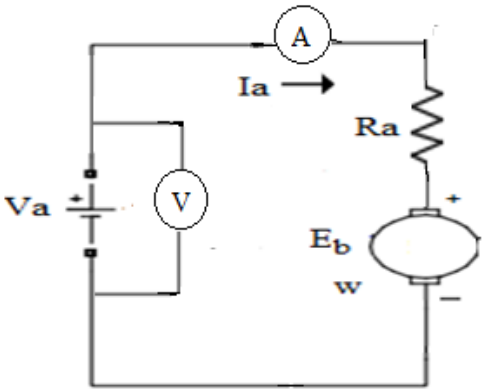

Fig.3.9 Test setup for determining K_b.

Table.3.1 No load test results to find K_b for PMDC motor.

Sl. No	**V_a (V)**	**I_a (A)**	**ω (rad/s)**	**$E_b = V_a - I_a R_a$ (V)**
1	0	0	0	0
2	4.7	3	65.5	2.6
3	6.0	3.4	94.3	3.6
4	7.1	3.85	119.9	4.5
5	8.0	4.2	139.9	5
6	9.0	5.05	152	5.5
7	10.0	5.7	168.9	6
8	11.0	6.35	187.9	6.5
9	12.0	7.05	206.2	7.1
10	13.0	7.6	228.1	7.7
11	14.0	7.8	253.3	8.5
12	15.0	8.0	278.5	9.4

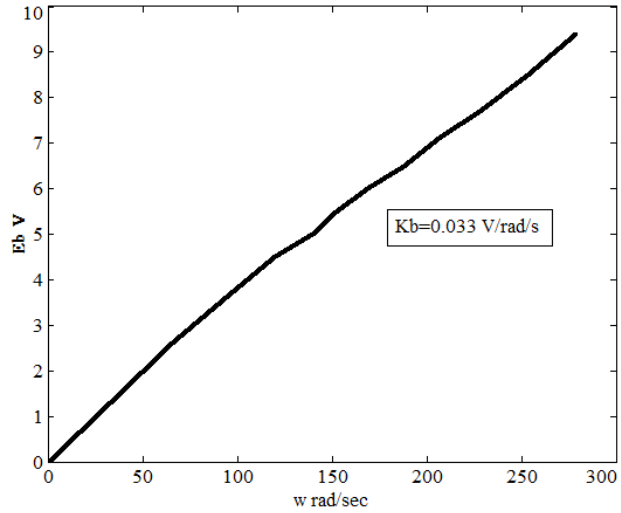

Fig.3.10 "ω vs. E_b" for PMDC motor.

3.3.3 Pump Load Equation:

"Speed (ω) vs. Torque (T)" plot of the pump is obtained experimentally for a head of 4 m (Table.3.2 and Fig.3.11). By curve fitting approach, the pump load equation (3.15) is derived. This is found to be of the same format as mentioned in the literature (Kolhe et al. 2004).

$$T = 4.8 \times 10^{-6}\ \omega^2 + 0.00019\ \omega + 0.092 \qquad (3.15)$$

Using basic equations (3.9) to (3.11) for PMDC Motor, equation (3.15) is written in terms of V_a & I_a as shown in equation (3.16).

$$4.4\ V_a^2 - 5.75\ V_a - 6.17\ V_a\ I_a + 2.15\ I_a^2 - 36.9\ I_a + 92 = 0 \qquad (3.16)$$

Table.3.2 "ω vs. T" of pump motor (4 m head) (Experimental).

Sl .No.	ω (rad/s)	T (Nm)
1	0	0.09
2	121.2	0.198
3	136.9	0.211
4	154.5	0.231
5	174.2	0.2475
6	183.3	0.28
7	192.4	0.31
8	201.5	0.34

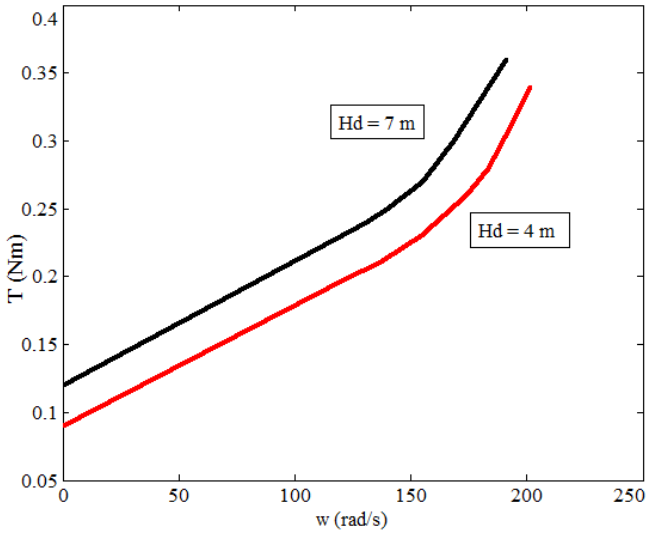

Fig.3.11 "ω vs. T" for pump at 4 m head.

3.3.4 Pump Flow Rate:

Relation between flow rate (Q L/s) and speed (ω) for a head of 4 m is obtained experimentally (Table 3.3) and plotted (Fig. 3.12). By curve fitting, the relation is represented by the equation (3.17).

$$Q = 0.0005\ \omega^2 - 0.041\ \omega - 0.008 \qquad (3.17)$$

The same procedure can be employed to obtain the flow rate for other heads. For example, proceeding in a similar fashion, flow rate relation is obtained for 7 m head also (Fig.3.13).

Table.3.3 Flow Rate of Pump (Experimental).

Sl. No.	**ω (rad/s)**	**Q (l/s)**
1	121.2	0.02
2	136.9	0.05
3	154.5	0.08
4	174.2	0.11
5	183.3	0.135
6	192.4	0.16
7	201.5	0.18

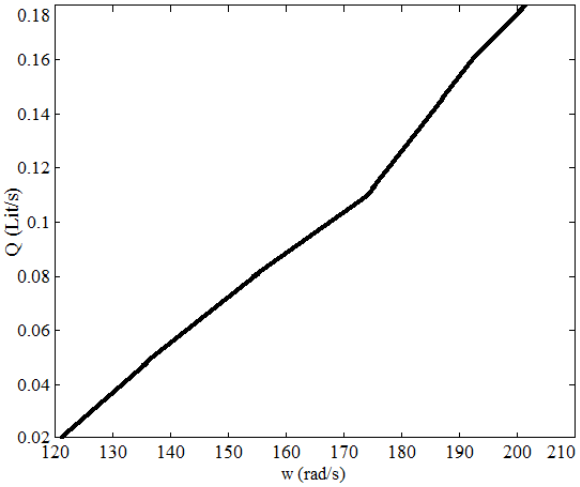

Fig.3.12 "ω vs. Q" for pump at 4 m head (Experimental).

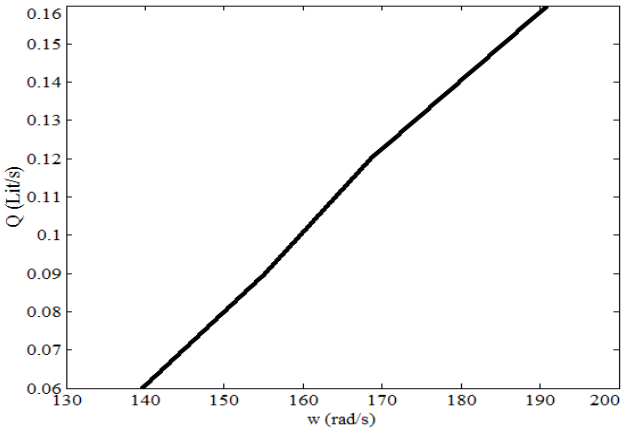

Fig.3.13 "ω vs. Q" for pump at 7 m head (Experimental).

3.3.5 Simulation of PMDC motor with pump load:

PMDC motor-pump model (Fig.3.14 & 3.15) is developed representing the permanent magnet as separate excitation with constant voltage source. Load equation, K_b, etc information derived in earlier section is made use of.

"V vs. ω" plot is obtained experimentally as well as by simulation. Simulation results are found to be in close proximity with the experimental results (Fig.3.16) thus validating the simulation model developed for the pump motor.

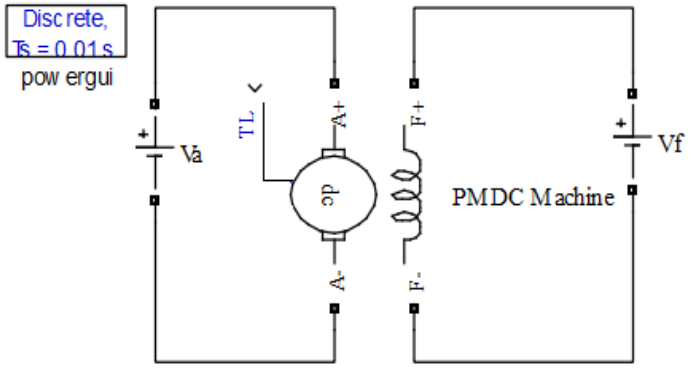

Fig.3.14 Simulation setup for PMDC motor on no load.

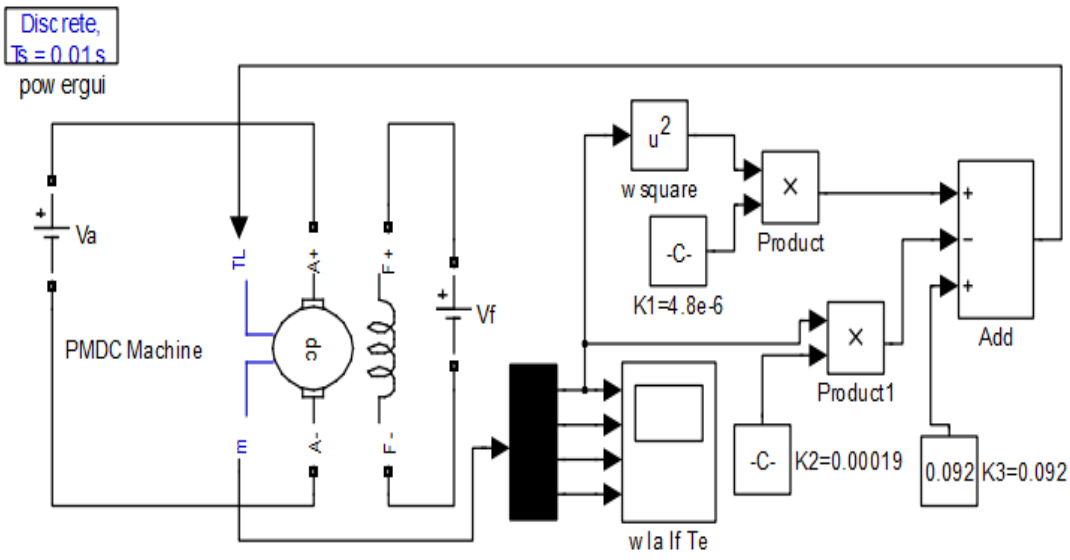

Fig.3.15 Simulation setup for PMDC motor with 4 m head pump load.

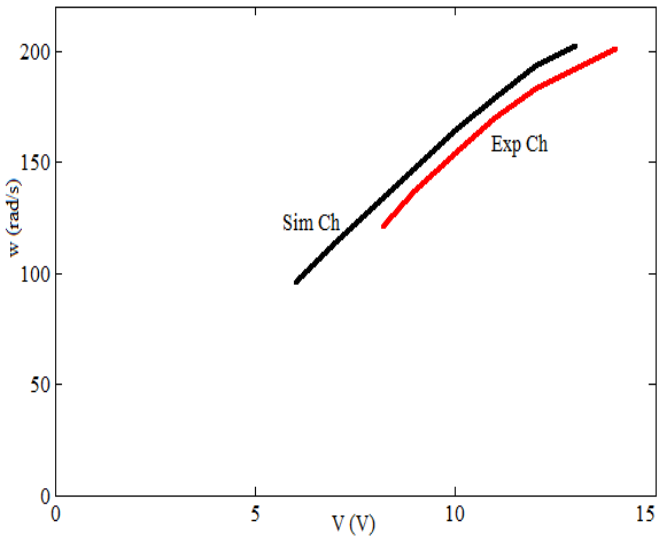

Fig.3.16 "Supply voltage (V) vs. Speed (ω)" for solar pump motor (Experimental & Simulation).

3.4 MPPT CONVERTER

MPPT converter is considered to have Cuk topology (Fig.3.17). This particular configuration is chosen for two reasons. First, it is versatile i.e. it is possible to do both step down & step up operations. Secondly, it has the non interruptive feature. Load is always connected to the solar panel whatever be the status of the switch in the converter. The power extraction from the solar panel is uninterrupted. Whereas in other converter configurations with the switch in series with the panel, whenever the switch is off, the power extraction from the panel is obstructed. This results in reduction in power harnessed, a serious disadvantage in solar PV domain where the basic idea is always to extract as much power as possible.

MOSFET is used as switch. Of the two options, MOSFET & IGBT, MOSFET is preferred due to its features like higher switching speed, lower switching losses and low voltage (<300 V) & medium power (<10 kW) application suitability.

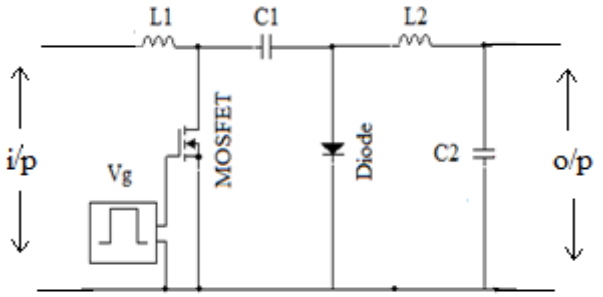

Fig.3.17 MPPT converter (Cuk topology).

3.4.1 Converter Design

The design equations (3.18 to 3.27) for Cuk converter (Rashid 2004) are given below.

$$V_0 = -\frac{D_r}{(1-D_r)} V_1 \quad (3.18)$$

$$I_1 = \frac{D_r I_o}{(1-D_r)} \quad (3.19)$$

$$\Delta I_{L1} = \frac{D_r V_1}{f L_1} \quad (3.20)$$

$$\Delta I_{L2} = \frac{D_r V_1}{f L_2} \quad (3.21)$$

$$\Delta V_{C1} = \frac{I_1(1-D_r)}{C_1 f} \quad (3.22)$$

$$\Delta V_{C2} = \frac{V_1 D_r}{8 C_2 L_2 f^2} \quad (3.23)$$

$$L_1 = \frac{D_r V_1}{f \Delta I_{L1}} \quad (3.24)$$

$$L_2 = \frac{D_r V_1}{f \Delta I_{L2}} \quad (3.25)$$

$$C_1 = \frac{I_1(1-D_r)}{\Delta V_{C1} f} \quad (3.26)$$

$$C_2 = \frac{V_1 D_r}{8 \Delta V_{C2} L_2 f^2} \quad (3.27)$$

where:

V_1: Input voltage (V); I_1: Input current (A); V_o: Output voltage (= V_a Load voltage) (V); I_o: Output current (= I_a, Load current) (A); D_r: Rated duty cycle; f: switching frequency (Hz);

ΔI_{L1}: Peak to peak ripple in current through L_1 (A)

ΔI_{L2}: Peak to peak ripple in current through L_1 (A)

ΔV_{C1}: Peak to peak ripple in voltage across C_1 (V)

ΔV_{C2}: Peak to peak ripple in voltage across C_2 (V)

Assuming: V_1 = 12 V; I_1 = 12.5 A; ΔI_{L1} = 0.1 A; ΔI_{L2} = 0.1 A; ΔV_{C1} = 1 V; ΔV_{C2} = 0.01 V; power capacity = 150 W; Switching frequency f = 20 kHz; Duty cycle range: 0.3 to 0.6. and using equations (3.24) to (3.27), the values of the different components are determined.

$L_1 = 4.2 \times 10^{-3}$ H; $L_2 = 7 \times 10^{-3}$ H; $C_1 = 400 \times 10^{-6}$ F; $C_2 = 40 \times 10^{-6}$ F.

3.4.2 Simulation Model of MPPT Converter

Simulation model for converter is developed (Fig.3.18) with the above design procedure as background. MOSFET is triggered by pulse generation block. Simulation is run with resistive load for different duty cycles applying an input voltage of 12 V d.c. Output voltage is noted. The simulation results are in close conformity with the experimental values (Fig. 3.19) validating the simulation model developed for the MPPT converter.

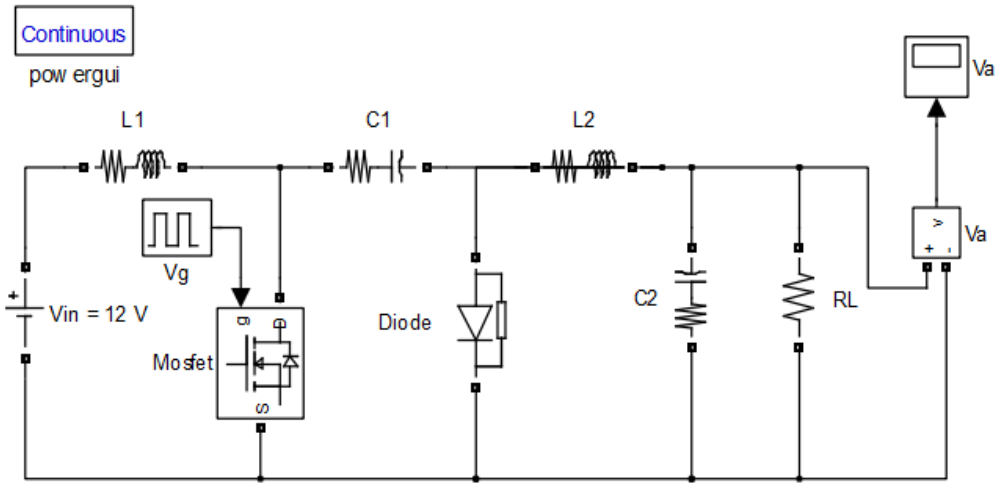

Fig 3.18 Simulation model for Cuk converter (with R load).

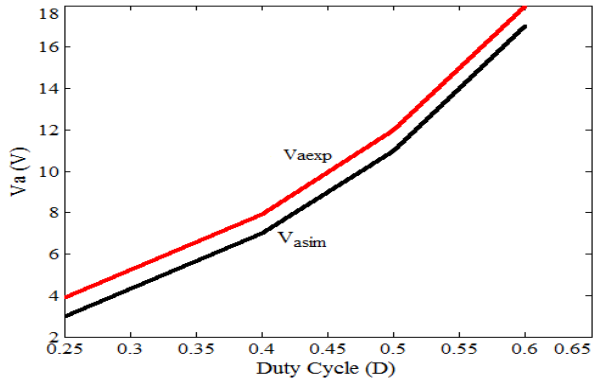

Fig.3.19 "D vs. V_a" characteristics for MPPT converter.

3.5 SIMULATION OF SYSTEM WITHOUT MPPT CONVERTER

With the help of basic component models presented in the earlier sections, different system models are developed. In this section, simulation model of the system with motor-pump connected directly to the solar panel (Fig.3.20) is developed (Fig.3.21). This configuration is also referred to as direct connected system as there is no MPPT converter.

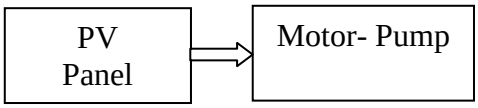

Fig.3.20 Direct connected solar pump.

Input required for this model is the information of radiation and the same is given in terms of I_{ph}. The output parameters are current & voltage for panel as well as motor (I_p= I_a, V_p= V_a); motor speed (ω) & torque (T). The simulation is run for different I_{ph} and plots of speed and output power as a function of I_{ph} are obtained (Fig.3.22).

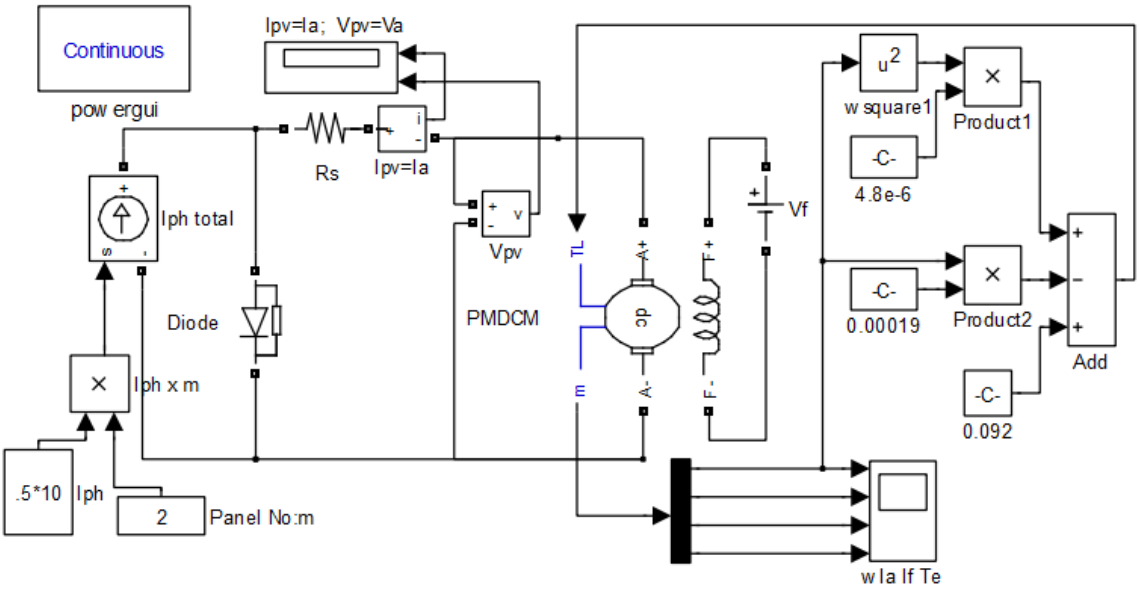

Fig.3.21 Simulation setup for solar pump without MPPT converter.

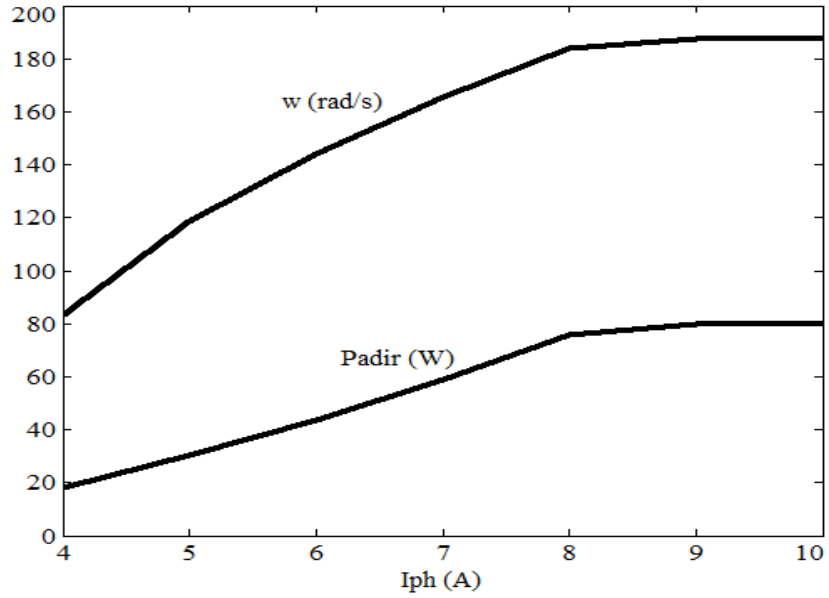

Fig.3.22 "I_{ph} vs. ω, P_{adir}" for solar pump without MPPT converter (Simulation).

3.6 SIMULATION OF SYSTEM WITH MPPT CONVERTER

In this section, simulation model of the system (Fig.3.1) "motor-pump connected to the solar panel through MPPT converter" is developed (Fig.3.23). The Inputs required for this module are: a) Radiation level (given in terms of I_{ph}). b) Duty cycle D for converter. The output parameters are: panel current & voltage (I_p, V_p), Motor current & voltage (I_a, V_a), Motor speed & torque (ω, T).

Maximum Power Point Tracking with panel power as reference ($MPPT_{PP}$)

In this section, the role of MPPT converter is demonstrated. For realising MPPT, non interruptive approach of tracking panel power is employed. In other words, panel power is taken as the reference. Such an approach can be referred to as $MPPT_{PP}$. This is more commonly employed at present. Using model in Fig. 3.23, the simulation is run for different I_{ph}. This means, at each radiation, duty cycle D is varied till panel power becomes maximum and corresponding power & speed values are noted. The plot of maximum power and speed as a function of I_{ph} is obtained (Fig.3.24).

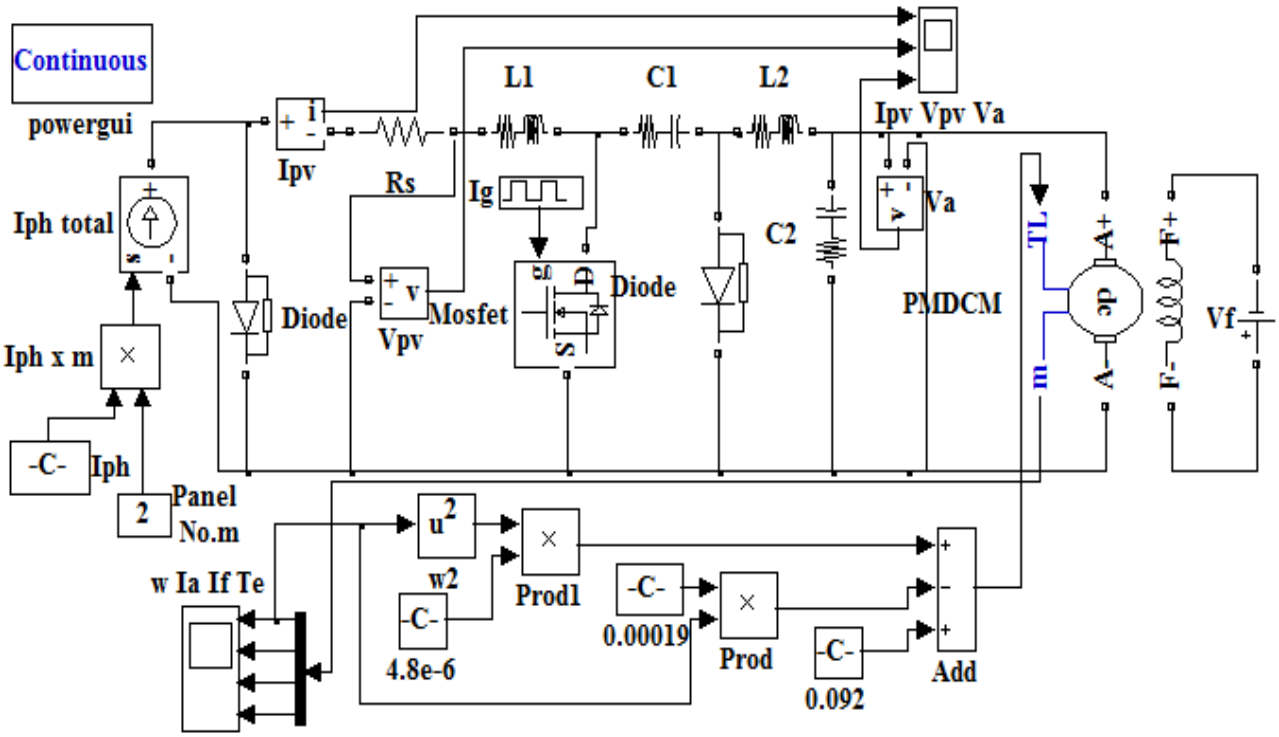

Fig.3.23 Simulation setup for solar pump with MPPT converter.

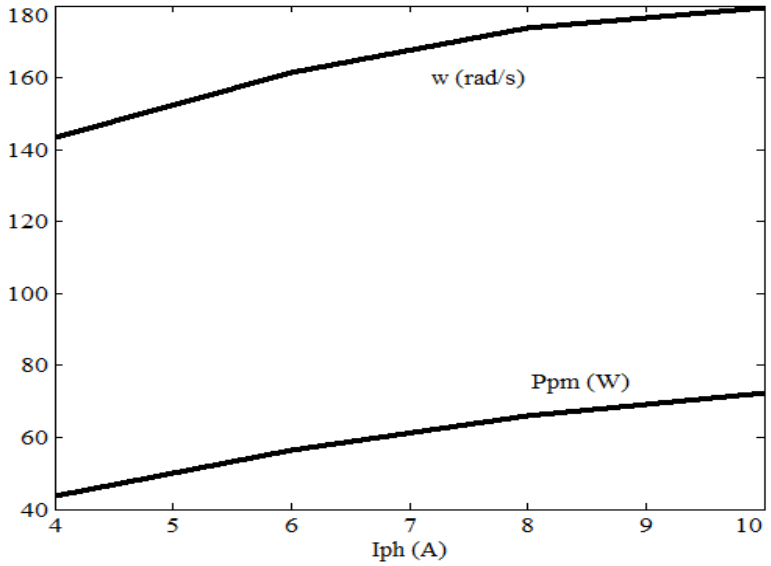

Fig.3.24 "I_{ph} vs. ω, P_{pm}" for solar pump with MPPT converter for $MPPT_{PP}$ (Simulation).

From the simulation work done, "I_{ph} vs. ω" and "I_{ph} vs. P" characteristics for both the cases (direct & with $MPPT_{PP}$) are given in Table 3.4 and plotted together (Fig.3.25 & 3.26). It is observed that output power & hence the speed (useful mechanical output power) is enhanced by employing MPPT converter. This feature is quite considerable at lower radiation values and decreases as radiation increases.

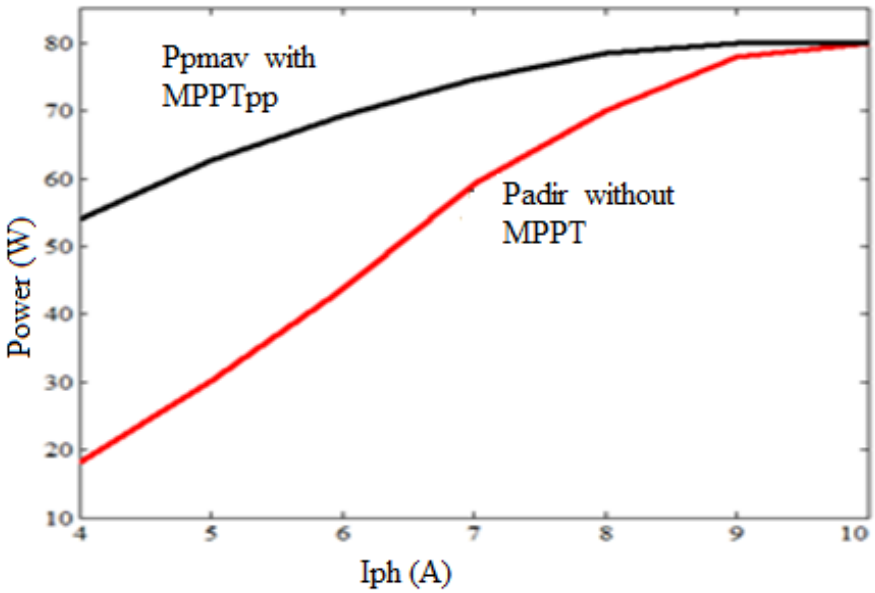

Fig.3.25 "I_{ph} vs. P" comparison for solar pump with $MPPT_{pp}$ & without MPPT (Simulation).

Table 3.4 Solar pump without MPPT and with $MPPT_{pp}$: Simulation results.

I_{ph} (A)	**without MPPT**		**with $MPPT_{pp}$**		
	P_{dir} (W)	**ω_{dir} (rad/s)**	**P_{mpp} (W)**	**P_{ampp} (W)**	**ω_{mpp} (rad/s)**
4	18.1	83.5	54.1	36.6	128
5	30.2	118.5	62.7	44	142
6	43.8	144.3	69.3	52.9	158
7	**60**	**160**	**74.7**	**61**	**165**
8	70	170	78.5	63	171
9	78	178	79.9	66	177
10	79.9	180	79.9	68.7	179

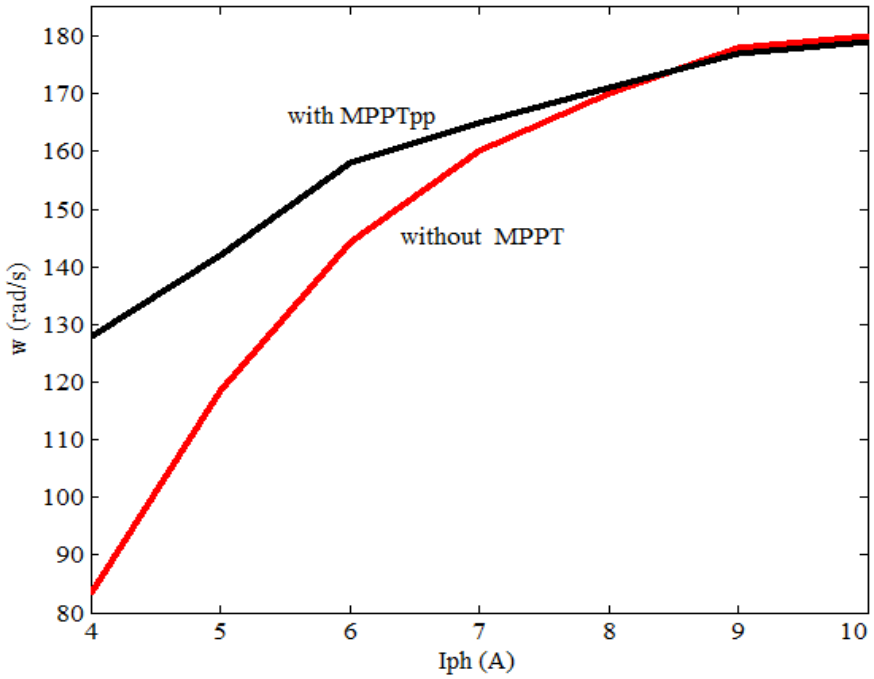

Fig.3.26 'I_{ph} vs. ω' comparison for solar pump with $MPPT_{pp}$ & without MPPT (Simulation).

Calculation of increase in output:

From the above simulation results, calculations are done to find increase in power and hence water yield from the pump. For this, sunshine availability on a typical day (Table 3.5) is considered which is found experimentally for the PV source. Assuming the current values at the starting of the hour to remain constant for that hour, I_{ph} availability can be put as in Table 3.6.

Without MPPT: Information from Table 3.4 & 3.6 is used while doing these calculations.

Energy generated & used / day = sum of product of power and duration at each I_{ph}

=18.1 x 2 + 30.2 x 1 + 43.8 x 2 + 60 x 1

= 214 Wh

Table 3.5 Typical sun shine over a day (Experimental).

Time of day	**I_{ph} (A)**	**Approximated I_{ph} (A)**
9 am	1.4	1
10 am	2.7	2
11 am	4.3	4
12 noon	5.9	5
1 pm	6.5	6
2 pm	7.0	7
3 pm	6.3	6
4 pm	4.8	4
5 pm	2.2	2
6pm	1.4	1

Table3.6 Availability of I_{ph} over a day (Experimental).

I_{ph} (A)	**Hours over a day (h)**
1	2
2	2
4	2
5	1
6	2
7	1

For the pump to lift water through a head of 4 m, minimum power required is 60 W. This is available when I_{ph} = 7A and the same is present for 1 h. Pump runs at 160 rad/s and corresponding flow rate is found to be 0.084 L/s from Fig. 3.12.

Water lifted = Duration (s) x Flow rate (L/s)

= 1 x 3600 x 0.084 = 302.4L

Since the solar PV source capacity is 148 W_p,

Water/ Watt of panel rating = 302.8/148 = 2.0 L/Wp

Assuming solar panel cost as Rs.110 per watt, upfront panel cost per unit volume of water lifted is = panel cost/water lifted = (110 x 148)/302.4 = Rs 53.8

With $MPPT_{pp}$: The same approach as followed for the case without MPPT converter explained above is followed here also. Enhancements are found comparing the values with the case without MPPT converter.

Energy generated / day = 54.1 x 2 + 62.7 x 1 + 69.3 x 2 + 74.7 x 1 = 384.2 Wh

Increase in generated energy = (384.2 - 214)/ 214 = 79.5 %

Energy used / day = 36.6 x 2 + 44 x 1 + 52.9 x 2 + 61 x 1 = 284 Wh

Increase in energy actually used = (284 - 214)/ 214 = 32.7 %

Minimum required power 60 W is available when I_{ph} = 7A and the same is present for 1 h. Pump runs at 165 rad/s and the corresponding flow rate is found to be 0.095 L/s using Fig. 3.12.

Water lifted = 1 x 3600 x 0.095 = 342 L.

% Increase in water harnessed = [(342-302.4)/302.4] x 100 = 13 %.

Water/Watt = 342/148 = 2.3 L/Wp

% Increase in water / watt = (2.3 - 2) / 2 = 13%.

Upfront panel cost per unit volume of water lifted = panel cost/water lifted = (110 x 148)/342 = Rs 47.6

3.7 IMPORTANT RESULTS FROM THIS CHAPTER

Through simulation testing, this chapter has demonstrated the role of MPPT converter in enhancing the output of solar pump. The method employed for MPPT is by tracking panel power ($MPPT_{pp}$). For the solar pump considered, it is found from simulation that:

- Increase in energy used per day is 32%.
- Increase in water harnessed is 13%.
- Increase in water harnessed / watt is 13%.

These benefits will be more pronounced when the insolation levels increase.

CHAPTER 4

NEW METHOD PROPOSED FOR SOLAR PUMPING: MPPT BY LOAD VOLTAGE TRACKING ($MPPT_{lv}$)

In this chapter, a new method developed for MPPT for solar pumping namely "MPPT by load voltage tracking ($MPPT_{lv}$)" is presented. Explanation for the new proposal is provided considering the resistive load first and then the motor-pump load. In each case theoretical background is given followed by results from simulation as well as experimental testing. An algorithm is also developed to show the performance of the proposal during continuously varying solar radiation.

Four papers are published covering some of the aspects of this chapter (Sl. No. 4, 8, 12 and 13 in the list of publications, pages: 154-156).

NEW PROPOSAL MADE:

An introspection and analysis of the V-I and V-P characteristics of the PV system with MPPT converter reveals an interesting feature. As the operating point is shifted from open circuit point to short circuit point on V-I characteristics by changing D, it is observed that:

- Panel voltage continuously decreases.
- Power drawn by the load increases first and then decreases.
- Corresponding load voltage Va also increases first and then decreases. Load power becomes maximum when the load voltage becomes maximum. This means for a particular radiation, there exists a specific motor voltage at which output power becomes maximum.

With this as the background, the new proposal is made as:

- Maximum load power P_a corresponds to maximum load voltage V_a.
- It is proposed to **employ load voltage V_a as a control parameter for varying the duty cycle of the converter in achieving MPPT**.

- V_a is to be continuously monitored and D continuously varied so as to realise maximum V_a which automatically ensures maximum output power at the corresponding radiation.
- This approach can be referred to as Maximum Power Point Tracking by load voltage tracking ($MPPT_{lv}$). It is basically a non interruptive approach. Here only one parameter i.e. V_a, needs to be monitored.
- $MPPT_{LV}$ is simpler than the maximum power point tracking by panel power tracking ($MPPT_{PP}$). Because in $MPPT_{PP}$ panel power P_p is monitored which requires monitoring V_p as well as I_p and then multiplying them to get P_p.
- In addition to making the control process simple, $MPPT_{lv}$ also gives higher output power as compared to $MPPT_{pp}$.

$MPPT_{lv}$ aims at making load power maximum. $MPPT_{pp}$ aims at making the panel power maximum anticipating the load power will also become more. The two approaches though look to be the same, are not so. Maximum panel power need not necessarily mean maximum load power. The amount of load power realized depends on the operating point on the PV curve and the efficiency of MPPT converter. The approach has to be to make the load power more rather than making the panel power more. Hence, in principle $MPPT_{lv}$ is superior to $MPPT_{pp}$. At the end of the day, what matters is the quantity of load power and hence the useful output realised. Otherwise the very purpose of MPPT is not served well.

4.1: NEW PROPOSAL $MPPT_{lv}$: SYSTEM WITH RESISTIVE LOAD

4.1.1 Theoretical Background:

The system with resistive load R along with other components like PV source and MPPT converter is considered (Fig.4.1). The converter (step down & step up) acts like a transformer with a transformation ratio $y = D/(1-D)$. The parameters can be referred from one side to the other as in the case of a transformer. Let R', V_a' & I_a' be the values of R, V_a & I_a respectively referred to panel side (Fig.4.2).

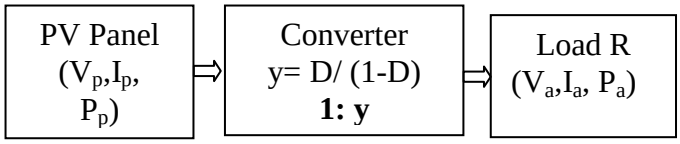

Fig.4.1. R load with MPPT converter.

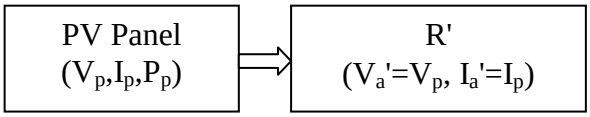

Fig.4.2. Load referred to panel side.

For this system the following equations can be written:

$$y = \frac{D}{(1-D)} \quad (4.1)$$

$$V_a = y\, V_p \quad (4.2)$$

$$y = V_a / V_p = I_p / I_a \quad (4.3)$$

Using equality of power,

$$I_p^2 R' = I_a^2 R \quad (4.4)$$

$$R' = (I_a / I_p)^2 R \quad (4.5)$$

$$R' = \frac{R}{y^2} \quad (4.6)$$

$$P_p = V_p\, I_p \quad (4.7)$$

$$P_a = V_a\, I_a \quad (4.8)$$

Assuming 100% efficiency for converter,

$$V_p\, I_p = \frac{V_p^{\,2}}{R'} = P_p = V_a\, I_a = \frac{V_a^{\,2}}{R} = P_a \quad (4.9)$$

$$V_a = \sqrt{P_a}\ \sqrt{R} = \sqrt{P_p}\ \sqrt{R} \quad (4.10)$$

$$V_a \propto \sqrt{P_a} \quad (4.11)$$

Hence theoretically, equations (4.10) and (4.11) indicate that V_a follows variations of P_a and P_p. As per the typical "V_p vs. P_p" characteristics (Fig. 2.2), P_p rises from zero, reaches maximum and decreases to zero. So do P_a and V_a. Thus V_a becomes maximum when P_a becomes maximum. Conversely, maximum load power P_a corresponds to maximum load voltage V_a. The equations derived above are applicable to motor-pump load also.

To establish validity of equation (4.11), an actual PV source is taken with the specifications as given in section 3.2. "V_p vs. I_p" characteristic is obtained experimentally at a radiation corresponding to I_{sc} = 5.8 A (Fig. 4.3). Pure resistance R = 2 Ω is considered as load. Using equation (4.6), R' is calculated for different values of D. By superimposing R' lines on the "V_p vs. I_p" plot of Fig. 4.3, different operating points (V_p, I_p) are obtained. With these, V_a, I_a, & P_p are obtained using equations (4.2), (4.3) & (4.7) and tabulated (Table 4.1). Plot of "D vs. V_a, P_a" (Fig. 4.4) shows that, with change in D, as load voltage V_a increases (decreases), load power P_a also accordingly increases (decreases). P_a becomes maximum when V_a becomes maximum. This is in accordance with equation (4.11).

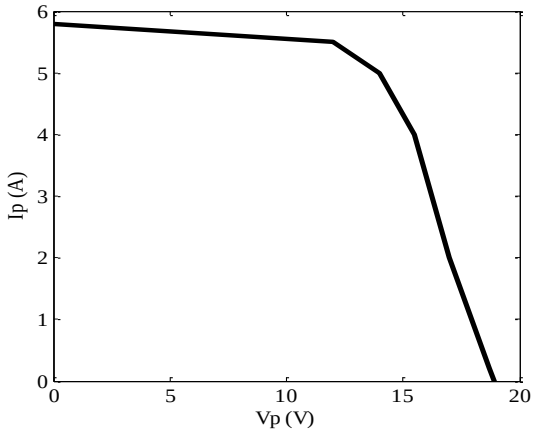

Fig.4.3 "V_p vs. I_p"of 148 W_p PV source (Experimental).

Table 4.1 Values derived from practical "V_p vs. I_p" characteristics for system with MPPT converter & R load at I_{sc} = 5.8 A.

D(%)	30	35	40	45	50	55
y =D/(1-D)	0.42	0.53	0.66	0.81	1.0	1.22
R' $=R/y^2$ (Ω)	11.3	7.1	4.5	3.0	2.0	1.34
$\mathbf{V_p}$ (V)	17.5	16.8	16.0	14.6	10.3	6.5
$\mathbf{I_p}$ (A)	1.5	2.3	3.5	4.4	5.1	5.2
$\mathbf{P_p}$ $=V_pI_p$ (W)	27.1	38.6	56	64.2	52.5	33.8
$\mathbf{V_a}$ $=yV_p$ (V)	7.35	8.9	10.5	**11.8**	10.3	7.9
$\mathbf{I_a}$ $=I_p/y$ (A)	3.6	4.3	5.3	5.4	5.1	4.26
$\mathbf{P_a}$ $=V_aI_a$ (W)	26.4	38.2	55.6	**63.7**	52.5	33.6

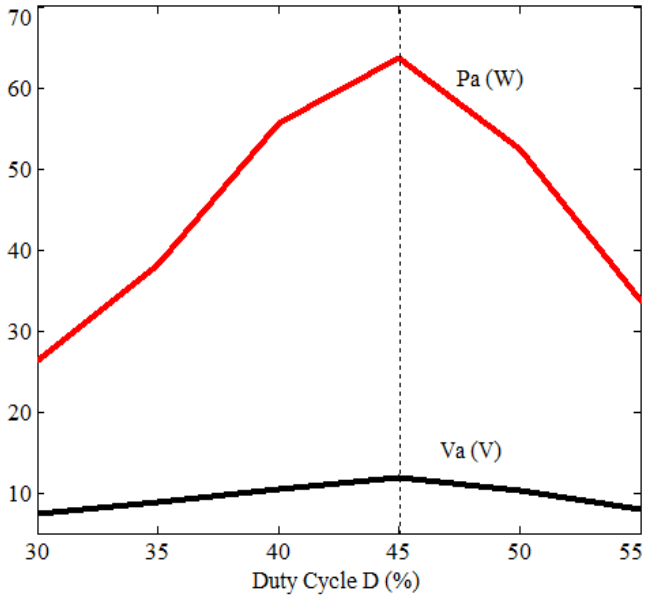

Fig. 4.4 "D vs. V_a, P_a" for R load (Theoretical).

4.1.2. Simulation Testing

This section deals with the simulation of PV system with the MPPT converter and R load (Fig.4.5).

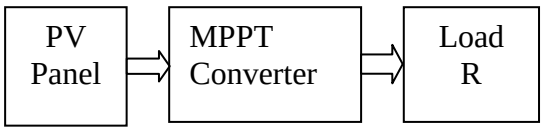

Fig.4.5 PV System with R load.

The simulation setup for the entire system is shown in Fig.4.6. Inputs required for this model are radiation level (given in terms of I_{ph}) and duty cycle D for converter. The output parameters are: I_p, V_p, I_a, V_a. The simulation is run for different I_{ph} and at each radiation for different values of D. The plots of load voltage (Fig.4.7) and load power (Fig.4.8) as a function of D are obtained. It is observed that at each radiation, power becomes maximum when the voltage V_a is maximum.

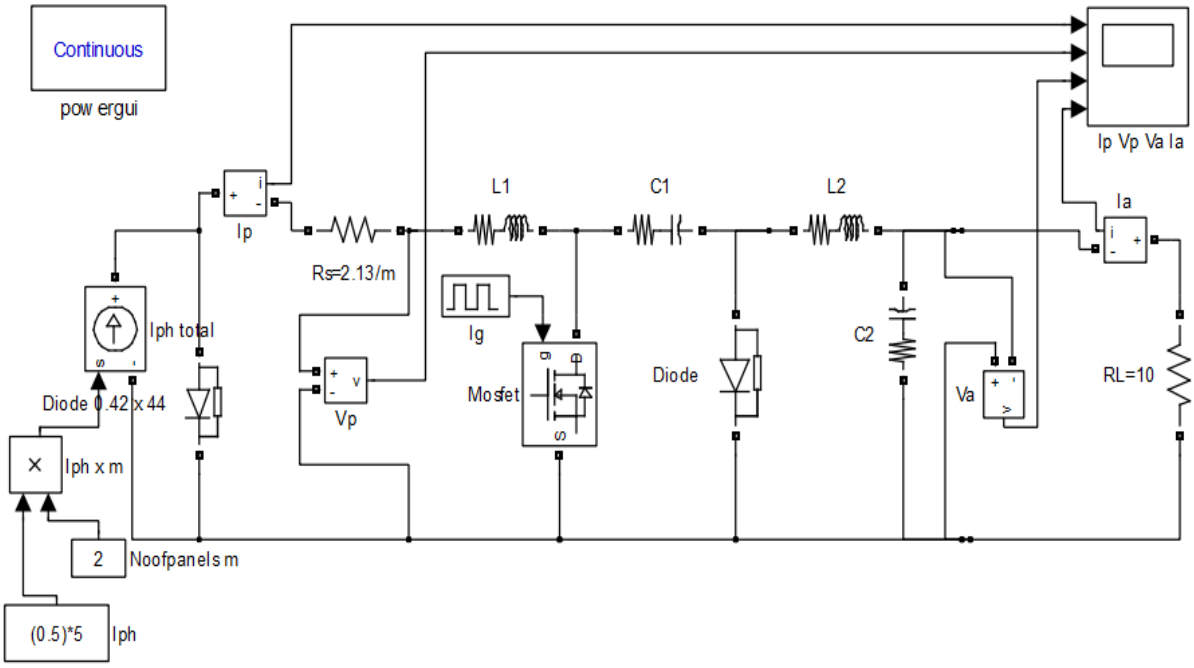

Fig.4.6 Simulation model for system with R load and MPPT converter.

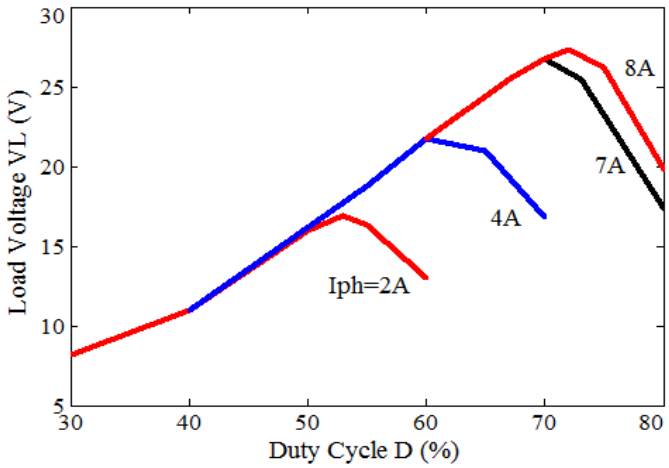

Fig.4.7 "Duty cycle vs. Load voltage" for R load with MPPT converter (Simulation).

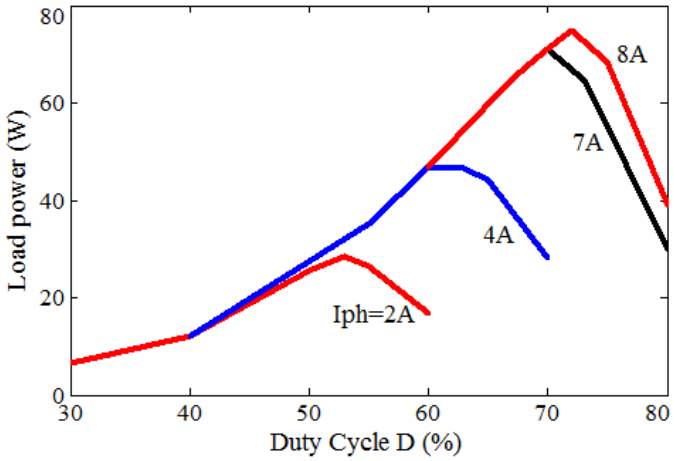

Fig.4.8 "Duty cycle vs. Load power" for R load with MPPT converter (Simulation).

Further, the simulation testing is done for the same I_{ph} values without MPPT converter and the power to load is found as a function of hour of day by mapping I_{ph} values onto hours of the day referring to experimental readings (Table 4.2).

Then the simulation is carried out with MPPT employing both $MPPT_{pp}$ & $MPPT_{lv}$ and the values of power are determined (Table 4.3 & 4.4). With these results different powers are plotted as a function of hour of day (Fig. 4.9). It is observed that power (P_{dir}) obtained with direct connection is less. Actual load power obtained employing MPPT is more. In that too, the load power P_{amlv} obtained with $MPPT_{lv}$ is more than the load power P_{ampp} obtained with $MPPT_{pp}$. However maximum available panel power P_{pmav} is more than the actual load powers.

Table 4.2. R load without MPPT (Simulation).

Time of Day	**Maximum available panel power P_{pmav} (W)**	**Power to load (without MPPT) P_{dir} (W)**
10.5	57	28.4
12.25	73	--do--
13	73	--do--
14.4	57	--do--
15.75	33	--do--
17.25	33	--do--

Table 4.3. $MPPT_{pp}$ for R load (Simulation).

Time of Day	**With $MPPT_{pp}$**	
	Maximum power generated by panel P_{pmpp} (W)	**Power to load at maximum power of panel P_{ampp} (W)**
10.5	56.4	44.1
12.25	72.2	63
13	72.2	63
14.4	56.4	44.1
15.75	32.4	16.9
17.25	32.4	16.9

Table 4.4 $MPPT_{lv}$ for R load (Simulation).

Time of Day	**With $MPPT_{lv}$**	
	Power generated by panel at maximum V_a P_{pmlv} (W)	**Power to load at maximum V_a P_{amlv} (W)**
10.5	49.5	47
12.25	67.4	65
13	67.4	65
14.4	49.5	47
15.75	31.9	28.5
17.25	31.9	28.5

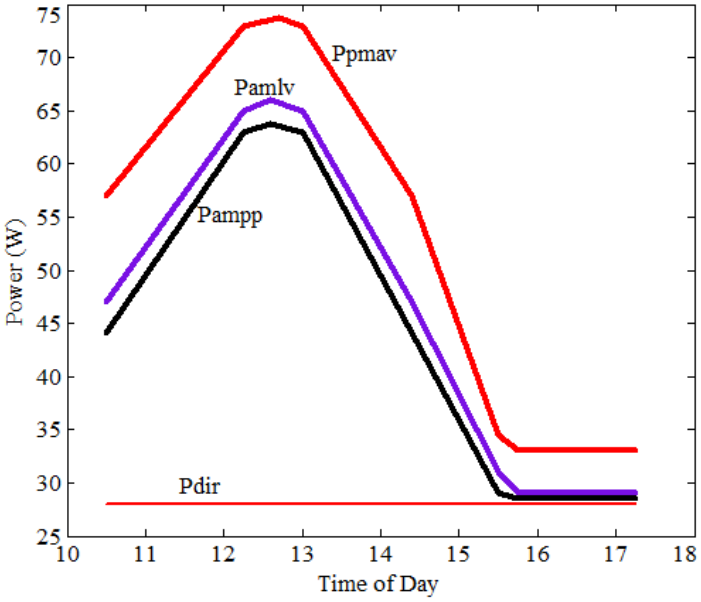

Fig. 4.9. "Hour of day vs. Different powers" for R load (Simulation).

4.1.3. Experimental Testing

The experimental setup is an open loop system. It consists of the PV source, MPPT converter and the resistive load connected as per the circuit diagram in Fig. 4.10. Necessary meters are added for measuring currents and voltages. The actual set up is shown in Fig.4.11. Load resistance is taken as 10 Ω. PV source and MPPT converter are taken with specifications mentioned in section 3.2 & 3.4.

MOSFET taken is PJ5NF06; 50 A, 60 V (device details given in Appendix III). The triggering signals for MOSFET are obtained by Pulse Width Modulated (PWM) Signal Wave Generator. These signals are strengthened by MOSFET driver IR 2110 (Appendix IV) and then applied to MOSFET gate. Diode module DF400 is taken. Practical component values employed for MPPT converter are: $L_1 = L_2 = 1$ mH, 0.1 Ω.; $C_1 = C_2 = 100 \times 10^{-6}$ F.

First the load is connected directly to panel and the voltage & current readings are taken. Then the load is connected through the MPPT converter. The duty cycle of the MOSFET is varied and different parameters like D, V_p, I_p, V_a and I_a are noted. This procedure is repeated for different radiations i.e. times of the day.

The following characteristics are obtained: a) " Duty cycle vs. Load voltage " (Fig.4.15) b) " Duty cycle vs. Load power " (Fig.4.16). It is observed that at each radiation, power becomes maximum when the voltage V_a is maximum which validates the theoretical finding.

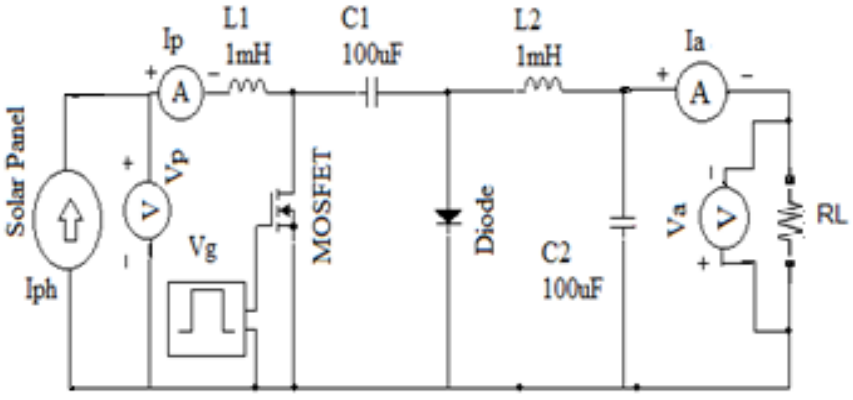

Fig. 4.10 Electric circuit for experimental testing (R load).

Fig.4.11 Experimental test set up for R load.

Fig.4.12 Solar PV panels used for experimentation.

Fig.4.13 Power Capacitors used for testing.

Fig.4.14 Inductors used for testing.

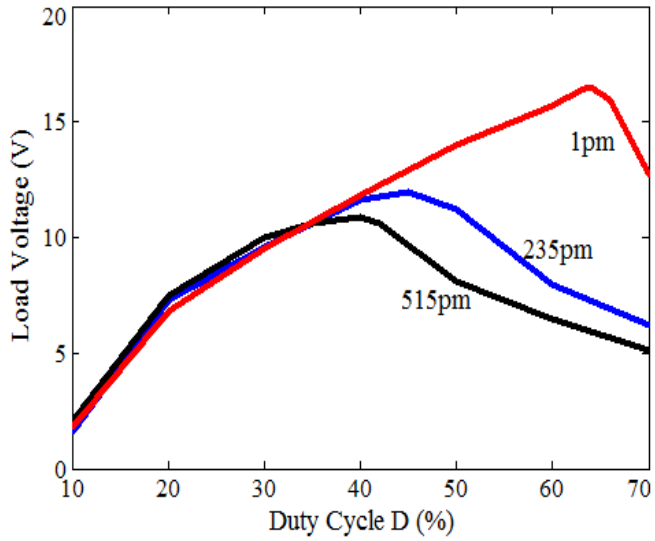

Fig.4.15 "Duty cycle vs. Load voltage" for R load with MPPT converter (Experimental).

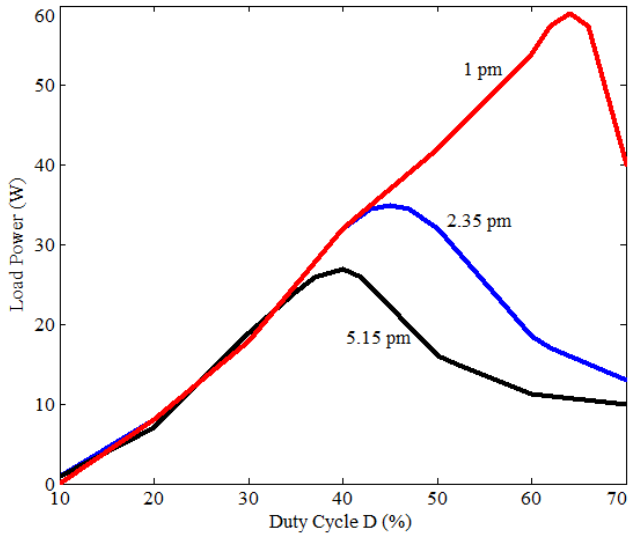

Fig. 4.16 "Duty cycle vs. Load power" for R load with MPPT converter (Experimental).

The experimentation is conducted at different hours of day. Each time, first the system without MPPT converter is considered and the values of power are noted (Table 4.5) and plotted (Fig. 4.17). Then the experimental testing is done with MPPT employing both $MPPT_{pp}$ and $MPPT_{lv}$. The values of power are noted (Table 4.6 & 4.7). With these results different powers are plotted as a function of hour of day (Fig.

4.18, 4.19 & 4.20). It is observed that power (P_{dir}) obtained with direct connection is less. Actual load power obtained employing MPPT is more. In that too, the load power P_{amlv} obtained with $MPPT_{lv}$ is more than the load power P_{ampp} obtained with $MPPT_{pp}$. However maximum available panel power P_{pmav} is more than the actual load powers.

Table 4.5. R load without MPPT (Experimental).

Time of Day	**Maximum available panel power P_{pmav} (W)**	**Power to load without MPPT P_{dir} (W)**
10.5	55	30.4
12.25	77	30.6
13	84	32
14.4	48	23.5
15.75	32.2	21.8
17.25	30	20

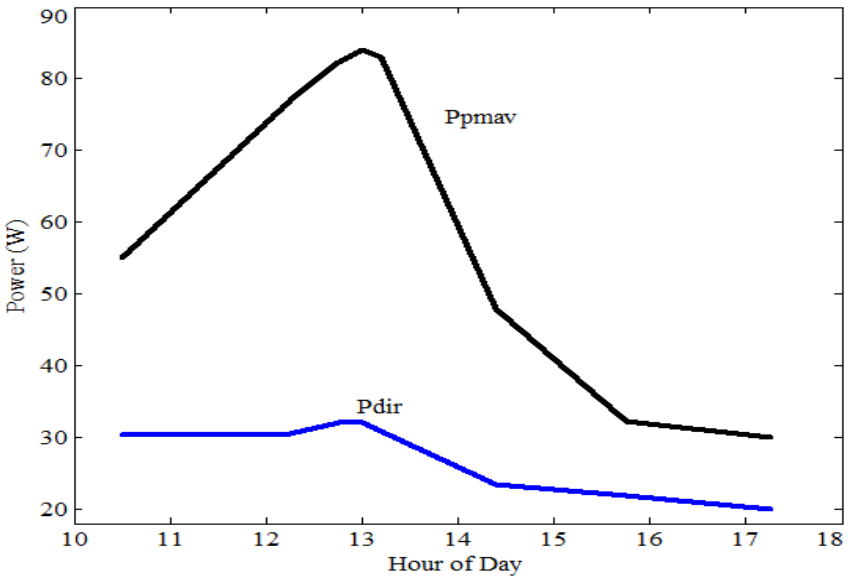

Fig.4.17 " Hour of Day vs. P_{pmav} & P_{dir} " R load without MPPT converter (Experimental).

Table 4.6. $MPPT_{PP}$ for R load (Experimental).

Time of Day	Maximum available panel power P_{pmav} (W)	With $MPPT_{pp}$	
		Maximum power generated by panel P_{pmpp} (W)	Power to load at maximum power of panel P_{ampp} (W)
10.5	55	50.2	45.18
12.25	77	72	46
13	84	70.1	40
14.4	48	45	27
15.75	32.2	32	23
17.25	30	30	21

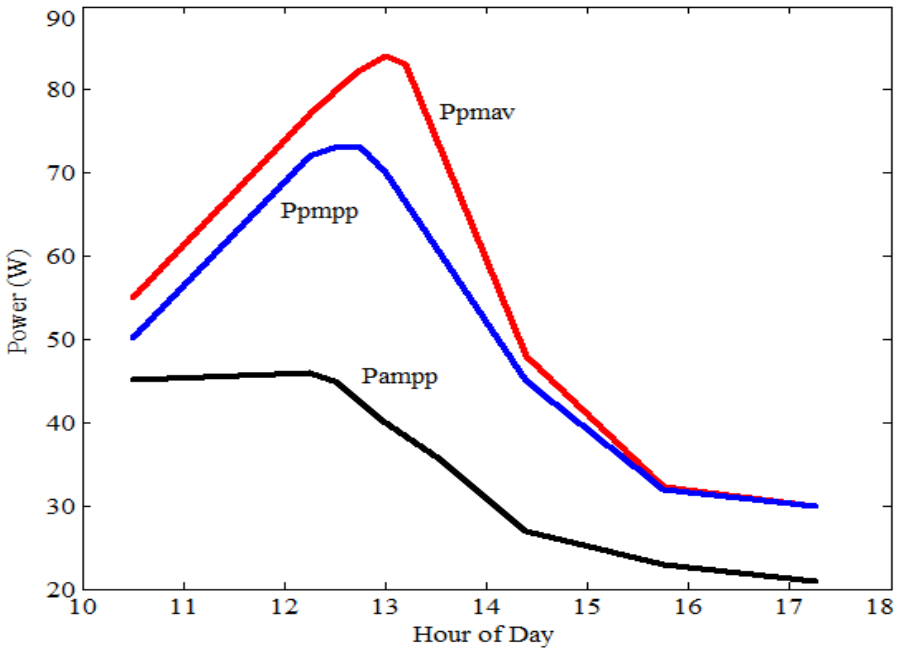

Fig.4.18 "Hour of day vs. P_{pmav} , P_{pmpp} & P_{ampp}" R load with MPPT converter employing $MPPT_{pp}$ (Experimental).

Table 4.7 $MPPT_{lv}$ for R load (Experimental).

Time of Day	Maximum available panel power P_{pmav} (W)	With $MPPT_{lv}$	
		Power generated by panel at maximum V_a P_{pmlv} (W)	Power to load at maximum V_a P_{amlv} (W)
10.5	55	50.2	45.18
12.25	77	61.18	55
13	84	64	59
14.4	48	40	32
15.75	32.2	32	23
17.25	30	30	21

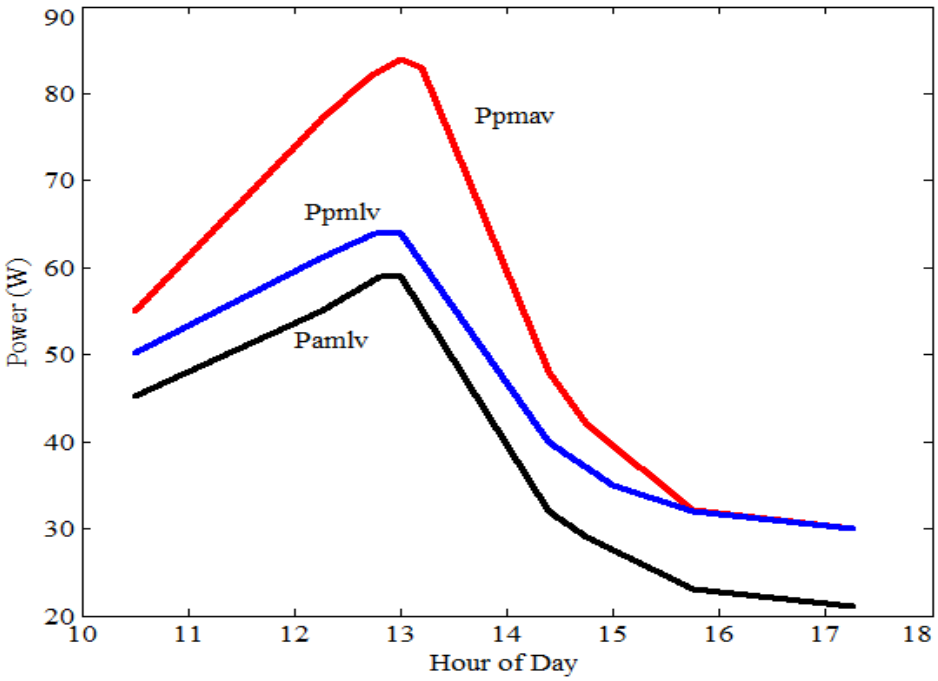

Fig.4.19 " Hour of day vs. P_{pmav}, P_{pmlv} & P_{amlv} " R load with MPPT converter employing $MPPT_{lv}$ (Experimental).

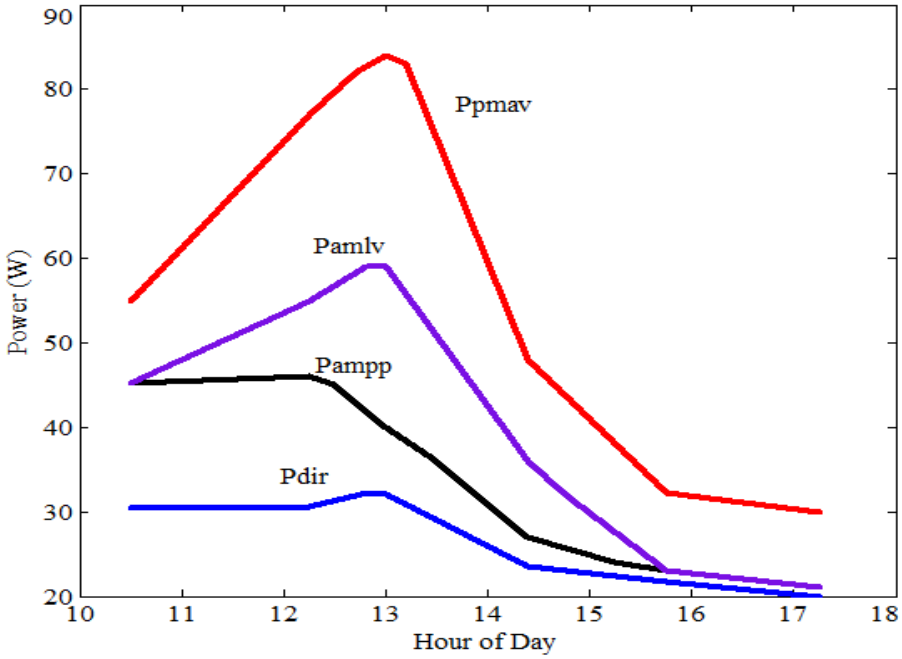

Fig.4.20 "Hour of day vs. P_{pmav}, P_{ampp}, P_{amlv} & P_{dir}" R load with MPPT converter (Experimental).

During experimentation, typical waveforms are observed (Fig. 4.21 to 4.24) and found to be in tune with theoretical patterns of a normal Cuk converter (Rashid 2004) thus validating the proper working of the MPPT converter. Fig 4.21 conveys the working of MOSFET as a switch. It can be observed that MOSFET is ON when the gate signal is high. Fig. 4.22 represents the capacitor (C_1) voltage. Fig. 4.23 shows the output voltage which is found to be almost constant as per the design expectation of the converter. Fig 4.24 represents the inductor (L_1) voltage. As expected, the time average of the inductor voltage over one cycle is zero.

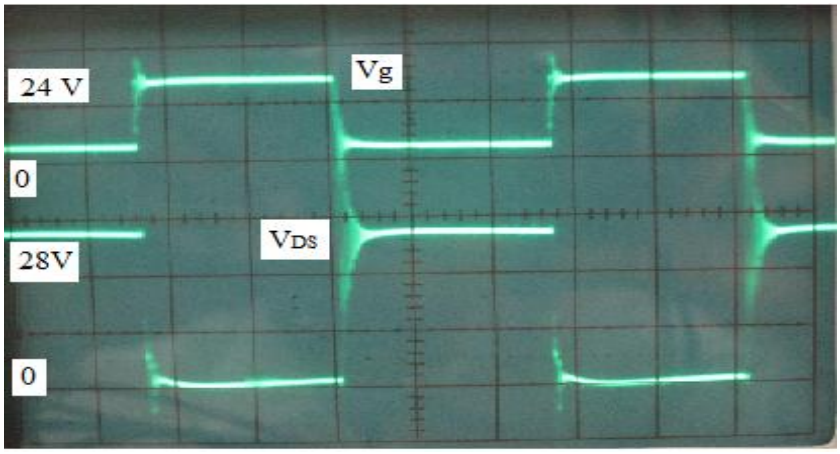

Fig.4.21 MPPT converter waveform (R load):

"Time vs. Gate voltage (V_g) and MOSFET voltage (V_{DS})".

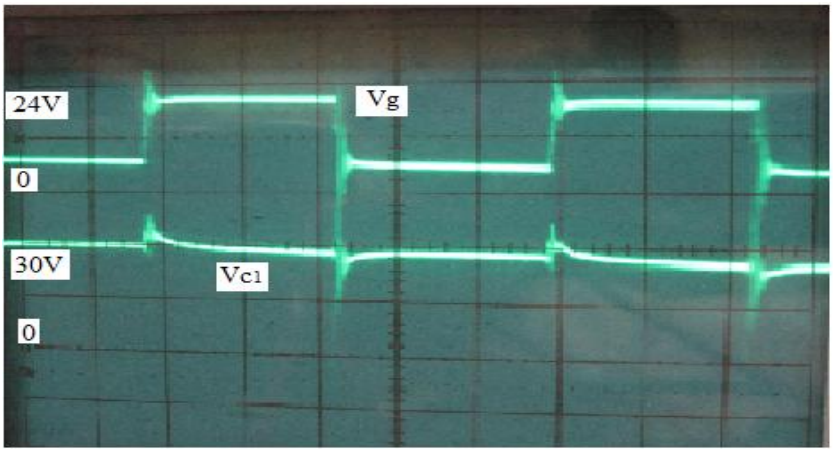

Fig.4.22 MPPT converter waveform (R load):

"Time vs. Gate voltage (V_g) and Capacitor (C_1) voltage (V_{C1})".

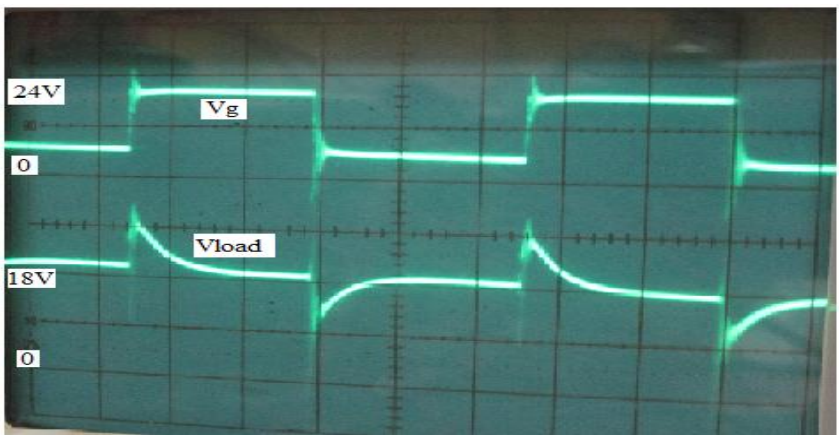

Fig.4.23 MPPT converter waveform (R load):

"Time vs. Gate voltage (V_g) and Load voltage (V_a)".

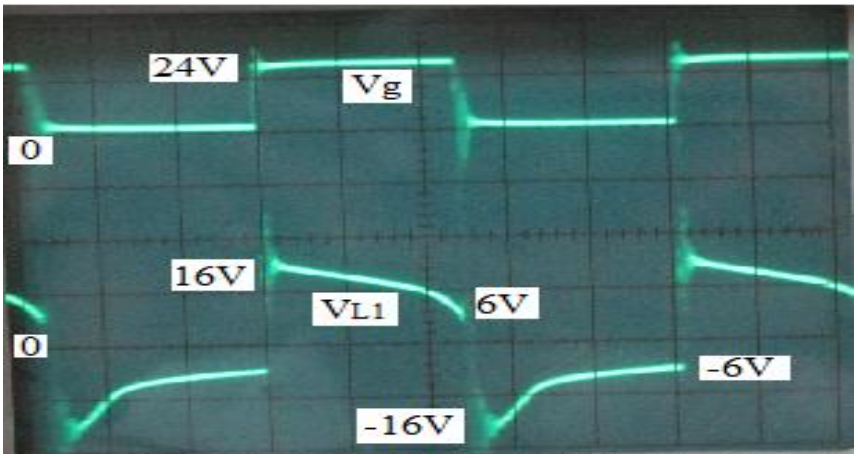

Fig.4.24 MPPT converter waveform (R load):
"Time vs. Gate voltage (V_g) and Inductor (L_1) voltage (V_{L1})".

4.2 NEW PROPOSAL $MPPT_{lv}$: SYSTEM WITH PUMP LOAD

4.2.1 Theoretical Background:

Here the system with solar PV source, MPPT converter and motor-pump load (4 m head) is considered (Fig 4.25). The pump load can be represented referred to panel side (Fig. 4.26). Proceeding in the same way as in section 4.1.1, the referred load equation (4.12) for pump is obtained using equation 3.16 of section 3.3.

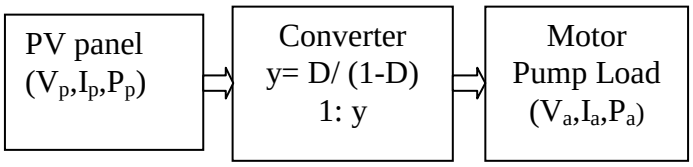

Fig.4.25 System with MPPT converter and pump load.

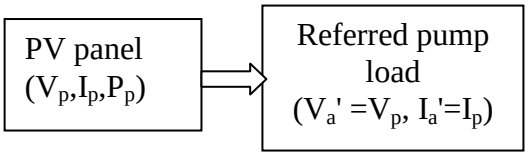

Fig.4.26 Pump load referred to panel side.

$$4.4y^2V_a'^2 - 5.75yV_a' - 6.17V_a'I_a' + 2.15\frac{I_a'^2}{y^2} - 36.9\frac{I_a'}{y} + 92 = 0 \qquad (4.12)$$

V_a'-I_a' curves are obtained for different D and then are superimposed with "V_p vs. I_p" curves of the PV source obtained experimentally at different radiations (Fig. 4.27). Intersection points are the operating points. It is observed from the plot that the operating points depend on the insolation level. They are also decided by the effective load impedance which is dictated by the value of switching duty cycle D of MPPT converter. Using these operating points, different plots such as "D vs. V_a" (Fig. 4.28) and "D vs. P_p" (Fig. 4.29) are plotted. It is found that at each radiation, panel power is maximum when V_a becomes maximum. V_a shows typical increase/decrease trend with the corresponding variations in P_p. This is valid with respect to load power P_a also assuming 100% efficiency for the converter as per the equation (4.9). Thus the theoretical inference "V_a follows variations of P_a" made for pure resistance load in section 4.1.1, is valid for pump load also.

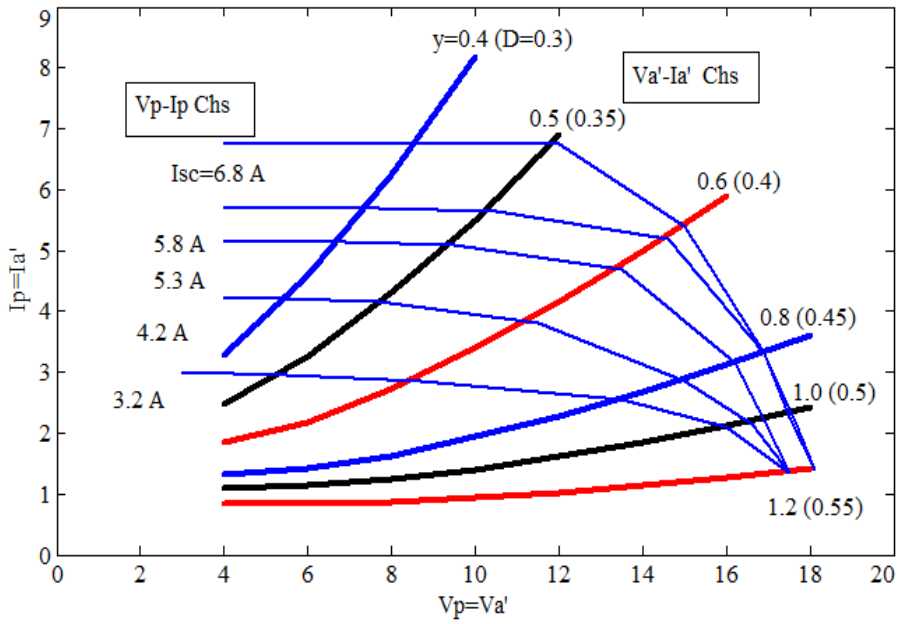

Fig.4.27 PV source and pump load characteristics superimposed.

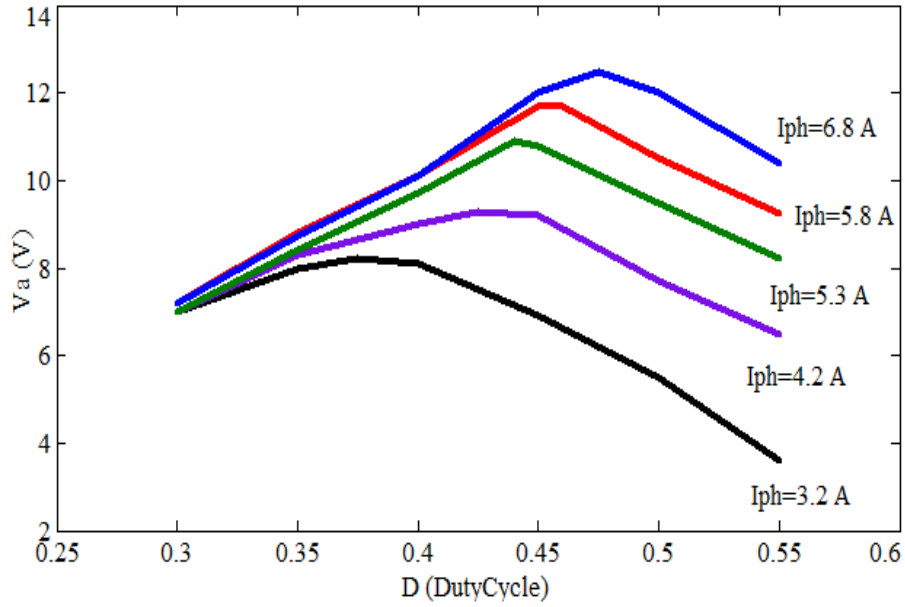

Fig.4.28. "Duty cycle vs. Load voltage" for pump load (Theoretical).

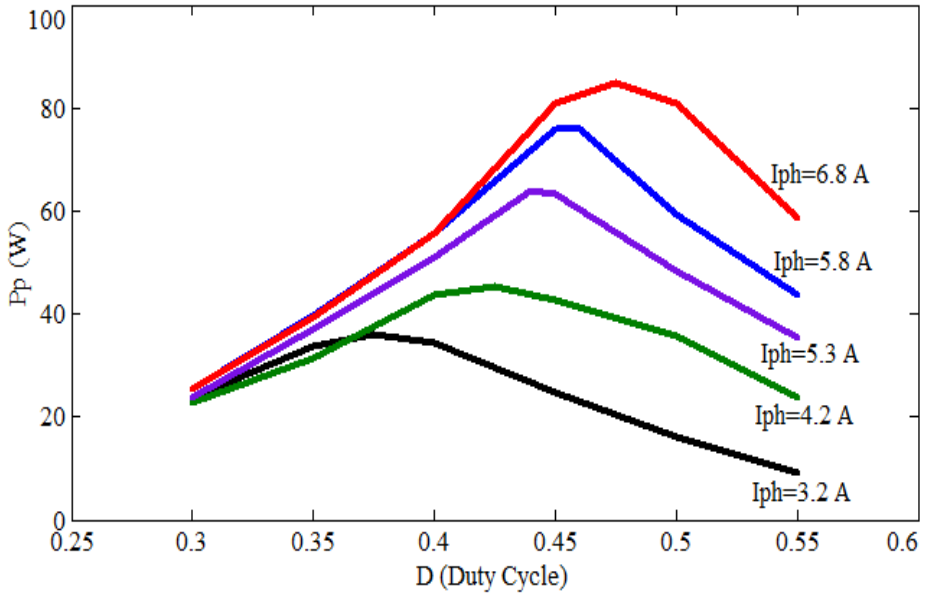

Fig.4.29 "Duty cycle vs. Panel power" for pump load (Theoretical).

4.2.2. Simulation Testing

The model developed for simulation testing is shown in Fig.4.30. Inputs required for this model are I_{ph} and D. The output parameters are: I_p, V_p, I_a, V_a, ω, and T. The simulation is run for different I_{ph} and at each radiation for different values of D. The plots of V_a (Fig.4.31) and P_a (Fig.4.32) as a function of D are obtained. It is observed that at each radiation, V_a shows 'increase-decrease' trend i.e. power becomes maximum when the voltage V_a is maximum.

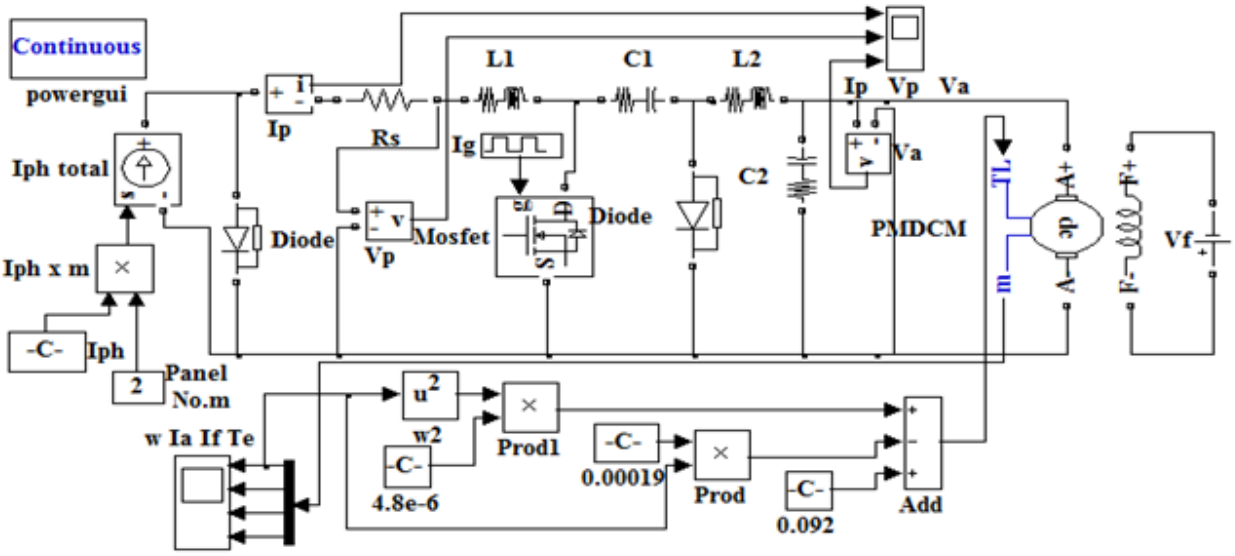

Fig.4.30 Simulation setup for pump load with MPPT converter.

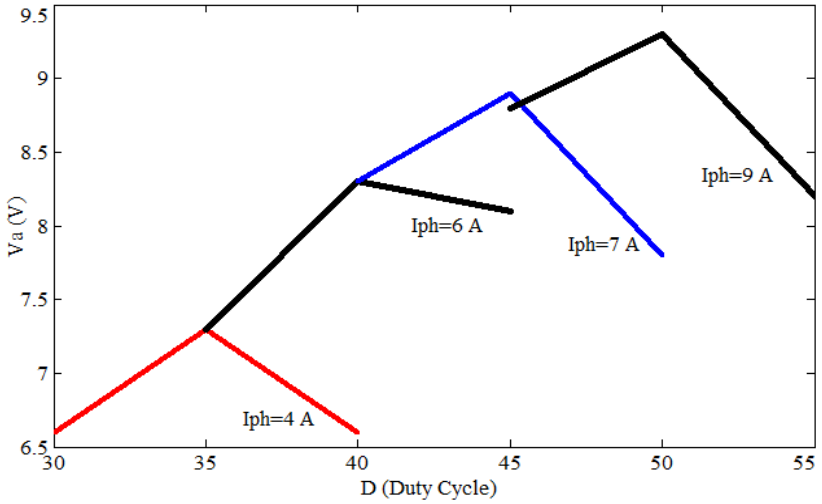

Fig.4.31 "Duty cycle (%) vs. Load voltage" for pump load with MPPT converter (Simulation).

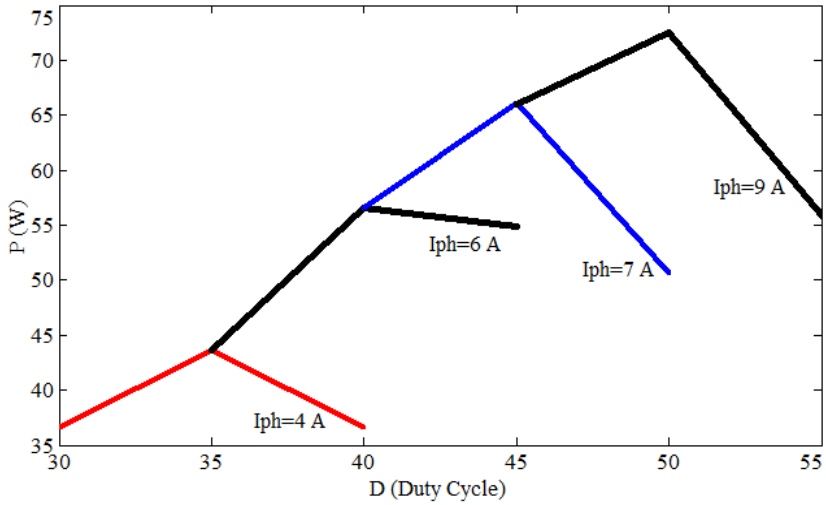

Fig.4.32 "Duty cycle (%) vs. Power" for pump load with MPPT converter (Simulation).

Further the simulation testing is done for these I_{ph} values without MPPT converter. Pump power and speed are determined (Table 4.8). Then the simulation testing is done with MPPT employing both $MPPT_{pp}$ and $MPPT_{lv}$ and the values of power and speed are found (Table 4.9). It is observed that power obtained and pump speed with direct connection is less.

With these results different powers (Fig. 4.33) and speeds (Fig. 4.34) are plotted. Actual load power obtained and pump speed are more when MPPT converter is employed. Also, the load power (P_{amlv}) and pump speed **(**ω_{mlv}) obtained with $MPPT_{lv}$ are more than the load power (P_{ampp}) and pump speed **(**ω_{mpp}) obtained with $MPPT_{pp}$.

Table 4.8 Solar pump without MPPT converter (Simulation).

I_{ph} (A)	**P_{dir} (W)**	**ω_{dir} (rad/s)**
4	18.1	83.5
5	30.2	118.5
6	43.8	144.3
7	60	160
8	70	170

Table 4.9 Solar pump with MPPT converter:

$MPPT_{pp}$ and $MPPT_{lv}$ (Simulation).

I_{ph} (A)	with $MPPT_{pp}$			with $MPPT_{lv}$	
	P_{mpp} (W)	P_{ampp} (W)	ω_{mpp} (rad/s)	P_{amlv} (W)	ω_{mlv} (rad/s)
4	54.1	36.6	128	43.6	143.3
5	62.7	44	142	55.8	160
6	69.3	52.9	158	62	161.6
7	74.7	61	165	66	173.7
8	78.5	63	171	69	173.9
9	79.9	66	177	72.5	179.8
10	79.9	68.7	179	74	179.5

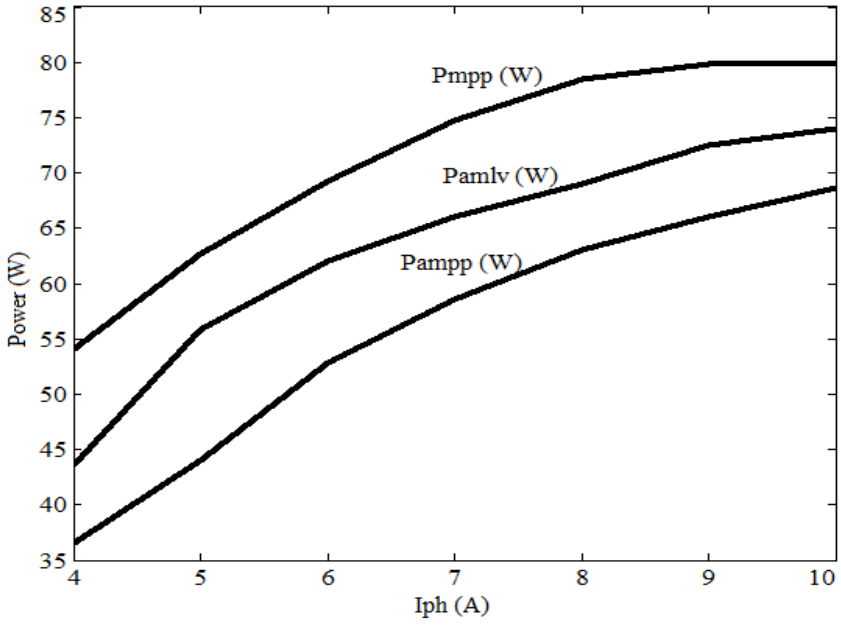

Fig. 4.33 "I_{ph} vs. Different powers" for solar pump with $MPPT_{pp}$ and $MPPT_{lv}$ (Simulation).

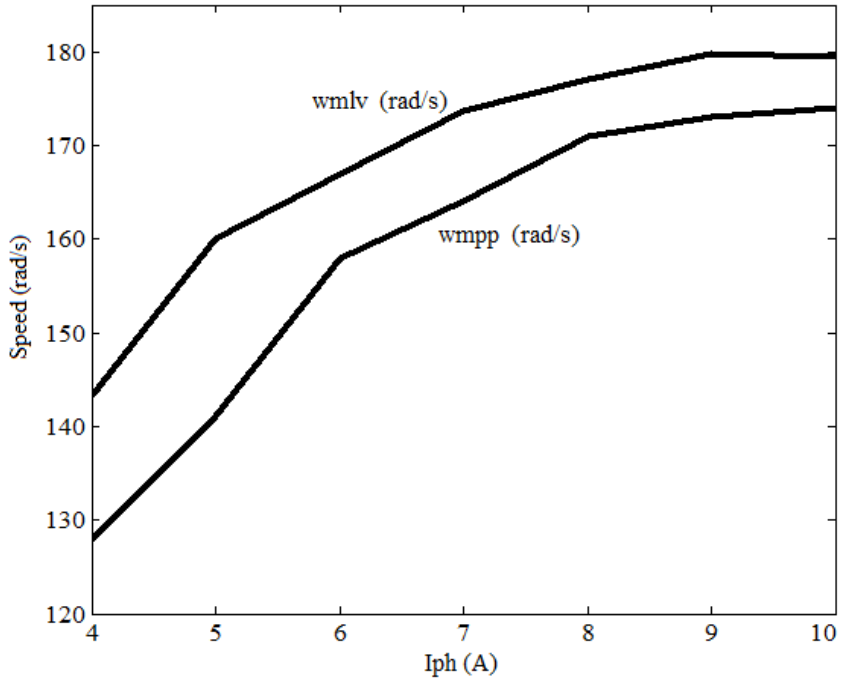

Fig.4.34 "I_{ph} vs. ω" for solar pump with $MPPT_{pp}$ and $MPPT_{lv}$ (Simulation).

Calculation of increase in output:

Here calculations are done to give an idea of the enhancements in power, speed and water yield. Though the simulation testing is done over a wide range of values for I_{ph}, it's better to select realistic insolations (i.e., I_{ph} values) and their duration over an entire day to get an idea of power spread over the day time. For this I_{ph} values are mapped onto hours of the day (Table 4.10) referring to experimentally obtained V-I characteristics of PV source. It can be determined how different insolations (I_{ph} values) on a typical day will translate in terms of energy harnessed and useful output.

Table 4.10 Duration of insolation.

I_{ph} (A)	**Duration (h)**
4	2
5	1
6	2
7	1

Without MPPT: Information from Table 4.8 & 4.10 is used while doing these calculations.

Energy generated (used)/ day = sum of product of power and duration at each I_{ph}.

= 18.1 x 2 + 30.2 x 1 + 43.8 x 2 + 60 x 1 = 214 W h

Minimum power to lift water for 4 m head is 60 W. This is available for 1 h at I_{ph}=7A.

Using the flow rate for the corresponding speed from Fig. 3.12,

Water lifted = Duration (s) x Flow rate (L/s) = 1 x 3600 x 0.084 =302.8 L

Since the solar PV source capacity is 148 W_p

Water/ Watt =302.8/148 = 2.0 L/W_p

Assuming solar panel cost as Rs. 110 per unit watt, upfront panel cost per unit volume of water lifted is = panel cost/water lifted = 148 x 110 / 302.8 = Rs 53.8

With $MPPT_{pp}$: Information from Table 4.9 & 4.10 is used while doing these calculations. The same approach as followed for the case without MPPT converter explained above is followed. Enhancements are found comparing the values with the case without MPPT converter.

Energy used / day = 36.6 x 2 + 44 x 1 + 52.9 x 2 + 61 x 1 = 284 W h

% Increase in energy used = (284-214)/214 = 32.7%

Minimum required power of 60 W is available for 1 h.

Water lifted = 1 x 3600 x 0.095 = 342 L.

% Increase in water harnessed = (342 - 302.8)/302.8 = 13 %.

Water/Watt = 342/148 = 2.3 L/W_p

% Increase in Water/Watt = (2.3 - 2)/ 2 = 13%

Upfront panel cost per unit volume of water lifted = (110 x 148)/342 = Rs 47.6

With $MPPT_{lv}$: Information from Table 4.9 & 4.10 is used while doing these calculations. The same approach as followed for the case without MPPT converter explained above is followed. Enhancements are found comparing the values with the case without solar pump.

Energy used / day = 43.6 x 2 + 55.8 x 1 + 62 x 2 + 66 x 1 = 333 W h

% Increase in used energy = (333 -214)/214 = 55.6%

Minimum required power 60 W is available when Iph = 6 A & 7 A.

6A is available for 2 h whereas 7A is available for 1 h.

Water lifted = 2 x 3600 x 0.085 + 1 x 3600 x 0.103 = 612 + 370.8 = 982.8 L.

% Increase in water harnessed = (982.8 - 302.8)/ 302.8 = 224%.

Water/Watt = 982.8/148 = 6.6 L/Wp

% Increase in Water/Watt = (6.6 - 2)/ 2 = 224%

Upfront panel cost per unit volume of water lifted = (110 x 148)/982.8 = Rs 16.5

It is clear from the above that there is increase in power and water yield when MPPT converter is employed. In that too, the gains with $MPPT_{lv}$ are more compared to those with $MPPT_{pp}$. It is also to be observed that, with $MPPT_{lv}$, there is remarkable decrease in cost per unit volume of water lifted.

4.2.3. Experimental Testing

Experimental test setup consists of the PV source, MPPT converter and the pump load connected as per the circuit diagram in Fig.4.35. Pump specifications are as in section 3.3 and the specifications of all other components are as mentioned in section 4.1.3. The pump and the overall set up are shown in Fig.4.36 & 4.37 respectively.

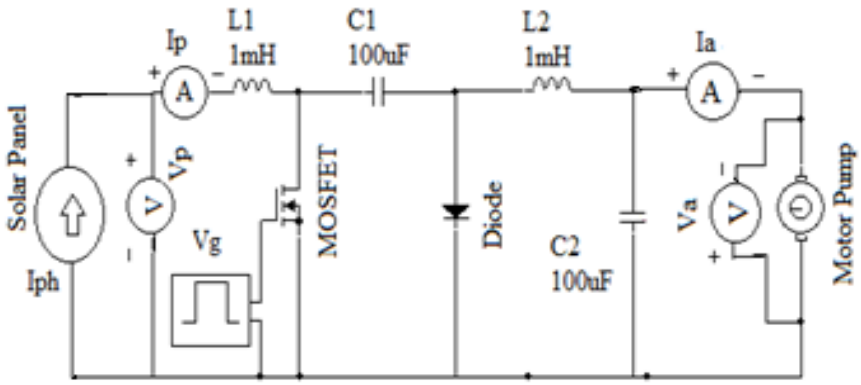

Fig.4.35 Experimental setup for pump load with MPPT converter.

Fig. 4.36 Solar pump used for experimentation.

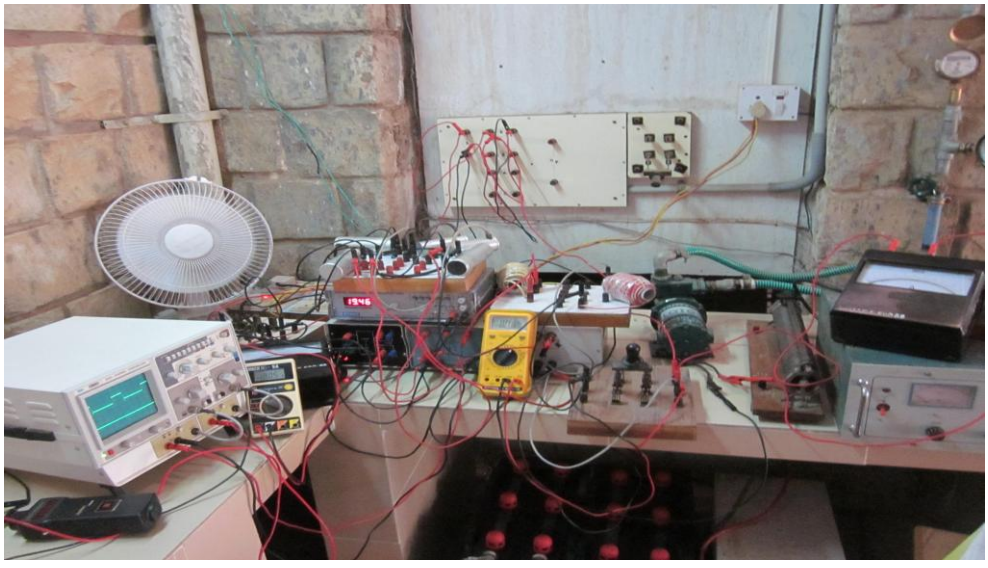

Fig.4.37 Experimental test set up for solar pump.

Typical waveforms are observed (Fig.4.38 to 4.41) in the course of experimentation. Fig.4.38 illustrates the functioning of MOSFET. It is ON when the gate signal is high. Fig.4.39 & 4.40 represent the inductor voltages. Their time average over one cycle is zero as expected. Fig.4.41 shows the output voltage, remaining almost constant as per the design. Thus the waveforms are in tune with those of a normal Cuk converter (Rashid 2004) thus confirming the proper working of the MPPT converter.

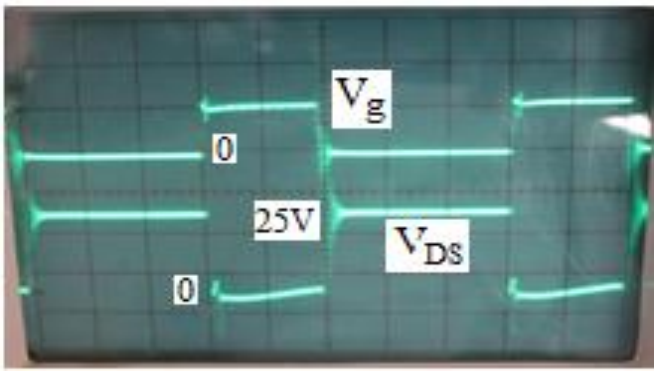

Fig.4.38 MPPT converter waveform: "Time vs. Gate voltage (V_g) and Voltage across MOSFET (V_{DS}).

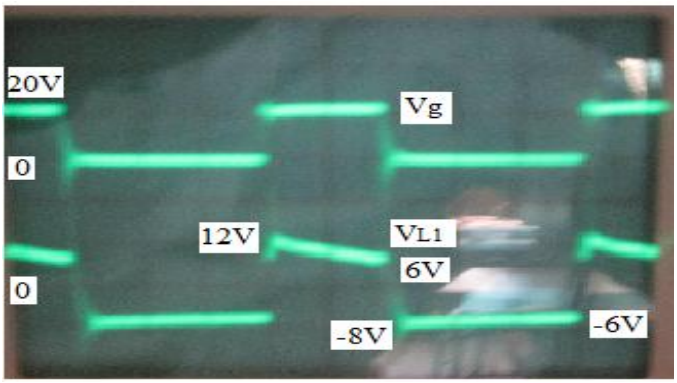

Fig.4.39 MPPT converter waveform: "Time vs. Gate voltage (V_g) and Inductor (L_1) voltage (V_{L1}).

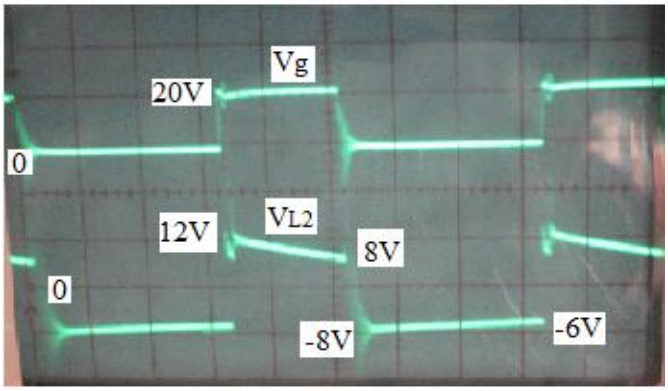

Fig.4.40 MPPT converter waveform: "Time vs. Gate voltage (V_g) and Inductor (L_2) voltage (V_{L2}).

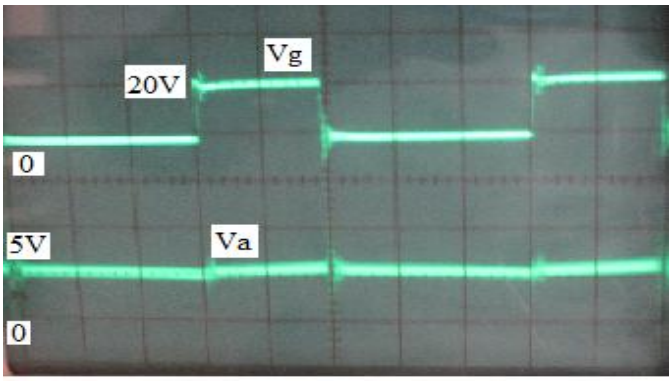

Fig.4.41 MPPT converter waveform: "Time vs. Gate voltage (V_g) and Motor voltage (V_a).

Testing is done without and with the MPPT converter. First the pump is run by connecting it to solar panel directly. Voltage, current and speed (ω_{dir}) readings are taken at different hours of day (Table 4.11). Then the pump is connected through the MPPT converter. The duty cycle of the MOSFET is varied and different parameters like D, V_p, I_p, V_a, I_a and ω are noted. This procedure is repeated for different radiations i.e. times of the day. Readings are taken for both the methods, $MPPT_{pp}$ and $MPPT_{lv}$ (Table 4.12 & 4.13).

Table 4.11 Solar pump without MPPT converter (Experimental).

Hour of day	**Maximum available panel power P_{pmav} (W)**	**Power to pump P_{dir} (W)**	**Pump speed ω_{dir} (rad/s)**
10	37.5	9.9	52.8
11	58.8	27.7	78
12	76	46.7	144
13	98	69.5	174.7
14	102	73.4	179.5
15	90	62.6	161.6
16	65	38.8	134.1
17	28.2	9.1	53.7
18	16	3.6	---

Table 4.12 Solar pump with MPPT converter employing $MPPT_{pp}$ (Experimental).

Hour of day	**Maximum available panel power P_{pmav} (W)**	**$MPPT_{pp}$**		
		Maximum power generated by panel P_{pmpp} (W)	**Power to pump at maximum panel power P_{ampp} (W)**	**Pump speed ω_{mpp} (rad/s)**
10	37.5	31.5	23	64.5
11	58.8	56.8	45.4	144
12	76	70.9	55	156
13	98	95	74	180
14	102	98	78	183
15	90	83	66	173
16	65	62.3	44	141
17	28.2	25.5	20.4	85
18	16	12.1	5.8	--

Table 4.13 Solar pump with MPPT converter employing $MPPT_{lv}$ (Experimental).

Hour Of Day	**Maximum available panel power P_{pmav} (W)**	**$MPPT_{lv}$**		
		Power generated by panel at maximum V_a P_{pmlv} (W)	**Power to pump at maximum V_a P_{amlv} (W)**	**Pump speed ω_{mlv} (rad/s)**
10	37.5	31.5	23	64.5
11	58.8	56.8	45.4	144
12	76	67.5	60.5	160
13	98	88	79	184
14	102	94	85	186
15	90	79	71.2	176
16	65	62.3	44	141
17	28.2	25.5	20.4	85
18	16	12.1	5.8	--

With the help of the experimental readings, the following characteristics are obtained:

a) Duty cycle vs. Load voltage (Fig.4.42) b) Duty cycle vs. Load power (Fig.4.43)

It is observed that at each radiation, power becomes maximum when the voltage V_a is maximum which is in tune with the theoretical finding. To drive home this feature more clearly, power and voltage curves corresponding to 5 pm radiation are plotted together (Fig.4.44). It can be seen that power becomes maximum when the load voltage V_a becomes maximum. Thus experimental results also validate the new proposal made for MPPT.

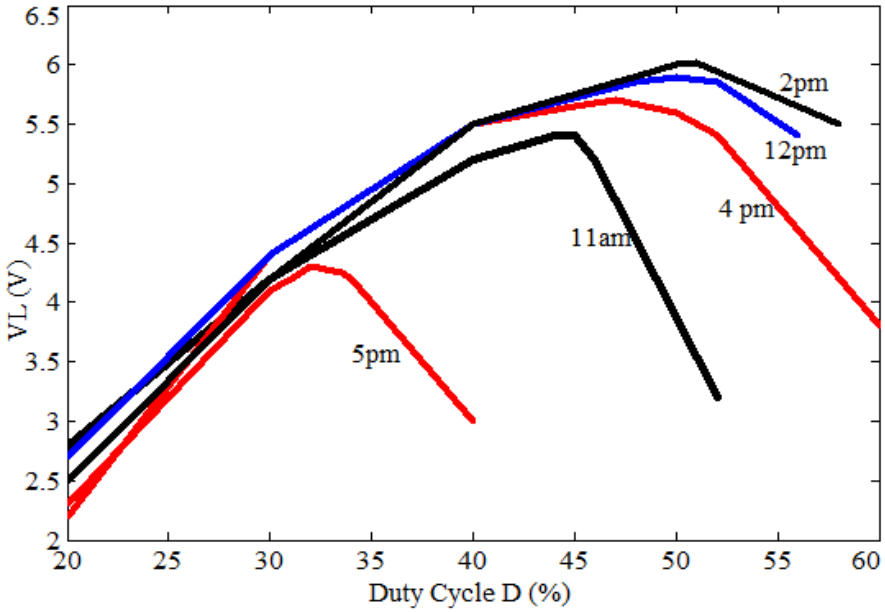

Fig. 4.42. "Duty cycle vs. Load voltage" for pump load (Experimental).

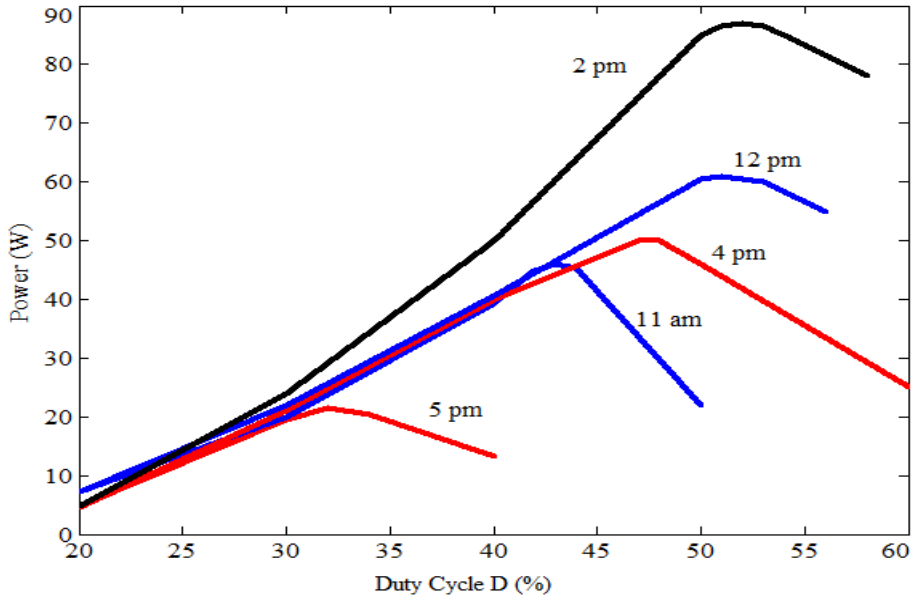

Fig.4.43. "Duty cycle vs. Power" for pump load (Experimental).

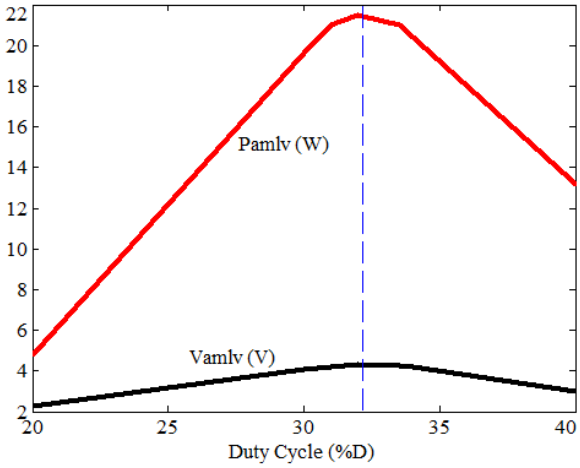

Fig 4.44 Solar pump with $MPPT_{lv}$: Power and Voltage curves at 5pm (Experimental).

Also from the experimental results, plots of "Time of day vs. Different powers" are obtained corresponding to the three cases: a) solar pump without MPPT b) pump with $MPPT_{pp}$ c) pump with $MPPT_{lv}$.

Variation of maximum available panel power (P_{pmav}) and power (P_{dir}) supplied to pump by direct (no MPPT) connection as a function of time of day is given in Fig.4.45.

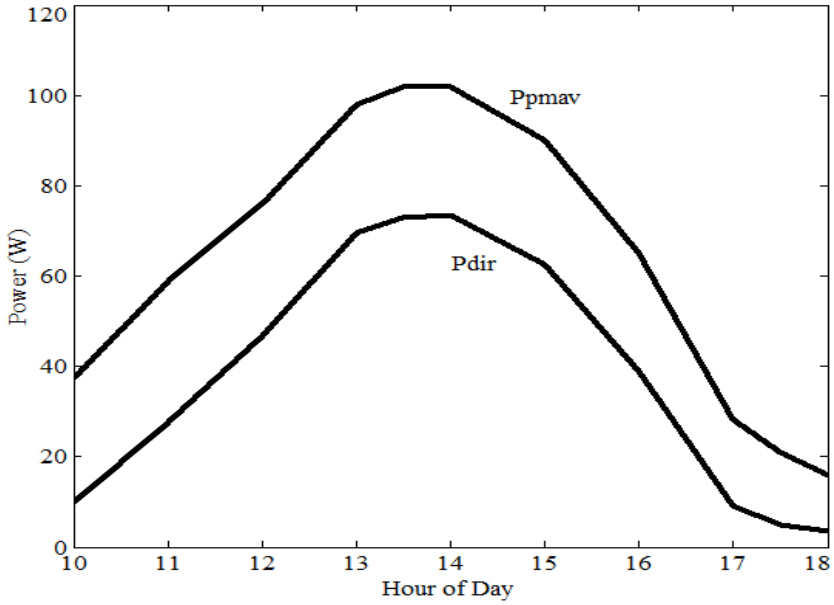

Fig.4.45 Solar pump without MPPT converter: "Hour of day vs. P_{pmav} & P_{dir}" (Experimental).

The case of pump with $MPPT_{pp}$ is depicted by Fig.4.46. It shows the maximum power generated by panel (P_{pmpp}) and power supplied to pump at maximum panel power (P_{ampp}) at different hours of the day. Fig.4.47 presents the situation when $MPPT_{lv}$ is employed. Here power generated by panel at maximum load voltage (P_{pmlv}) and power supplied to pump at max load voltage (P_{amlv}) are shown.

A comparison between the different approaches is provided in Fig.4.48. All the three powers, P_{dir}, P_{ampp} and P_{amlv} are given simultaneously. It is observed that power with direct connection is the least of the three. Power with MPPT converter is more. In that too, power with MPPT employing load voltage tracking ($MPPT_{lv}$) is more than that with panel power tracking($MPPT_{pp}$). This clearly brings out the fact that making generated power i.e., panel power maximum does not mean load power is maximum. Hence approach of aiming at maximum panel power anticipating maximum load power is not always right. Instead the approach has to be to aim at maximum load power itself. This is exactly the gist of the new proposal ($MPPT_{lv}$) made for harnessing maximum load power.

Comparative idea about pump speeds is given in Fig. 4.49. It is clear that the pump runs at higher speed with $MPPT_{lv}$ as compared to direct connection.

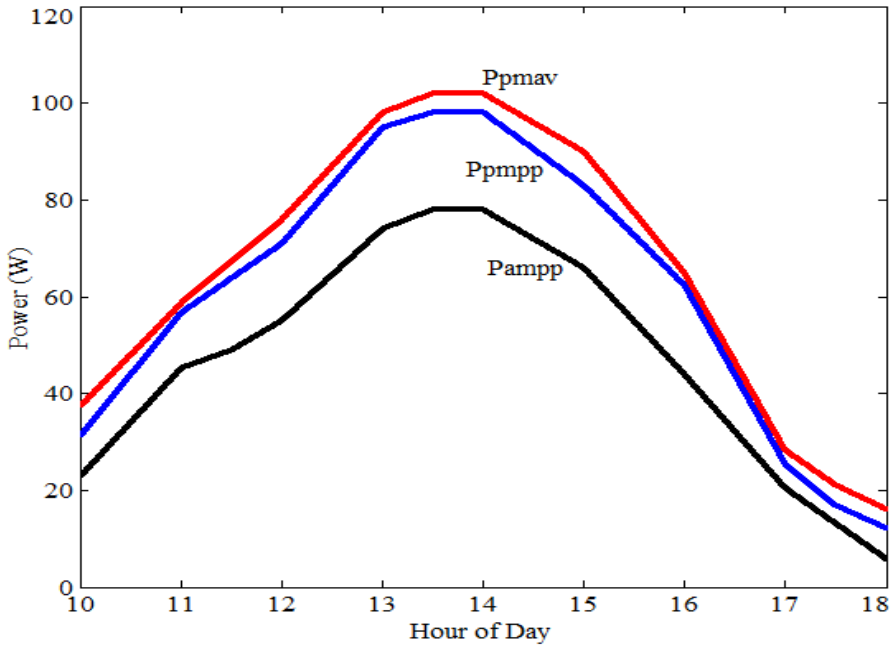

Fig.4.46 Solar pump with MPPT converter employing $MPPT_{pp}$:
"Hour of day vs. P_{pmav}, P_{pmpp} & P_{ampp}" (Experimental).

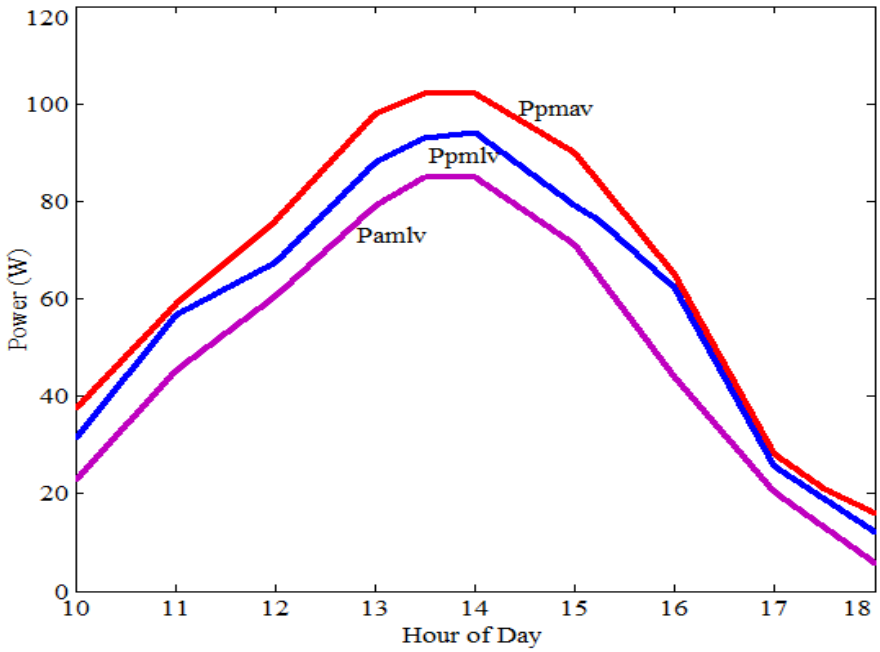

Fig.4.47 Solar pump with MPPT converter employing $MPPT_{lv}$: "Hour of day vs. P_{pmav}, P_{pmlv} & P_{amlv}" (Experimental).

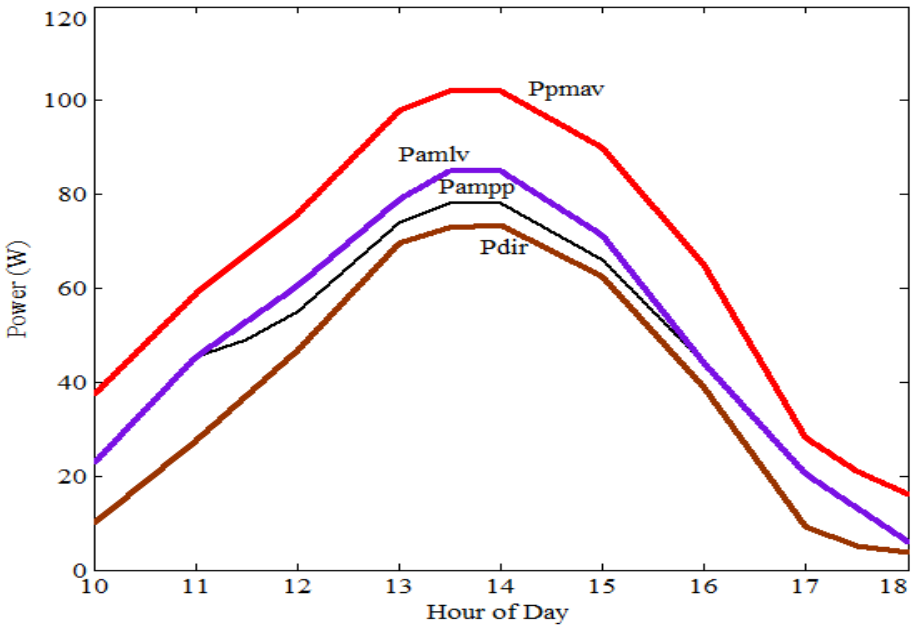

Fig.4.48 Solar pump with MPPT converter: "Hour of day vs. P_{pmav}, P_{ampp}, P_{amlv} & P_{dir}" (Experimental).

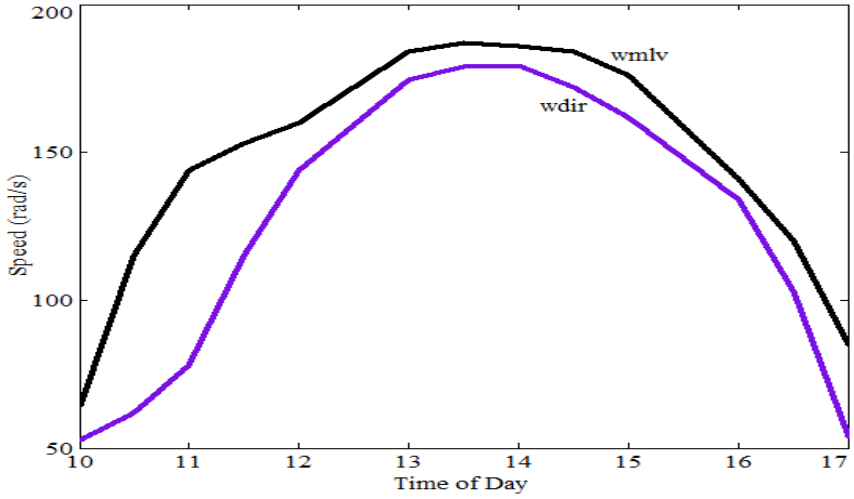

Fig.4.49 Solar pump: "Hour of day vs. ω_{mlv} (with $MPPT_{lv}$) and ω_{dir} (No MPPT) " (Experimental).

Calculation of increase in output:

To get an idea of the range of benefits, the following calculations are done. These are on same lines as in section 4.2.2.

Without MPPT: Information from Table 4.11 and Fig. 4.45 is made use of for the calculations. Energy generated (used) /day when the pump is operating without MPPT converter is obtained by time integration of P_{dir} curve in Fig 4.45.

Energy generated (used) /day = 250 W h

It's observed from Fig. 4.45 that minimum power of 60 W to start pumping is available for 2 h. Speeds for these durations are noted. Corresponding average flow rates are found from Fig. 3.12. Water lifted is determined as,

Water lifted = Duration (s) x Flow rate (L/s)

= 1 x 3600 x 0.11 + 1 x 3600 x 0.1 = 756 L

Since solar PV source capacity is 148 W_p, Water/ Watt =756/148 = 5.1 L/W_p

Assuming panel cost as Rs. 110 per watt, upfront panel cost per unit volume of water lifted is = panel cost/water lifted = 148 x 110 / 756 = Rs 21.5

With $MPPT_{pp}$: Information from Table 4.12 and Fig. 4.46 are made use of.

Energy used / day = 317 W h

Increase in energy used = (317-250)/250 = 26.8%

It's observed from Fig.4.46 that minimum power of 60 W to start pumping is available for 2.5 h. Speeds for these durations are noted. Corresponding average flow rates are found from Fig.3.12. Water lifted is determined as,

Water lifted = 0.5 x 3600 x 0.085 + 1 x 3600 x 0.12 + 1 x 3600 x 0.11

= 981 L

% Increase in water harnessed = (981 - 756)/756 = 29.7 %.

Water/Watt = 981/148 = 6.6 L/W_p

% Increase in Water/Watt = (6.6 - 5.1)/5.1 = 29 %.

Upfront panel cost per unit volume of water lifted is = (110 x 148)/981 = Rs 16.5

With $MPPT_{LV}$: Information from Table 4.13 and Fig. 4.47 are made use of.

Energy used / day = 350 W h

Increase in used energy = (350 -250)/250 = 40%

It's observed from Fig.4.47 that minimum power to start pumping i.e. 60W is available for 3.5 h. Corresponding average flow rates are found from Fig.3.12. Water harnessed is determined as,

Water lifted = 1 x 3600 x 0.094 + 1 x 3600 x 0.13 + 1 x 3600 x 0.12+ 0.5 x 3600 x

0.084 = 1689 L

% Increase in water harnessed = (1689 - 756)/ 756 = 123%.

Water/Watt = 1689/148 = 11.4 L/W_p

% Increase in Water/Watt = (11.4 - 5.1)/5.1 = 123 %.

Upfront panel cost per unit volume of water lifted is = (110 x 148)/1689 = Rs.9.6

It is clear from the above that there is increase in power and water yield when MPPT converter is employed. In that too, the gains with $MPPT_{lv}$ are more compared to those with $MPPT_{pp}$. It is also to be observed that, with $MPPT_{lv}$, there is remarkable decrease in cost per unit volume of water lifted. With increase in insolation, the additional gains also go on increasing.

4.3 ALGORITHM FOR IMPLEMENTING MPPT BY LOAD VOLTAGE TRACKING ($MPPT_{lv}$)

The simulation models developed in the earlier section were of open loop type and discrete in nature. They were run at specific I_{ph} (or insolation) values. Proposed new method for MPPT was demonstrated running the model at a specific I_{ph} each time separately. In this section an algorithm is developed (Fig. 4.50) to implement the proposal $MPPT_{lv}$ for time changing insolation. For this, closed loop simulation model is developed and perturb & observe (P&O) approach is employed.

4.3.1 Working of Algorithm:

The algorithm adjusts D automatically so as to make V_a maximum. This results in the harnessed power becoming maximum. Let V_a and V_{ref} indicate present and previous load voltages respectively. Also, let D and D_{ref} indicate present and previous duty cycles respectively. D is incremented by a small value Δ. V_a is measured and compared with V_{ref}. If V_a is more than V_{ref}, then the trend of change in D is right. Hence D is further increased. If V_a is less than V_{ref}, the inference is that the

trend of change in D is not right. Hence D is decremented by Δ. Even if $V_a = V_{ref}$, the operating point is perturbed a little by incrementing D by Δ and the effect on V_a is observed. Accordingly D is changed. Thus, the process of ascertaining that V_a is maximum is continuously put in action. This automatically ensures the load power is maximum.

The algorithm is implemented with the help of MATLAB program and SIMULINK simulation model.

4.3.2 MATLAB Program for Algorithm:

MATLAB program developed for implementing the $MPPT_{lv}$ algorithm is given in Fig. 4.51. Initially, D & V_a are set to zero. This is accomplished by the commands: 'persistant' and 'isempty'. The value of V_a is taken from the simulation model. The controller employed is of proportional type. In each pass, D value is altered by an amount "change". It is kept very small so that the program will work properly and will not become unstable. At the end of each pass, V_{ref} & D_{ref} are reset to the present values of V_a & D.

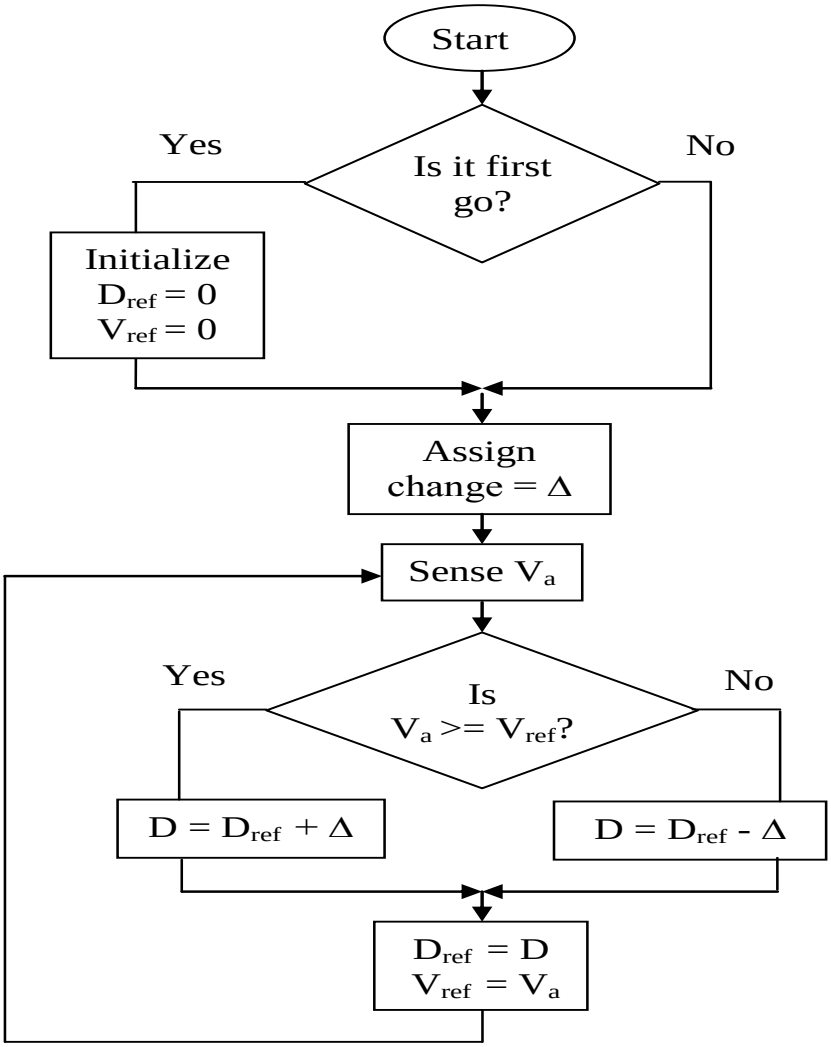

Fig.4.50 Algorithm for $MPPT_{lv}$.

```
function D = aa1RPid1(VL)
   % DEFINE VARIABLES
persistent Vref;
persistent Dref;
change = 0.000005;
    % INITIALIZING
if isempty(Vref)
   Vref=0;
end
if isempty(Dref)
   Dref=0;
end
    % GET LOAD VOLTAGE VL
    % 'P' IMPLEMENTATION
x=abs(VL-Vref);
 if x>=0 && x<=0.1
  m=0.3;
  else if x>0.1 && x<0.5
  m=0.2;
  else if x>0.5 && x<10
  m=0.1*x;
  else
  m=1;
      end
      end
 end
Ch = m*change;            % END OF "P" IMPLEMENTATION
    % CHANGE IN D
if  VL >= Vref;
   D = Dref + Ch;         %INCREMENT D
   else
   D = Dref - Ch;         %DECREMENT D
end
    %RESETTING
Dref=D;
Vref = VL;
```

Fig.4.51 Program for implementing $MPPT_{lv}$ algorithm.

4.3.3 Simulation Model and Results:

Simulation models are developed for resistive as well as pump loads. These are run using the MATLAB program obtaining the results which demonstrate the implementation of algorithm

4.3.3.1 R load with $MPPT_{lv}$

Simulation Model

Simulation model developed is shown in Fig. 4.52. Feedback signal from the load (output) side is averaged and sent to MATLAB program. From there the value of D is obtained. Repeating sequence block generating triangular waveform and relational operator are employed to generate the firing pulses for the MOSFET. Relational operator gives high output if the triangular waveform value is less than or equal to D value. Hence, as D increases, the duty cycle also increases. Saturation block helps to limit D to finite value.

Averaging of the feedback signal will improve the performance. 'Start' block is used to initiate the program at the beginning. It is simply an initial value of D. Repeating sequence block generating rectangular waveforms is used to feed different I_{ph} of different durations depicting the time changing radiation. Load resistance is taken as 10 Ω.

Results

The model is run with time changing I_{ph} as input. Corresponding D, V_a and P_a are observed. The results are given in Fig 4.53. It is observed that for each I_{ph}, V_a and hence P_a become the corresponding maximums. This means that, due to the algorithm, at each radiation, D automatically changes tracking the maximum voltage which corresponds to the maximum load power. The results from algorithm match with the values obtained from discrete simulation tests for each I_{ph} value, thus validating the proposal of $MPPT_{lv}$.

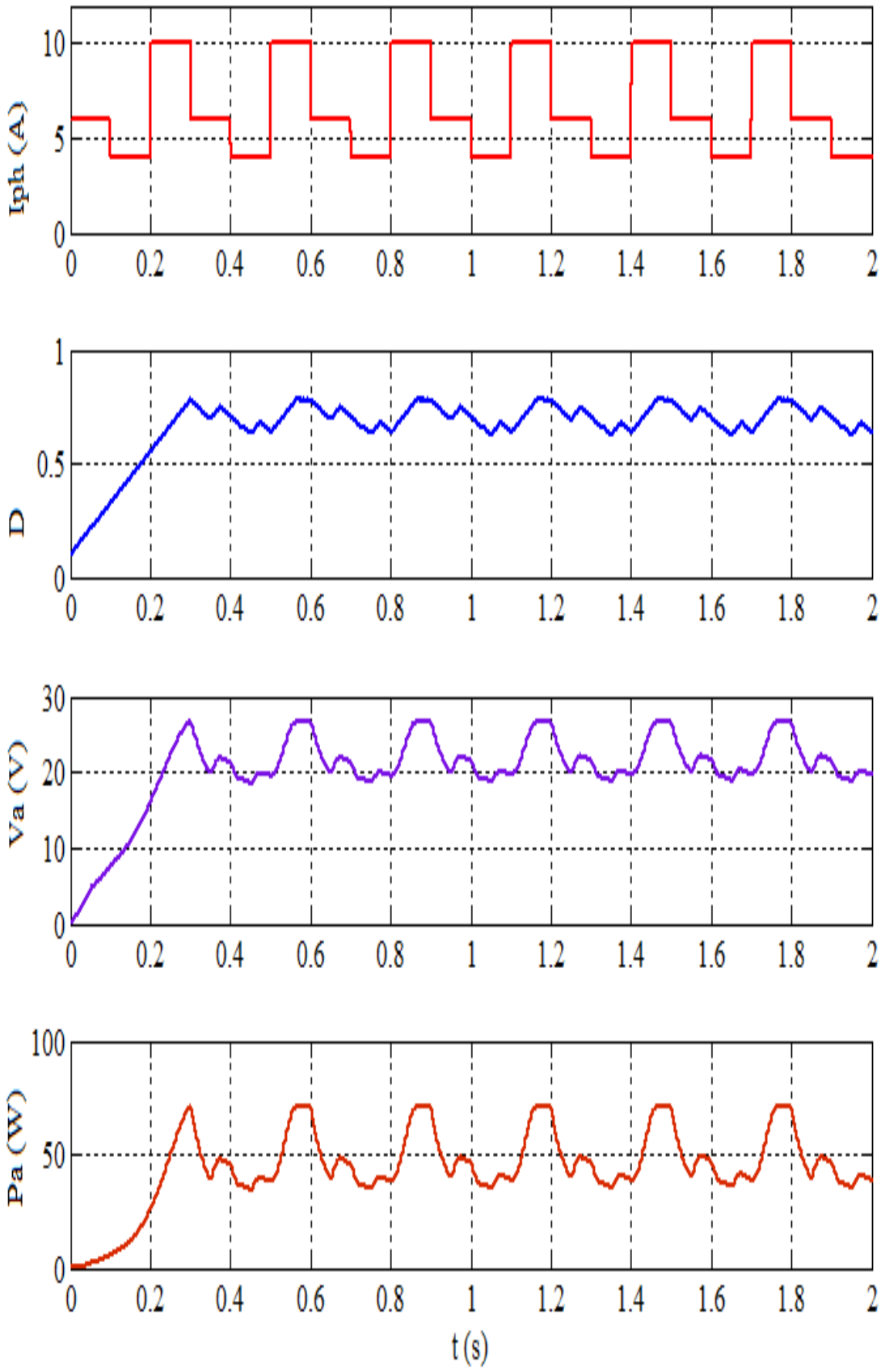

Fig.4.53 Results of $MPPT_{lv}$ algorithm for R load.

4.3.3.2 Solar Pump with $MPPT_{lv}$

Simulation Model

This model (Fig 4.54) is the same as that for R load discussed above except for the change in the load which is now taken as pump. Working of the model is also on the same lines as explained above.

'Start' block is critical and sensitive typically in this model as some initial voltage is required for the motor to start operating. Value of 'change' is another critical aspect. It is to be kept as less as possible for stable and proper operation of the algorithm. It's a basic model, there can be improvements over it.

Results

The model is run with time changing I_{ph} as input. Corresponding D, V_a and P_a are observed. The results are given (Fig 4.55). It is observed that for each I_{ph}, V_a and hence P_a become the corresponding maximums. This means that, due to the algorithm, at each radiation, D automatically changes tracking the maximum voltage which corresponds to the maximum load power thus validating proposal of $MPPT_{lv}$.

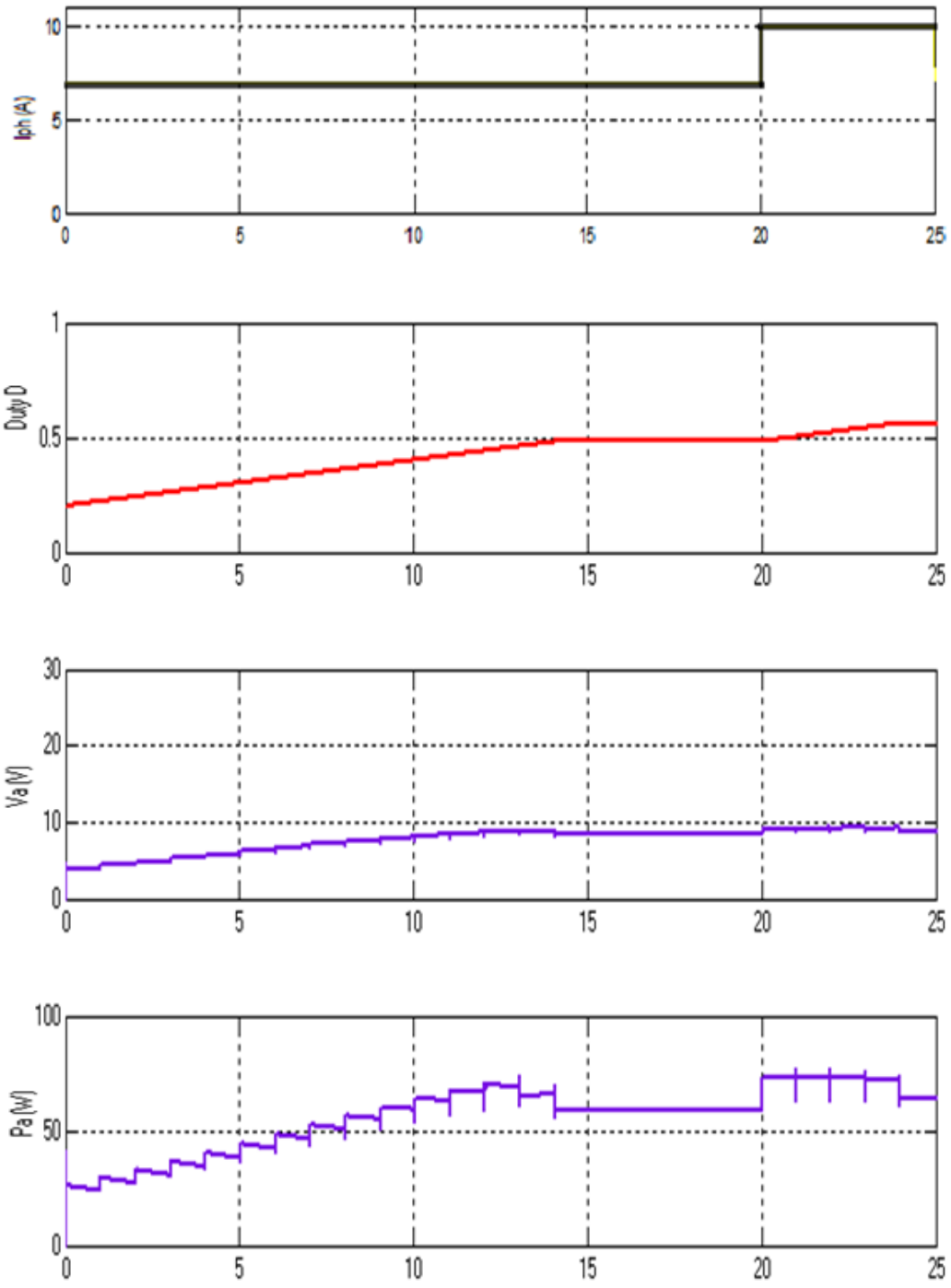

Fig.4.55 Results of $MPPT_{Iv}$ algorithm for pump load.

4.4 IMPORTANT RESULTS FROM THIS CHAPTER

This chapter has proposed a new approach to realise MPPT. The proposal is to track load voltage ($MPPT_{lv}$) in contrast to more commonly employed method of tracking panel power ($MPPT_{pp}$). Main advantage $MPPT_{lv}$ is its simplicity. Through theoretical, simulation as well as experimental approaches, the chapter has shown the implementation and validation for the proposed new method ($MPPT_{lv}$).

By both simulation and experimental testing, $MPPT_{lv}$ is shown to yield improvement in the performance of solar pump as compared to $MPPT_{pp}$. Results obtained from experimentation are given in Table 4.14. It is observed that for solar pump with $MPPT_{lv}$, the energy and water harvested have increased whereas the cost per litre of water lifted has decreased. Thus $MPPT_{lv}$ offers dual advantage of simplicity and increase in output.

Table 4.14 Improvement in performance of solar pump due to $MPPT_{lv}$ (Experimental results).

	$MPPT_{pp}$	$MPPT_{lv}$
% Increase in energy used	26.8	40
% Increase in water harnessed	29.7	123
% Increase in Water harvested/Watt	23	55.3

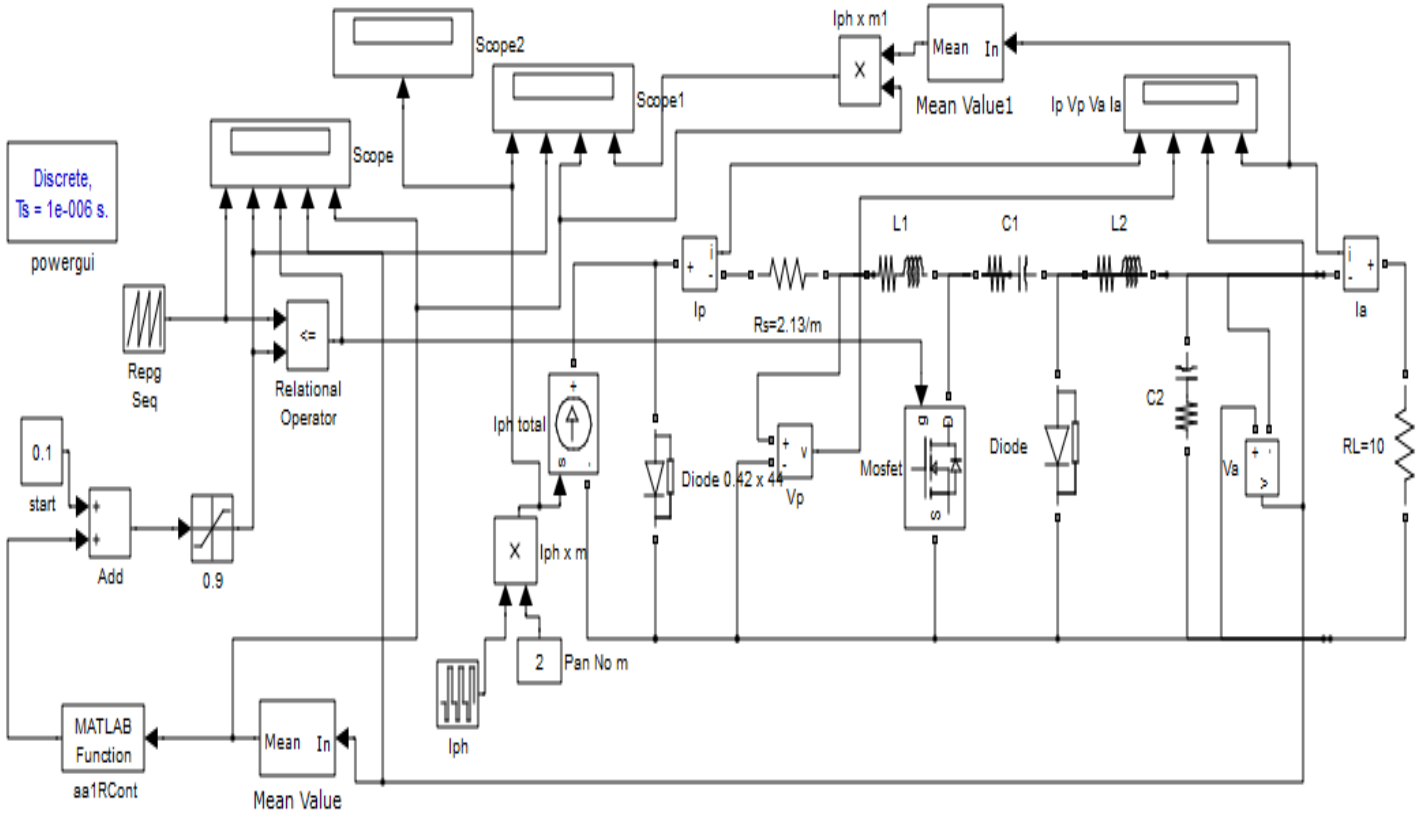

Fig.4.52 Simulation model for implementing $MPPT_{lv}$ algorithm for R load

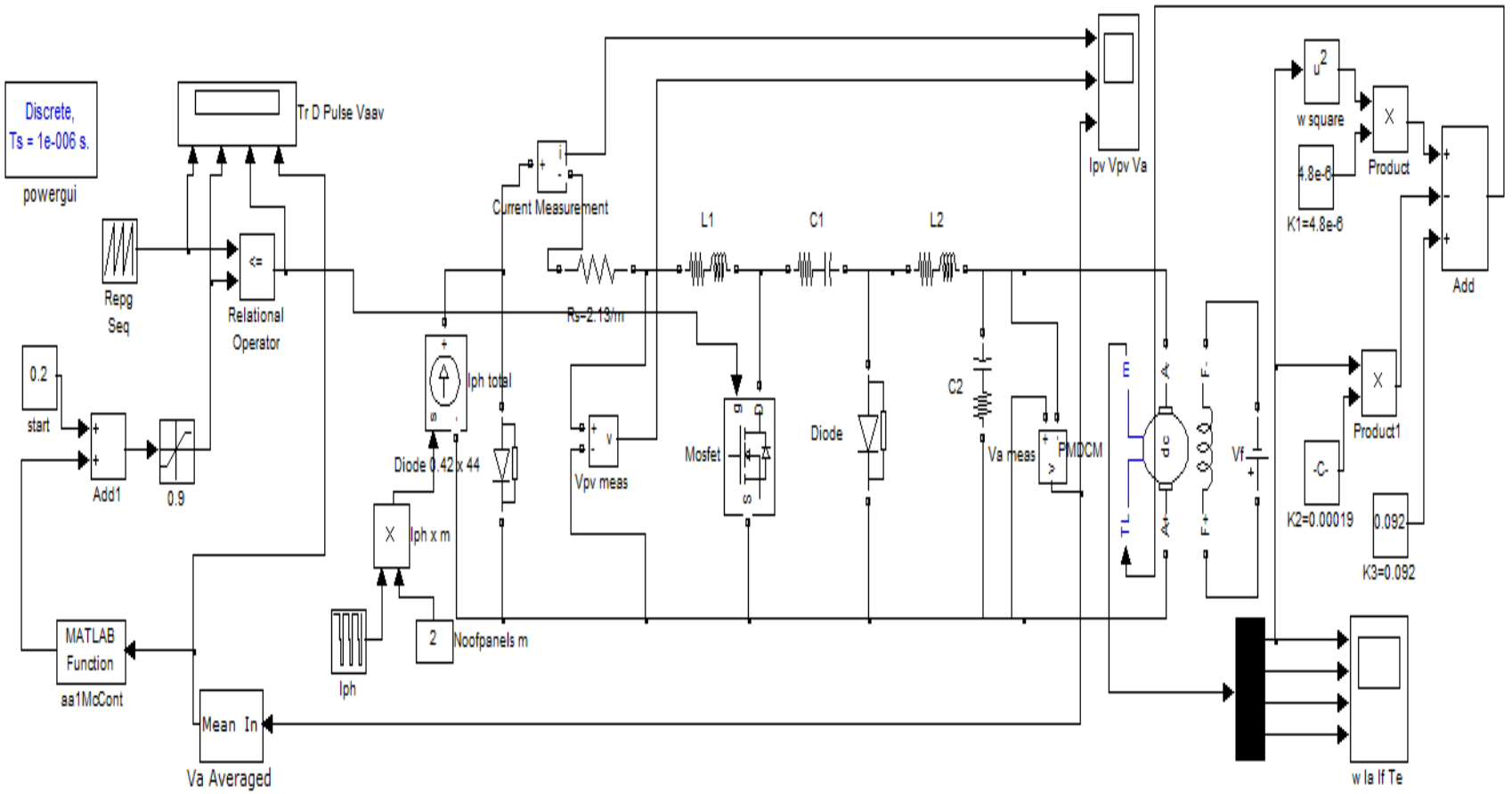

Fig.4.54 Simulation model for implementing $MPPT_{lv}$ algorithm for pump load.

CHAPTER 5

INDIVIDUAL FLOOR STORAGE METHOD : A NOVEL STRATEGY PROPOSED FOR SOLAR PUMPING IN MULTI FLOORED BUILDINGS

Present chapter deals with water lifting aspects in multi floored buildings. To begin with, the details of a survey conducted regarding water lifting practice are presented. Next, the present practice of water lifting in multi floored buildings and the proposed novel strategy are explained. Theoretical background for the new proposal is given. Then, the application of proposed strategy for solar water pumping is explained taking an example of a two floored building.

Seven papers are published covering some of the aspects of this chapter (Sl. Nos. 1-3, 5-7 and 9 in the list of publications, pages: 154,155).

5.1 SURVEY

A survey was conducted to understand the existing water lifting system and practice. The objective was to use the inputs from the survey to explore the opportunities for improvements in solar water lifting application.

5.1.1 Findings from the Survey

Locality of Survey: Survey was carried out in a domestic locality in the city of Dharwad (India), covering 300 houses (Table 5.1). The widespread use of pumps is quite evident from the fact that 90% of the households have pumps and that too electric ones.

Table 5.1. Locality of survey.

Locality of survey	**Gandhinagar, Dharwad, India**
Total number of houses surveyed	300
Number of houses with pumps (electrical)	270

Type of Buildings: Due to escalating site cost, there is an increasing tendency to go for multifloored buildings in urban areas. For the locality under consideration (Table 5.2), about 75% are with only ground floor (GF). 25% houses have additional floors like first floor (FF) & second floor (SF).

Table 5.2 Type of houses.

Type of House	**Number of houses**
Only GF	225
Two floored: GF + FF	69
Three floored: GF + FF + SF	6
Total	300

Water Source for Pump: Two sources, municipal water and bore wells, act as inputs to the pumps (Table 5.3). Most of the houses (80%) have the sumps storing the municipal supplied water as the source whereas others (20%) have their own bore wells.

Table 5.3 Water source for pump.

Source	**Number of houses**
Sump	216
Bore well	54
Total	270

Water Lifting Methodology: In most of the houses, water is stored from municipal supply in a sump at ground level. This water is lifted up using pump to an overhead (OH) tank placed above the topmost floor and stored in it. Then it's brought down to different floors and supplied to the utility points of the corresponding floors.

Suction and Delivery Heads: In case of sump-fit pumps, the suction head is 1.5 to 2.0 m (Table 5.4). Position of OH tank and hence delivery head depends on the number of floors. Majority of houses (75%) are with only GF requiring a head capability of 5 to 7 m.

Table 5.4: Suction and delivery heads.

Type of Head		**Head (m)**	**Percentage of houses**
Suction head (Hs)		1 to 2	100
Delivery head (H_d) (position of OH tank)	GF building	4	75
	GF+FF building	7	23
	GF+FF +SF building	10	2

Sump Pump Details: Most of the pumps (about 85%) for single floored houses are of single phase ac, 0.375 kW, monoblock centrifugal type (Table 5.5) working for 0.5 to 0.75 h every day. Pumps of the same rating are employed for both single and two floored houses.

Table 5.5 Sump pump details.

Type of pump	Centrifugal, monoblock
Pump Ratings	1-phase a.c., 0.375 kW
Total Head	Up to 30 m (for most of the pumps)

5.1.2 Comments Regarding Survey Findings

From the details of the survey explained above, two important observations are made regarding net pumping head and position of storage tank. They open up opportunities to system designers and engineers for introducing new efficient methods in pumping practice and trying for optimization of pump design.

Total Pumping Head: Presently pumps of the same capacity are being employed immaterial of whether the house is single or two floored type. The head capability of these pumps is 30 m. However as is observed from survey, most of the houses are with only GF with a total head requirement of 5 to 7 m. Then it means that pumps are oversized. This makes them costly and bulky. Instead pumps can be specially designed and optimized to meet the requirement of the single floored buildings only. This results in cost and size reduction of pumps with improved efficiency. These developments reach large number of customers as the number of customers in this group are in majority. Thus there is a big customer segment to be specially treated and hence commercially explored.

Storage Tank Position: The water lifting methodology presently practised for multi floored buildings employs single OH tank placed above the topmost floor. This particular observation is explored further in the present research study and the details are given in the ensuing sections.

5.2 NEW STRATEGY FOR PUMPING IN MULTI FLOORED BUILDINGS

5.2.1 Water Lifting in Multi floored Buildings - Present Practice

Presently, in multi floored buildings, a single OH tank is placed above the topmost floor. All the water is lifted up to that height and then brought down to lower floors (Fig.5.1). This method can be referred to as "Top Floor Storage Method (TFSM)". Here, even the water required at lower heights is unnecessarily lifted to higher levels. For example, let a two floored building be considered with ground floor (GF) and first floor (FF). Here OH tank is placed on the top of the FF at a height of approximately 7 m. This position of the tank is alright for the FF water requirement. But, for the GF, though water is required at just 4 m height, it is lifted up to 7 m and then brought down. Such a lifting of water to unnecessary large heights means more energy consumption which is wastage. This is the demerit of TFSM.

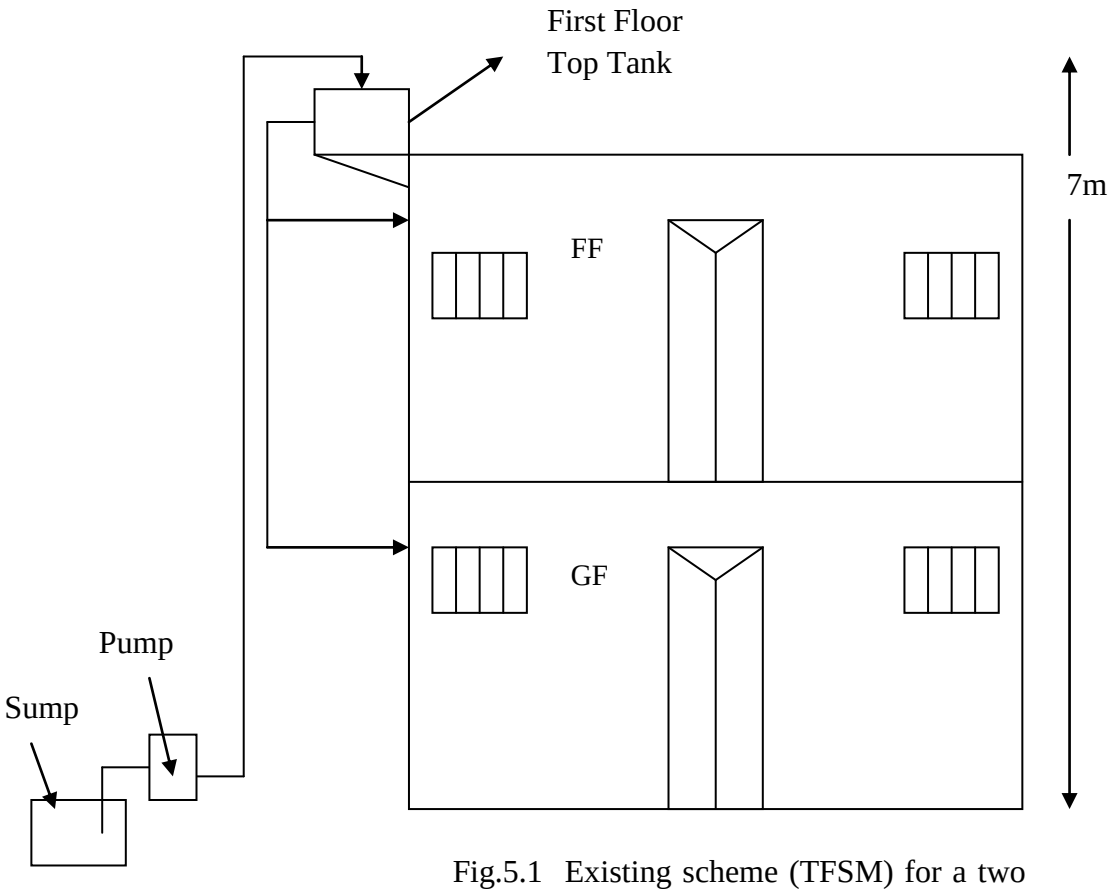

Fig.5.1 Existing scheme (TFSM) for a two floored building.

5.2.2 IFSM: The New Strategy

To overcome the demerit of TFSM, a new strategy "Individual Floor Storage Method" (IFSM) is proposed. According to this proposal, instead of one single large OH tank on topmost floor, small tanks at each floor height are to be employed supplying water to corresponding floor (Fig.5.2). Independent pipe line is laid from pump to each floor tank through a multi output valve. Water is pumped to each floor tank independently using the valve. This method avoids wastage of energy as the water is pumped to the required optimum heights only. Conversely, for a particular amount of energy consumed, IFSM yields more water output.

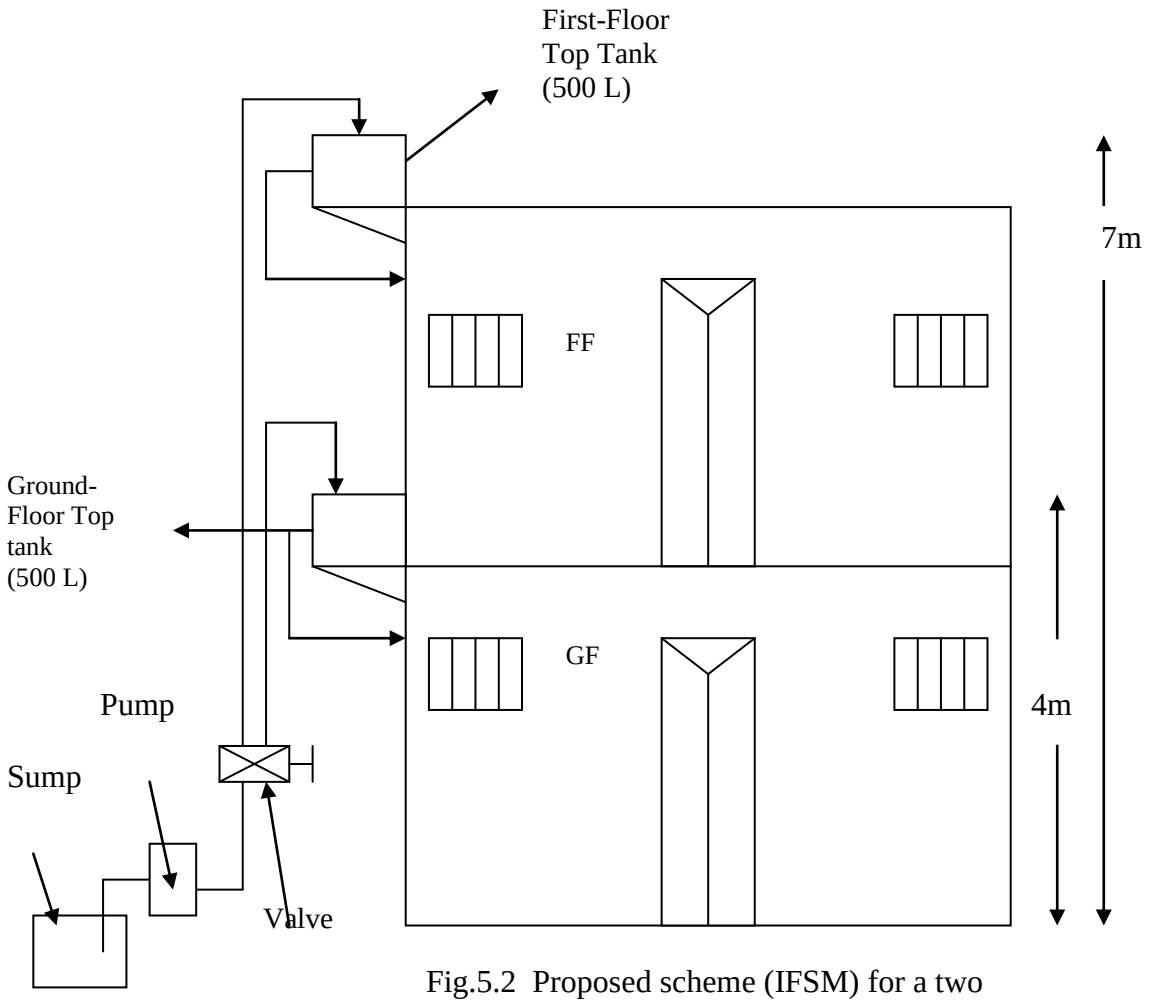

Fig.5.2 Proposed scheme (IFSM) for a two floored building.

5.2.3 Theoretical Background

In this section theoretical explanation for the energy saving aspect of IFSM is given. The energy required for lifting water with both the methods TFSM & IFSM are determined for a multi floored building thus demonstrating theoretically the benefit of IFSM. Let the features of the building be:

- Number of floors = n
- Height of each floor = h m (assuming uniform floor height)
- Water required per floor per day = m L = m kg
- Water is available in a sump at ground level of the building and suction head $H_s = 0$.

From the fundamentals of physics, the work done or energy spent (W) in lifting a mass of m kg through a height of h m is given by equation (5.1).

$$W = mgh \text{ J} \qquad (5.1)$$

where g = acceleration due to gravity = 9.81 m/s^2. The system is assumed as ideal to make the mathematical treatment simple. Hence only static head is taken in to account neglecting the pipe friction head.

TFSM: Supplying water for this building with TFSM means lifting n x m L water/day through a height of n x h m. Using equation (5.1), energy required per day (E_{tf}) for TFSM is given by equation (5.2).

$$E_{tf} = (nm)g\,(nh) = n^2mgh \text{ J} \qquad (5.2)$$

IFSM: Supplying water for this building with IFSM means lifting daily m L water through a height of h m for first floor, through $2h$ m for second floor, etc. up to through nh m for the topmost i.e., n^{th} floor. Total work done is the sum of the individual works done for each floor. Using equation (5.1), energy required per day for IFSM (E_{if}) is given by,

$$E_{if} = mgh + mg(2h) + \ - - \ - + mg(nh) \qquad (5.3)$$

$$= \frac{mghn(n+1)}{2} \quad \text{J} \qquad (5.4)$$

Saving in energy: From equations (5.2) & (5.4), the ratio of the energy values can be obtained as shown in equation (5.5).

$$\frac{E_{if}}{E_{tf}} = \frac{(n+1)}{2\,n} \qquad (5.5)$$

From equation (5.5), it's observed that the energy required is less with IFSM compared to that with TFSM. Hence IFSM leads to saving in energy. Using equations (5.2) & (5.4), expression for saving in energy can be obtained as given in equations (5.6 & 5.7).

$$Saving\ in\ energy = E_{tf} - E_{if}$$

$$= n^2\, mgh - \frac{n(n+1)mgh}{2}$$

$$= \frac{n(n-1)}{2}\, mgh \qquad (5.6)$$

$$= \frac{(n-1)}{2n}\ n^2\, mgh$$

$$= \frac{(n-1)}{2n}\, E_{tf} \qquad (5.7)$$

$$\%\ Saving\ in\ energy = \frac{(E_{tf} - E_{if})}{E_{tf}} \times 100 \qquad (5.8)$$

Using equation (5.8) values of energy saved for different floor numbers are calculated (Table 5.6 & Fig 5.3). It is observed that the percentage saving in energy is remarkable for lower number of floors. Theoretically, the energy saving depends on: i) the number of floors and ii) the magnitude of water lifted. In a practical situation, the floor heights may not be uniform. Also the pump discharge at different heights will not be the same. It changes non linearly. Hence the actual saving in energy depends on all these factors. The analysis can be extended to the case of non uniform floor heights also by substituting the corresponding floor heights in the relevant

equations. Suction head, wherever present and considerable, can be accounted for by adding it to delivery head (H_d) and thus getting total head (H) as $H = H_s + H_d$.

Table 5.6 Energy saving with IFSM (Theoretical).

Floor Number (n)	E_{if} / E_{tf}	**Energy Saving (%)**
1	1	0
2	0.75	25
3	0.66	34
4	0.62	37.5
5	0.6	40

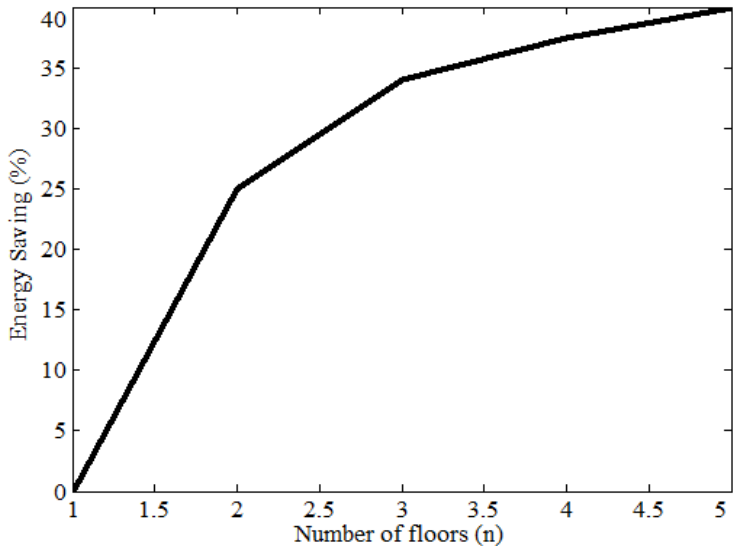

Fig. 5.3 Energy saving with IFSM (Theoretical).

5.2.4 Experimental validation:

For demonstrating the experimental validation of IFSM, water lifting in two floored building shown in Fig 5.1 is considered. Water is lifted from the sump (depth = H_s = 1.2m) at the GF to the OH tank. The pump has the same specifications as given in section 3.3. Minimum power, corresponding flow rates and the energy consumed for different delivery heads (H_d) are found experimentally (Table 5.7 & Fig 5.4).

Here two cases are considered: a) Fixed water requirement per day and b) Fixed energy consumption per day. With the first case the amount of energy required for a particular amount of water to be lifted is determined. With the second case, the amount of water lifted for a particular amount of energy consumed is found. For each case both the methods i.e. TFSM and IFSM are employed and the results obtained thus validating the proposal of IFSM.

Table 5.7 Flow rate and energy consumed for pump.

H_d (m)	**Input Power (W)**	**Flow Rate Q (L/s)**	**Energy consumed (kWh/ L)**
4 (GF tank level)	60	0.08	0.20×10^{-3}
7 (FF tank level)	70	0.03	0.66×10^{-3}

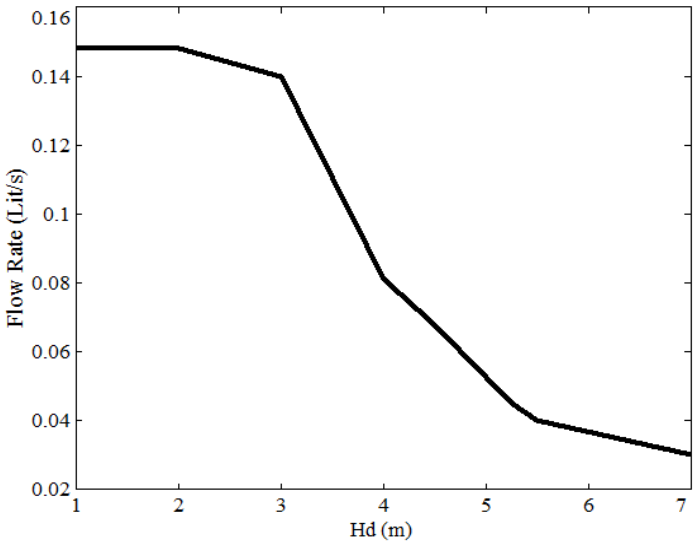

Fig. 5.4 "Head vs. Flow rate" for pump.

5.2.4.1 Fixed Water Per Day

Let water requirement per floor per day be 150 L.

TFSM (Fig.5.1)**:** Since there are 2 floors, total water required for both the floors is 300 L /day. It is proposed to have one OH tank of 500 L capacity kept on the FF roof top (tank inlet point being 7 m above ground level). Water is lifted from sump up to 7 m height. For pumping the required 300 L /day, the electric energy required/day is calculated using values from Table 5.7 corresponding to H_d = 7 m. This is obtained as:

Electric energy required/day = Volume of water lifted x Energy consumed/Litre

$= 300 \times (0.66 \times 10^{-3}) = 0.2$ kWh.

IFSM (Fig.5.2)**:** Water required per floor per day is 150 L. To meet the total water requirement by the new strategy, IFSM, it is proposed to provide two 250 L tanks: one on GF top (tank inlet point 4 m above ground) supplying water to GF and the other on FF top (tank inlet point 7 m above ground) supplying water to FF. Water is lifted from sump up to 7 m while filling FF tank whereas lifting is only up to 4 m while filling GF tank. Two-way valve helps in selecting the tank to be filled. For pumping the required 150 L/day to each tank, the total electric energy required per day is calculated using values from Table 5.7 corresponding to H_d = 4 m and H_d = 7 m respectively.

Electric energy required/day = Energy required for lifting water to GF tank + Energy required for lifting water to FF tank

$= 150 \times (0.20 \times 10^{-3}) + 150 \times (0.66 \times 10^{-3})$

$= 0.03 + 0.099 = 0.13$ kW h.

This is less than that required with TFSM.

Saving of energy = 0.2 - 0.13 = 0.07 kW h/day

% Energy saving = (0.07/ 0.2) x 100 = 35 %.

5.2.4.2 For fixed value of energy

Let 0.2 kWh of energy be spent per day on pumping.

TFSM: Single OH tank of 500 L is kept on FF top. It is filled by running the pump consuming total energy of 0.2 kWh or 0.2 x 10^3 Wh per day. While pumping to this head, the pump draws power of 70 W.

Running time of pump = (0.2 x 10^3) / 70 = 2.85 h.

Taking flow rate from Table 5.7,

Water lifted to FF tank = 2.85 x 3600 x 0.03 = 300 L.

IFSM: Two OH tanks each of 250 L capacity are taken. One is housed on GF top and the other on FF top. Let the total energy spent with IFSM also be 0.2 kWh per day. Of this let 0.05 kWh be spent on pumping to GF tank and 0.15 kWh on pumping to FF tank. Power drawn is 60 W while pumping to GF tank and is 70 W while pumping to FF tank.

Running time of pump when supplying GF tank = (0.050 x10^3) /60 = 0.83 h

Taking flow rate from Table 5.7,

Water lifted to GF tank = 0.83 x 3600 x 0.08 = 240 L

Running time of pump when supplying FF tank = (0.150 x10^3) /70 = 2.14 h

Taking flow rate from Table 5.7,

Water lifted to GF tank = 2.14 x 3600 x 0.03 = 231 L

The amount of water pumped to each floor with different methods are given in Table 5.8. It can be observed that at each floor 50% more water is obtained by using IFSM compared to that by TFSM.

Table 5.8 Water lifted with TFSM & IFSM (Experimental).

Floor	GF	FF
Water lifted/day by TFSM (L)	150	150
Water lifted/day by IFSM (L)	240	231

Additional Expenditure:

As compared to TFSM, IFSM requires two OH tanks, additional plumbing work and valve. The cost of one 500 L PVC tank and that of two 250 L PVC tanks is almost the same. Hence there is no additional cost regarding the OH tanks. It is assumed that there is provision to keep individual floor tanks and hence no need of additional civil construction for this. Extra plumbing work & valve require additional expenditure which is approximately Rs. 1000. This being one time investment is affordable to the pump users.

5.3 APPLICATION OF IFSM FOR SOLAR WATER PUMPING

In solar pumping system without battery (Fig 5.5), the motor-pump unit is connected directly to the solar panel. Water is transferred to an OH tank whenever the solar power is available. OH tank itself acts as a storage element. However the position of OH tank is critical. It decides the overall efficiency of operation and hence the amount of water pumped. Obviously, "Individual Floor Storage Method (IFSM)" the new method proposing energy saving position of OH tanks, is appropriate for solar water pumping system employing OH tanks as storage elements.

IFSM is complimentary to the aspect of harnessing maximum energy from solar PV panel discussed in the earlier chapter. IFSM can be incorporated in addition to implementing MPPT.

This section discusses application of IFSM for solar water pumping without battery backup. To begin with, present and proposed methods are explained. Then, IFSM proposal is narrated with an example of a two floored building.

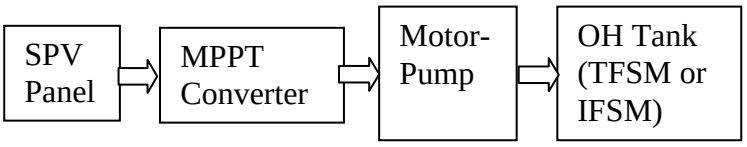

Fig.5.5. Solar pumping in multi floored buildings with MPPT converter.

5.3.1 Solar water pumping with TFSM:

Presently solar water pumping in multi floored buildings is done by top floor storage method (Fig 5.6). As discussed in section 5.2, this approach is not efficient. It demands excess energy as the water is lifted to higher levels unnecessarily. For a particular value of installed capacity of solar panel, it results in lesser water yield. Conversely for a particular amount of water to be lifted per day, the capacity of the solar panel required will be more which leads to higher cost. Hence TFSM is not suitable for solar water pumping application.

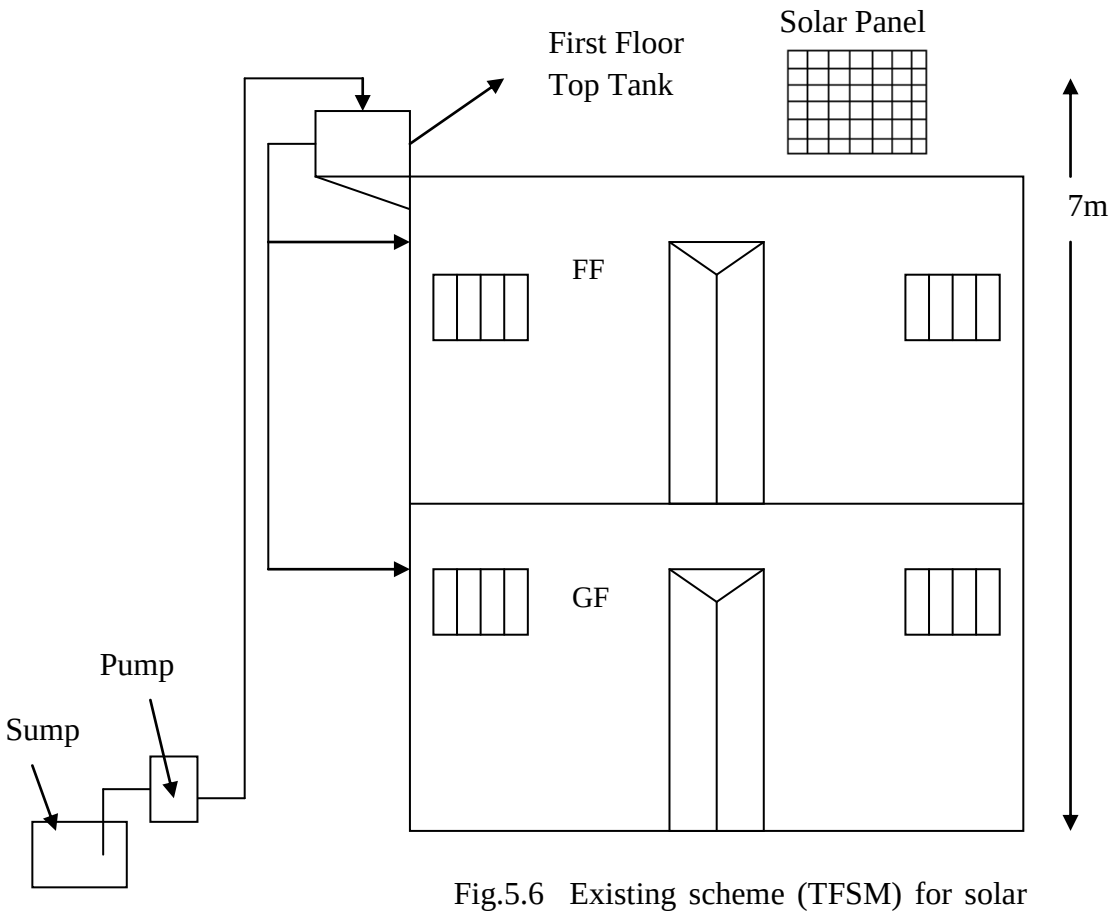

Fig.5.6 Existing scheme (TFSM) for solar pumping in a two floored building.

5.3.2 Solar water pumping with IFSM:

Instead of TFSM, individual floor storage method is proposed for solar water pumping in multi floored buildings (Fig 5.7). As explained in section 5.2, this approach overcomes the demerit of TFSM. Here water is pumped to the required optimum heights thus avoiding wastage of energy. Hence is suitable for solar PV application as solar power is quite precious. Minimum power required for pumping to lower level tank is lesser than that for higher level tank. Pumping to lower level tank happens at a lesser radiation compared to that for higher level tank. Thus IFSM enables use of panels for more duration. The amount of water lifted will be more for a particular capacity of solar panel. Conversely, for a particular amount of water to be

lifted, the PV panel size needs to be less. The direct consequence of this is a decrease in the initial cost. This is a significant advantage particularly with respect to solar pump as its main demerit is high cost per unit volume of water lifted.

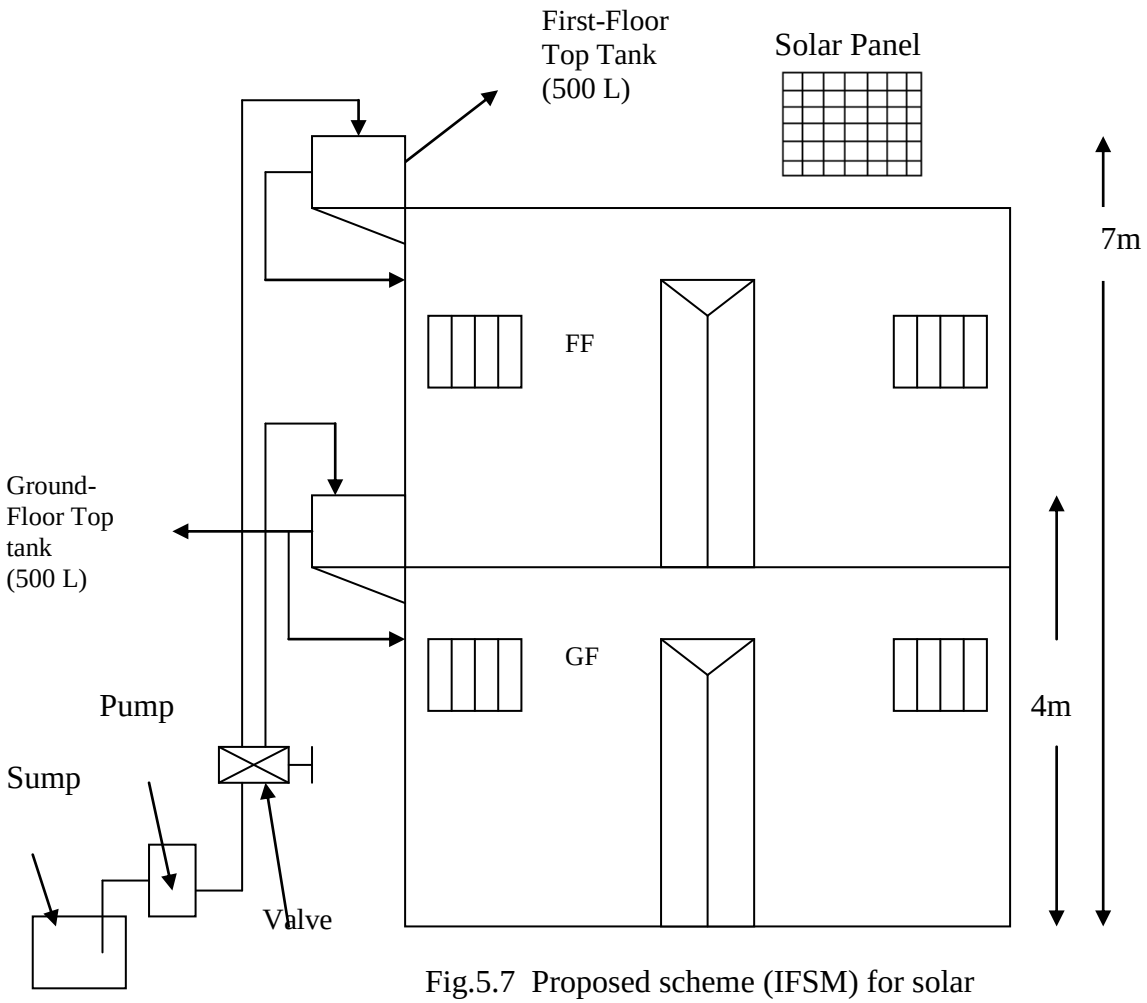

Fig.5.7 Proposed scheme (IFSM) for solar pumping in a two floored building.

5.3.3 Example of application of IFSM:

The application of the proposed method for solar pumping system is presented considering an example of providing solar pumping system to a two floored (GF + FF) house. The house is supposed to have the following features: It is located at Dharwad, Karnataka, India (Latitude: $15^0$28' Longitude: $75^0$1'). Solar pumping system is of direct coupled type (Fig. 5.5). There is no battery backup. MPPT is assumed to be incorporated. This means maximum power from the PV panel is available continuously.

Pump used earlier (section 3.3) is used here also. Minimum power to start pumping and the corresponding flow rates for different delivery heads (H_d) were found experimentally and are given in Table 5.7 & Fig 5.4.

Two cases are considered: a) With a particular rating PV panel and b) With a particular water requirement per day. In the first case, the amount of water lifted for a particular amount of energy harnessed per day is found. In the second case, the size of solar panel required for a particular amount of water to be lifted is determined. For each case both the methods i.e. TFSM and IFSM are worked out and the results obtained to bring out the advantage of employing IFSM for solar pumping.

5.3.3.1 With a particular rating PV panel:

148 Wp solar PV source considered earlier (section 3.2) is used here also. Maximum power curve for this source is obtained experimentally and given in Fig. 5.8. Water obtained per day with both the methods, TFSM and IFSM, is determined as shown below.

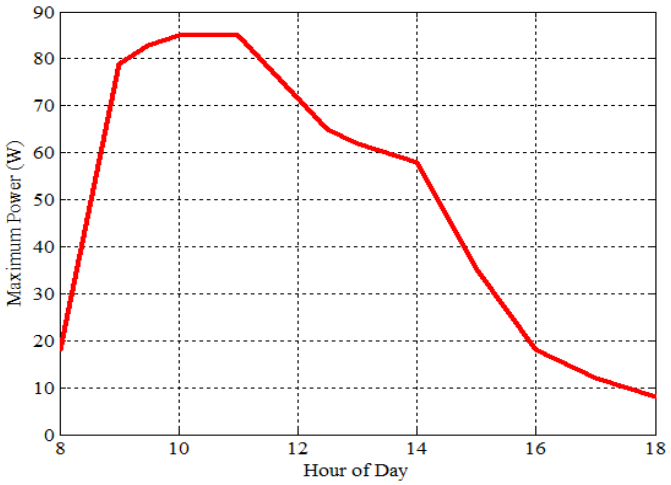

Fig 5.8 Maximum power curve for 148 W_p solar panel.

TFSM based proposal: The proposed set-up for TFSM is as shown in Fig 5.6. One PVC tank of 1000 L capacity is placed on FF top. Water is lifted from the sump to OH tank (H_d = 7 m) and stored. From there it's supplied to ground floor and first floor. Features of the major components are to be as given in Table 5.9.

Table 5.9 Major components for TFSM
(with particular rating PV panel).

Item	**Features**
PV panel size	148 W_p, 12 V.
OH tank	1000L PVC tank on FF top.
Pump	70-100 W, 12 V d.c., total head : 9 m, surface mounted.

Minimum power required for pumping to FF tank level is 70 W. From the panel characteristics (Fig 5.8) it is observed that power available is more than or equal to 70 W for 3 h. Hence pumping happens for about 3 h. Using flow rate from Table 5.7,

Water lifted = Flow rate x Duration of pumping

= 0.03 x (3 x 3600) = 324 L

Water lifted per watt of panel capacity = Water lifted/ Panel rating

$= 324/148 = 2.1\ L/W_p$

IFSM based proposal: The proposed set-up for IFSM is as shown in Fig 5.7. Two PVC tanks each of 500 L capacity are provided, one on GF top and the other on FF top. Pipe line is to be laid from pump to each tank separately through two way valve. The same pump proposed for TFSM is selected here also. It is observed from the tests that, minimum power required to pump water is 60 W for GF tank and 70 W for FF tank (Table 5.7). Taking this aspect in to account, water is lifted from the sump to FF tank (H_d = 7 m) when available power is more than or equal to 70W and to GF tank (H_d = 4 m) when the available power is between 60 to 70 W using two way valve. Features of the major components for IFSM are to be as shown in Table 5.10.

Table 5.10 Major components for IFSM
(with particular rating PV panel).

Item	**Features**
PV panel size	148 W_p
OH tank	Two 500 L PVC tanks (one for each floor).
Pump	70-100 W, 12V d.c., total head: 9 m, surface mounted.
Pipe line	Independent pipeline with two way valve.

From the panel characteristics (Fig. 5.8) it is observed that power available is more than or equal to 70 W for 3 h and is within 60 to 70 W (i.e., ≥60 W & <70 W) for 1.0 h.

Hence pumping is done for 1.0 h for GF tank. Using flow rate from Table 5.7,

Water lifted = 0.08 x (1.0 x 3600) = 288 L

Pumping is done for 3 h for FF tank. Using flow rate from Table 5.7,

Water lifted to FF tank = 0.03 x (3 x 3600) = 324 L

Total water lifted = 288+ 324 = 612 L

Increase in water yield = [(612- 324) / 324] x 100 = 88%.

Water lifted per watt of panel capacity = 612 /148 = 3.7 L/W_p

Details of duration of pumping and water lifted are given in Table 5.11. It can be observed that IFSM enables use of panels for more duration leading to enhancement in water supplied to each floor by more than 80%. With TFSM, the pumping happens for 3 h whereas with IFSM the pumping happens for 3 + 1 = 4 h. This is happening because of the possibility of pumping even at lower power due to the provision of the GF tank. Otherwise this power would have gone unharnessed.

Table 5.11 Duration of pumping & water lifted (with particular rating PV panel).

Method	TFSM	IFSM	
Panel size	148	148	
H_d (m)	7 (FF tank)	4 (GF tank)	7 (FF tank)
Q (L/s)	0.03	0.08	0.03
Pumping duration (h)	3	1.0	3
Water lifted (L)	324	288	324
		Total: 612	

A comparative idea of cost calculations for both the methods is given in Table 5.12. It's assumed there is provision like landing space of staircase to keep the GF top tank. Hence no additional civil construction is required for this purpose. FF tank is kept on FF roof top. Cost of one 1000 L PVC tank is the same as the cost of two 500 L

PVC tanks. Tank cost is taken as Rs. 2.7/L. Cost of PV panel is taken as Rs.110 /W_p. Additional cost of Rs.1000 is allotted for IFSM towards 2-way valve and additional pipeline to be provided from pump to ground floor tank. The additional expenditure is of the order of 4%. This is not much compared to the increase in the additional water yield which is more than 80%. The effective cost per litre of water lifted daily is appreciably less.

Table 5.12 Cost calculations of TFSM & IFSM
(with particular rating PV panel).

Method	TFSM	IFSM
Cost of panel (Rs) @ Rs. 110/W_p	16280	16280
Pump cost (Rs)	5000	5000
Tank cost (Rs) @ Rs 2.7/L	2700	1350+1350 = 2700
Normal plumbing and others (Rs)	1000	1000
Additional expenditure (Rs) (additional plumbing & 2 way valve)	- - -	1000
Total cost (Rs)	24980	25980
Water yield (L)	324	612 (88% more)
Additional Expenditure		(25980-24980)/24980 = 4%
Effective total cost/Litre of water lifted (Rs/L)	24980/324 = 77	25980/ 612 = 41 {decrease: (77-41)/77 = 46% }

5.3.3.2 With a particular water requirement per day

Here the application of IFSM for solar water pumping for a particular volume of water requirement per day is presented taking the same two floored house and pump considered in section 5.3.3.1. Let the water requirement be 150 L/day for each floor (total: 300 L/day). Tests are conducted on different rating panels to find the peak power availability at different times of the day. Two panels (148 Wp & 124Wp) are selected which are found to meet the requirement in the present case. Their peak power availability is plotted in Fig 5.8 & 5.9. Power plots for both 148 Wp & 124 Wp sources are given simultaneously in Fig. 5.10 to drive home clearly the duration of pumping to different floor tanks in both the methods.

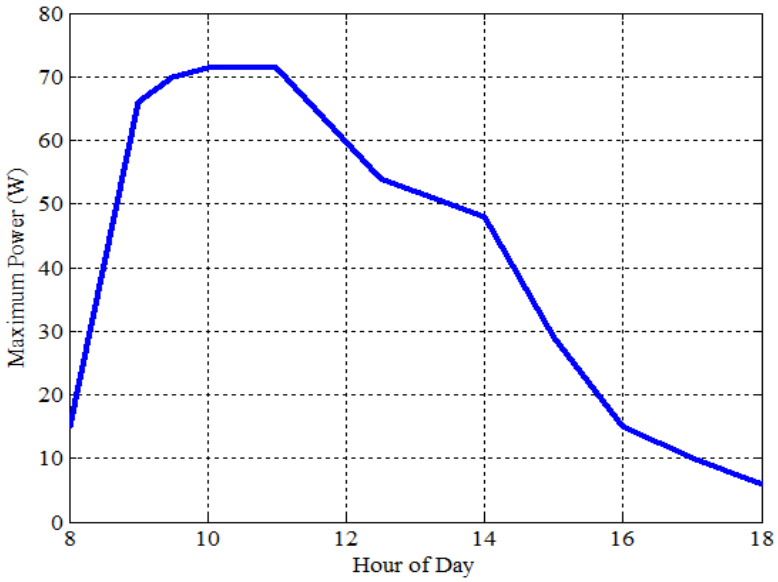

Fig 5.9 Maximum power curve for 124 W_p solar panel.

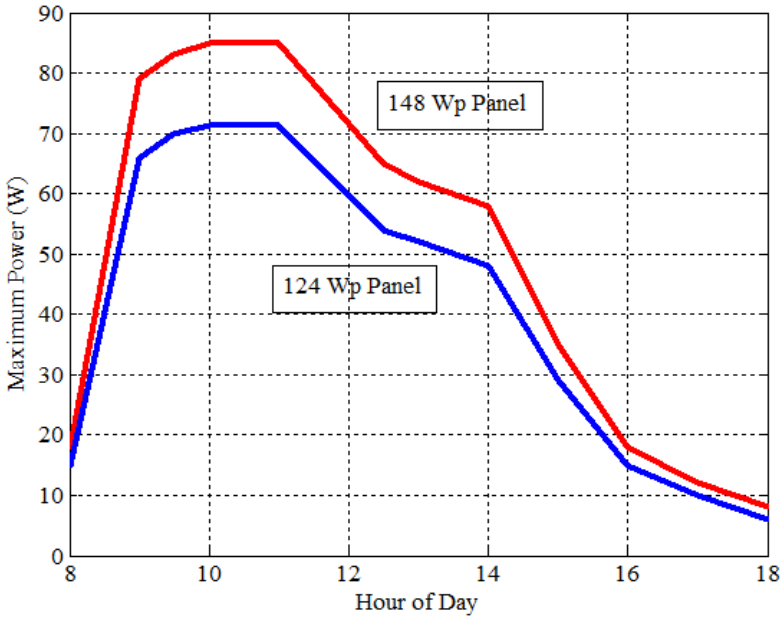

Fig 5. 10 Maximum power curves for 148 & 124 W_p source.

TFSM based proposal: The set-up for TFSM is as shown in Fig 5.6. One PVC tank of 500 L capacity is placed on FF top. Water is lifted from the sump to OH tank (H_d = 7 m) and stored. From there it's supplied to GF and FF. Features of the major components are to be as given in Table 5.13.

Table 5.13 Major components for TFSM (with particular water requirement/day).

Item	**Features**
PV panel size	148 W_p, 12 V.
OH tank	500 L PVC tank on FF top.
Pump	70-100 W, 12 V d.c., total head : 9 m, surface mounted.

Minimum power required for pumping to FF tank level is 70 W. From the panel characteristics (Fig 5.8) it is observed that power available is more than or equal to 70 W for 3 h. Hence pumping happens for about 3 h.

Water lifted = Flow rate x Duration of pumping

= 0.03 x (3x3600) = 324 L

Water lifted per watt of panel capacity = 324 /148 = 2.1 L/Wp

IFSM based proposal: The proposed set-up for IFSM is as shown in Fig 5.7. Two PVC tanks each of 250 L capacity are provided, one on GF top and the other on FF top. Pipe line is to be laid from pump to each tank separately through two way valve. 124 W_p panel is selected. Features of the major components for IFSM are to be as shown in Table 5.14. The same pump proposed for TFSM is selected here also.

Table 5.14 Major components for IFSM
(with particular water requirement/day).

Item	**Features**
PV panel size	124 W_p
OH tank	Two 250 L PVC tanks (one for each floor).
Pump	70-100 W, 12V d.c., total head: 9 m, surface mounted.
Pipe line	Independent pipeline with two way valve.

From the panel characteristics (Fig. 5.9) it is observed that power available is more than or equal to 70 W for 1.5 h and is within 60 to 70 W (i.e., ≥60 W & <70 W) for 1.5 h. Hence pumping is done for 1.5 h for GF tank. Taking flow rate from Table 5.7,

Water lifted = 0.08 x (1.5 x 3600) = 432 L

Pumping is done for 1.5 h for FF tank. Taking flow rate from Table 5.7,

Water lifted to FF tank = 0.03 x (1.5 x 3600) = 162 L

Total water lifted = 432 + 162 = 594 L.

Water lifted per watt of panel capacity = 594 /124 = 4.8 L/W_p

A comparative idea of different aspects for both the methods is given in Table 5.15. For the same minimum water supply of 150 L/day for each floor, TFSM employs 148 W_p panel whereas IFSM employs just 124 W_p panel resulting in downsizing of panel.

Table 5.15 Duration of pumping & water lifted
(with particular water requirement/day).

Method	TFSM	IFSM	
Panel Size	148 W_p	124 W_p	
Hd (m)	7 (GF tank)	4 (GF tank)	7 (IF tank)
Q (L/s)	0.03	0.08	1.75
Pumping Duration (h)	3	1.5	1.5
Water Lifted (L)	324	432	162
		Total: 594	

Cost and Saving Calculations

- The panel and OH tank ratings proposed above satisfy the water requirement for a normal sunny day. During cloudy days, the water yield reduces. Hence it is necessary to select higher size for panel and OH tank so as to provide certainty and consistency of water supply. Due to increased size of panel, the water pumped will be more than the normal requirement. Larger size of OH tanks will help to store this additional water. During cloudy or no-sun day, the

water pumped will be less than required. Then the backup storage in the tanks will come handy thus ensuring consistent water supply. Although increasing the sizes leads to increase in cost, it is inevitable.

- Decision regarding 'how much higher size is to be opted' is taken by taking in to account the information regarding the availability of radiation over the year at the location of interest. In the absence of such an information, usual approximate approach practised is to have the sizes increased by two times. Hence in the present case OH tank and panel sizes are increased by two times (Table 5.16). Proceeding in the same way as detailed in 5.5.3.1, a comparative idea of cost calculations for both the methods is given in Table 5.17.
- Saving or downsizing in PV panel capacity =148 x 2 - 124 x 2 = 48 W_p
- % Saving in peak power rating = 48/(148 x 2) = 16 %
- Saving in overall cost = 41260 - 36980 = Rs. 4280
- % Saving in initial expenditure = 4280/41260= 10.3 %

It can be observed from Table 5.17 that there is decrease in the required size of the panel by 16%. This results in decrease in panel cost. In addition to that, it also results in decrease in the area required for housing the panels. This is also a significant advantage particularly when the area available is limited or costly. Area required is approximately 1sqm for a 10A, 12V panel. In the case of roof top solar applications the area available for housing the panels is limited taking into account the shades coming due to adjoining buildings. Whereas for solar application in fertile land, the effective cost of area employed for housing solar panels turns out to be costly increasing the overall cost of the solar system. Hence the decrease in the required size of solar panel has multiple benefits.

Table 5.16 Panel sizing done accounting for cloudy days.

Method	TFSM	IFSM	
Panel size (W_p)	148 x 2 = 296	124 x 2 = 248	
OH tank size (L)	500 x 2 = 1000 (FF tank)	250 x 2 = 500 (GF tank)	250 x 2 = 500 (FF tank)

Table 5.17 Cost calculations accounting for cloudy days
(with particular water requirement/day)

Method	TFSM	IFSM
Cost of panel @ Rs. 110 /W_p	296 x 110 = 32560	248 x 110 = 27280
Pump Cost (Rs)	5000	5000
Cost of tank @ Rs 2.7/L	1000 x 2.7 = 2700	(500 x 2.7)+(500 x 2.7) = 2700
Plumbing and others (Rs)	1000	1000
Additional Expenditure (Rs)	- - -	1000 (additional plumbing & two way valve)
Total cost (Rs)	41260	36980
Monetary Saving (Rs)		4280
% Saving in initial expenditure		10.3 **%**

5.4 IMPORTANT RESULTS FROM THIS CHAPTER

This chapter has proposed a new strategy "Individual Floor Storage Method (IFSM)" for solar pumping in multi floored buildings. It is an improvement over the existing " Top Floor Storage Method (TFSM)". For the example of solar pumping for a two floored house, it is found that:

- For a specific rating of solar panel, IFSM results in more than 80 % increase in water harvested. Additional expenditure is only 4 %. The cost per litre of water is reduced by 46%.
- For a specific water requirement per day, IFSM leads to decrease in required size of solar panel by 16% and initial cost by 10% accounting for cloudy days. Additional advantages are the related reduction in floor area required and maintenance.

CHAPTER 6

DISCSSIONS & CONCLUSION

This chapter presents the discussions covering critical observations and concerns regarding the research work carried out. Then the scope for future work in the light of the experience of the present work is presented. Finally the concluding remarks are made summarising the entire work.

6.1 DISCUSSIONS

Solar pumping with MPPT by Load Voltage Tracking ($MPPT_{lv}$)

- Major advantage of $MPPT_{lv}$, the new method proposed for MPPT, is its simplicity as compared to the present more commonly employed method $MPPT_{pp}$.
- Another advantage of $MPPT_{lv}$ is the enhancement of output power to the pump load. Improvement in load power and hence the water output might seem to be less when looked at laboratory test results wherein the aspect of cloudy or no-sun days is not accounted for. But in real time application, this aspect needs to be considered and is taken care of by over sizing the solar panels. The extent of over sizing with $MPPT_{lv}$ is less compared to that with $MPPT_{pp}$ as the water yield with the former method is more. For examle, over sizing by 2 times is better than over sizing by 3 times the rated panel size. This leads to reduction in panel cost, maintenance cost and area required for panels. Thus overall economy becomes better.
- Major problem faced during practical testing with solar panel was the sudden and unexpected variation of insolation. It posed the problem of inconsistency of results obtained. This was managed by taking readings at many intervals so that few inconsistent values in between could be easily neglected. However this problem can be overcome by having an artificial sun and solar test setup within the laboratory.
- Lot of time is taken for each trial during discrete simulation testing of solar pump model and also during simulation implementation of $MPPT_{lv}$ algorithm for pump

load when working under 'normal mode'. An attempt was made to overcome this problem using 'accelerated mode' provision in the SIMULINK software. But with that, the performance was erratic and unstable for most of the times. Hence the 'normal mode' itself was employed.

Individual Floor Storage Method (IFSM) for Solar Pumping

- As a concept, IFSM is simple and economic.
- Another advantage of IFSM is that it leads to uniform distribution of dead weight as water storage is distributed on different floors.
- One concern generally raised is that the expenses for construction of new building with IFSM will be high compared to that with TFSM. The perception seems to be that in TFSM the over head (OH) tank is placed on the topmost terrace which is 'naturally available' whereas for IFSM additional special construction is necessary. In reality it's not so. Even in TFSM, the structural design has to account for the extra load due to OH tank being placed. For a new building, the cost for both the approaches is almost the same. Actually the cost of IFSM building will be slightly less (Deven et al. 2006).
- IFSM demands small structural modifications in existing buildings to position water tanks at different floors. However this provision can easily be made in design stage itself for new buildings.
- IFSM results in reduction in energy required for a specific requirement of water to be lifted. In other words, for a particular value of energy spent, the amount of water lifted with IFSM is more than that with TFSM. The increase in water output (or energy saving) depends on how much energy is spent on water lifting purpose for each floor i.e. pump performance as a function of head.
- IFSM yields greater benefits i.e. larger water harvesting (or higher energy saving) if implemented for multi floored buildings with large water consumption like hospitals, hostels, flat complexes etc. In the present day scenario of increasing number of multi floored buildings and escalating energy costs, proposed IFSM is more appropriate compared to the existing TFSM.

6.2 SCOPE FOR FUTURE WORK

- In the present work, though the MPPT converter was designed and implemented, the focus was more on validating the new proposal made for MPPT. Actual efficiency of the converter was found to be less, being in the range of 80-85%. The converter design needs to be fine tuned so as to get high efficiency of operation. Only when the converter efficiency gets enhanced, the advantage of any MPPT method will fully get translated as useful output power to the load thereby resulting in higher useful output from the load.
- It is required to develop an efficient hardware module for automatic closed loop control implementing $MPPT_{lv}$.
- In the process of simulation study, it was observed that maximum power harnessing can be done by varying the magnetic field of the DC motor even without MPPT converter. The magnetic field approach rather than electronic approach for realising MPPT seems to be more simple, rugged and reliable. But the problem is regarding the mechanism of changing the magnetic field as the brushed DC motor considered is of permanent magnet type wherein basically the field is fixed. The author made an attempt to explore the possibility of making the field variable in the existing motor itself but was not successful. This aspects deserves further probe. It opens up an altogether different field of work requiring development of a brushed PMDC motor with the field system which is derived using permanent magnets but still controllable in nature. This leads to "Variable Flux brushed PMDC motor for solar water lifting application". Details of the observations made in this regard are presented in appendix V.
- For solar pumping in multistoried buildings, IFSM necessitates devising proper control mechanism of directing water from pump to different floor OH tanks. Accomplishing this manually using a multi output valve is easy in situations where dedicated human operator is available. However an automatic setup, can also be provided.

6.3 CONCLUSION

Water pumping is an important application of solar PV power. However growth in the number of solar pumps is not promising. It is mainly due to higher cost per unit volume of water pumped and complex technology. These issues can be addressed by harnessing more power per unit installed capacity of the solar panel and making the system simple.

Present research work has dealt with the aspect of harnessing more power from PV panel using maximum power point tracking (MPPT) for water pumping application. The study is done considering a standalone water pumping system consisting of solar PV source feeding brushed PMDC motor coupled to centrifugal pump without battery backup.

Literature review indicates that different MPPT approaches are employed. Some of them are non interruptive and more accurate but highly complicated whereas others are simple but interruptive and less accurate. Present more commonly employed MPPT method is the one which employs panel power as the control parameter ($MPPT_{pp}$). But it is more complicated as it requires measurement of two parameters i.e. panel voltage as well as current and then multiplying them to obtain power value. Hence there is need for a method which is non interruptive, simple as well as accurate.

Simulation models are developed for the considered solar pumping system using MATLAB-SIMULINK. Simulation testing is done taking the cases of with and without MPPT converter. The role of MPPT converter in increasing the power harnessed and speed of the pump is demonstrated employing $MPPT_{pp}$ method.

Present thesis has proposed a novel method for accomplishing MPPT. The proposal is that load side voltage is to be used as control parameter for adjusting the duty cycle (D) of MPPT converter. Making load side voltage (V_a) maximum results in power also becoming maximum. Here the load voltage is tracked and D is continuously adjusted to make V_a maximum. This automatically ensures maximum power to the load. This method, "Maximum Power Point Tracking with load voltage

monitoring ($MPPT_{lv}$)" is independent of the ambient temperature. In this method, only one parameter i.e., V_a is to be sensed and hence is simpler than $MPPT_{pp}$.

The new proposal $MPPT_{lv}$ is substantiated by theoretical explanation and results from simulation. Experimental testing is also carried out and the results validate the proposal made. For pump load considered, the speed is proportional to motor voltage. As the motor voltage is made maximum, the speed also becomes maximum. This results in more water output as the water discharge of the pump at a particular head is directly proportional to the speed. It is found from the experimental testing that, due to the application of MPPT converter, increase in the output energy per day is 26.8% with $MPPT_{pp}$ and 40% with $MPPT_{lv}$. The corresponding increases in water harnessed are 29 % and 123 % respectively. It is clear that the proposed new method $MPPT_{lv}$ gives higher energy output and water yield. Thus the new method proposed has the dual advantage of simplicity and increased output.

An algorithm is developed to implement the proposal made for time changing solar insolations. The results show that at each insolation D varies automatically so that V_a and hence P_a are optimum at the corresponding insolation.

Another outcome of the research work is the development of a new strategy for solar pumping system for multi floored buildings. Position of over head (OH) storage tank in multi floored buildings is critical. The OH tank itself acts as the storage element. Presently “Top Floor Storage Method (TFSM)” is employed in multi floored buildings. A single OH tank is placed above the topmost floor. All the water is lifted up to that height and then brought down to lower floors. Here, even the water required at lower heights is unnecessarily lifted to higher levels resulting in more energy consumption, which is wastage. To overcome this demerit, a new strategy “Individual Floor Storage Method (IFSM)” is proposed. According to this, instead of one single large OH tank on topmost floor, small tanks at each floor height are to be employed supplying water to corresponding floor. Independent pipe line is laid from pump to each floor tank through a multi output valve. Water is pumped to each floor tank independently using the valve. Since the water is pumped to the required optimum heights only, it avoids wastage of energy. For a particular quantity of

available solar energy, the amount of water lifted will be more as IFSM enables use of panels for more duration. In other words, for a particular amount of water to be lifted, the photo voltaic (PV) panel size needs to be less. The direct consequence of this is a decrease in the cost. This is a significant advantage particularly with respect to solar pump as its main demerit is high cost.

For the example of a 2 floored house considered, with IFSM the increase in the water yield is more than 80%. Additional expenditure required is only 4% . Effective total cost per unit water lifted is appreciably reduced. On the other hand for a fixed volume of water requirement, the downsizing of solar panel is 16% with the corresponding decrease in initial cost of 10%. Due to downsizing of the solar panels there are additional benefits like reduction in maintenance cost and area required for panels. These gains will be more pronounced when the solar pumping system is designed accounting for the cloudy or no-sun days.

IFSM is complimentary to the aspect of harnessing maximum energy from solar PV panel discussed earlier. It can be incorporated in addition to implementing MPPT. IFSM demands small structural modifications in existing buildings to position water tanks at different floors. However this provision can easily be made in design stage itself for new buildings. IFSM necessitates devising proper control mechanism for directing water from pump to different floor tanks. Accomplishing this manually using a multi output valve is easy in situations where dedicated human operator is available.

The two new proposals, $MPPT_{lv}$ & IFSM made in this research work, giving increased water yield from the solar pump for a particular capacity of solar panel, are expected to increase the acceptability of solar PV water pumps and thus contribute to their growth.

APPENDIX I

IMPORTANT MPPT METHODS

a) MPPT BY PANEL POWER TRACKING ($MPPT_{pp}$): PERTURB & OBSERVE (P&O) ALGORITHM

MPPT by panel power tracking ($MPPT_{pp}$) is realised by P&O algorithm. It is simple, easy to implement and hence more commonly used in practice. It is known as "hill climbing" method. Fig. A.I.1 shows a PV module's output power curve as a function of voltage at constant insolation and module temperature. Let the PV module be operating at a point which is away from the maximum power point (MPP). In this algorithm the operating voltage of the PV module is perturbed by a small increment, and the resulting change of power, *P*, is observed. If the *P* is positive, then it is supposed that it has moved the operating point closer to the MPP. Thus, further voltage perturbations in the same direction should move the operating point towards the MPP. If the *P* is negative, the operating point has moved away from the MPP, and the direction of perturbation should be reversed to move back towards the MPP. Fig. A.I.2 shows the flowchart of this algorithm.

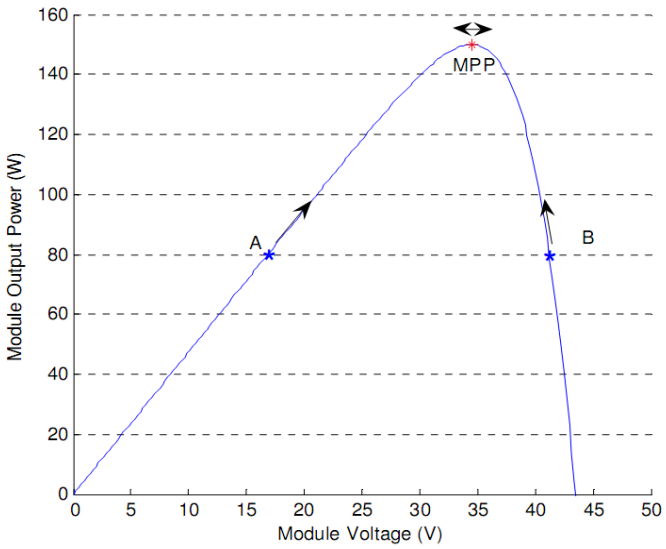

Fig. A.I.1 Power curve of PV module: P&O method.

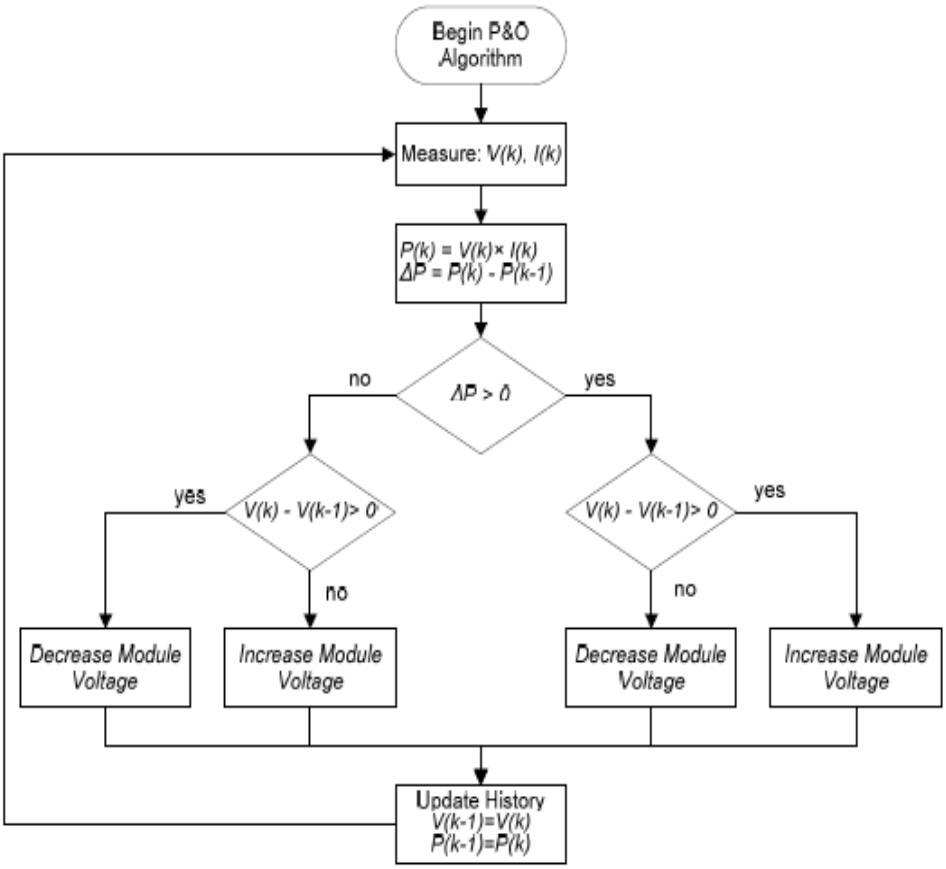

Fig. A.I.2 Flow chart of P&O algorithm.

b) MPPT BY INCREMENTAL CONDUCTANCE (IC) METHOD

This method overcomes the problem of the P&O algorithm under rapidly changing atmospheric conditions. It is based on the idea that the slope of *P-V* curve becomes zero at the MPP (Fig. 2.2).

$dP/dV = 0$ at MPP (A.I.1)

$(dP/dV) > 0$ on the left of MPP (A.I.2)

$(dP/dV) < 0$ on the right of MPP (A.I.3)

The above equations are written in terms of voltage and current as follows.

$$(dP/dV) = d(V.I)/dV = IdV/dV + VdI/dV = I + VdI/dV \quad \text{(A.I.4)}$$

If the operating point is at the MPP, the equation (A.I.4) becomes:

$$I + VdI/dV = 0 \quad \text{(A.I.5)}$$

$$dI/dV = -(I/V) \quad \text{(A.I.6)}$$

If the operating point is on the left side of the MPP, the equation (A.I.4) becomes:

$$I + VdI/dV > 0 \quad \text{(A.I.7)}$$

$$dI/dV > -I/V \quad \text{(A.I.8)}$$

If the operating point is at the right side of the MPP, the equation (A.I.4) becomes:

$$I + VdI/dV < 0 \quad \text{(A.I.9)}$$

$$dI/dV < -I/V \quad \text{(A.I.10)}$$

In the equations (A.I.6), (A.I.8) & (A.I.10), left side represents incremental conductance of the PV module and the right side of the equations represents its instantaneous conductance.

Fig. A.I.3 shows the flowchart of this algorithm. The algorithm starts with measuring the present values of PV module voltage and current. Then, it calculates the incremental changes, *dI* and *dV*, using the present values and previous values of voltage and current. The main check is carried out using the relationships in the equations (A.I.6), (A.I.8), and (A.I.10). If the condition satisfies the inequality (A.I.8), it is assumed that the operating point is at the left side of the MPP thus must be moved to the right by increasing the module voltage. Similarly, if the condition satisfies the inequality (A.I.10), it is assumed that the operating point is at the right side of the MPP, thus must be moved to the left by decreasing the module voltage. When the operating point reaches at the MPP, the condition satisfies the equation (A.I.6), and the algorithm bypasses the voltage adjustment.

At the end of cycle, it updates the history by storing the voltage and current data that will be used as previous values in the next cycle. Another important check included in this algorithm is to detect atmospheric conditions. If the MPPT is still operating at the MPP (condition: $dV = 0$) and the irradiation has not changed (condition: $dI = 0$), it takes no action. If the irradiation has increased (condition: $dI > 0$), it raises the MPP voltage. Then, the algorithm will increase the operating voltage to track the MPP. Similarly, if the irradiation has decreased (condition: $dI < 0$), it lowers the MPP voltage. Then, the algorithm will decrease the operating voltage. In

practice, the condition $dP/dV = 0$ (or $dI/dV = -I/V$) seldom occurs because of the approximation made in the calculation of dI and dV. Thus, a small margin of error should be allowed.

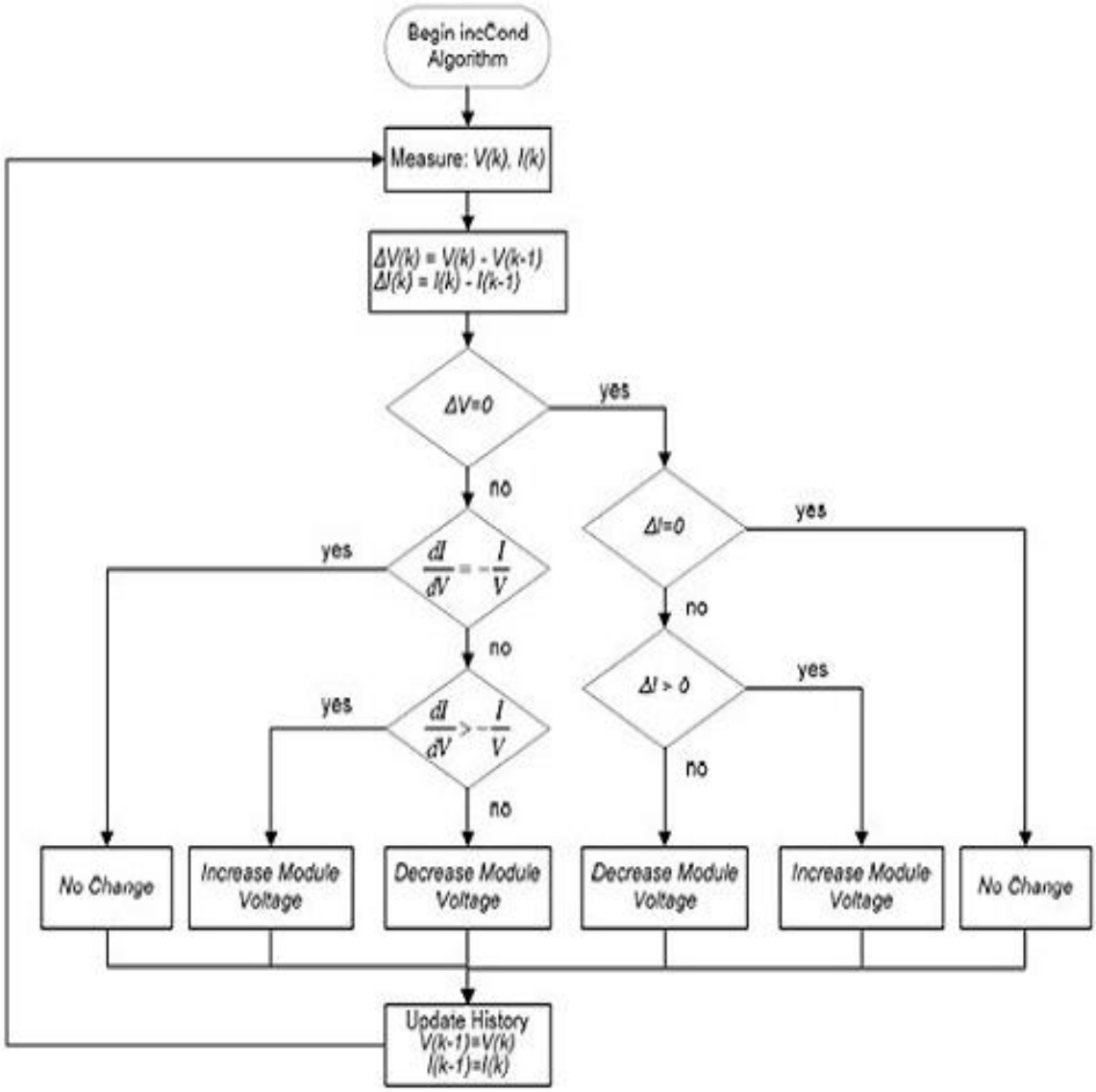

Fig.A.I.3 Flow chart of IC algorithm.

APPENDIX II

MATLAB/ SIMULINK: OVERVIEW

MATLAB stands for ”Matrix Laboratory”. It's a high-level language for technical computing developed by The Math Works Incs. In the present research work, MATLAB Version 7.7. 0.471(R2008b) (9.10.2008) is employed. MATLAB is a technical computing environment providing advanced analyses, data visualization, and the framework to develop customized algorithms. The open MATLAB language enables the sharing of ideas and the development of solutions. Interfaces to other programming languages, including Fortran and C, are provided. With more than 600 mathematical, statistical, and engineering functions, MATLAB gives immediate access to high-performance numerical computing. This functionality is extended with interactive graphical capabilities for creating plots, images, surfaces, and volumetric representations. The functionality is further extended with add-on toolboxes.

Simulink, which provides a graphical design environment for modeling and simulating complex systems, is also available on this service. It supports linear and nonlinear systems, modeled in continuous time, sampled time, or a hybrid of the two. Simulink provides a graphical user interface (GUI) for building models as block diagrams. Simulink also includes a comprehensive block library of sinks, sources, linear and nonlinear components, and connectors. If these blocks do not meet the needs, however, one can create their own blocks. The simulation results can be seen while the simulation runs using scopes and other display blocks. Different parameters can be changed and the effects can be seen for "what if" exploration. The simulation results can be put in the MATLAB workspace for post processing and visualization. Simulink software is tightly integrated with the MATLAB environment. It requires MATLAB to run, define and evaluate model and block parameters. Simulink can also utilize many MATLAB features. For example, Simulink can use the MATLAB environment to define model inputs, store model outputs for analysis and visualization, perform functions within a model through integrated calls to MATLAB operators and functions.

STB55NF06 STB55NF06-1 STP55NF06 STP55NF06FP

N-CHANNEL 60V - 0.015 Ω - 50A TO-220/TO-220FP/I²PAK/D²PAK STripFET™ II POWER MOSFET

TYPE	V_{DSS}	$R_{DS(on)}$	I_D
STP55NF06	60 V	<0.018 Ω	50 A
STB55NF06-1	60 V	<0.018 Ω	50 A
STB55NF06	60 V	<0.018 Ω	50 A
STP55NF06FP	60 V	<0.018 Ω	50 A(*)

- TYPICAL $R_{DS}(on)$ = 0.015 Ω
- EXCEPTIONAL dv/dt CAPABILITY
- 100% AVALANCHE TESTED
- SURFACE-MOUNTING D^2PAK (TO-263) POWER PACKAGE IN TUBE (NO SUFFIX) OR IN TAPE & REEL (SUFFIX "T4")
- THROUGH-HOLE I^2PAK (TO-262) POWER PACKAGE IN TUBE (SUFFIX "-1")

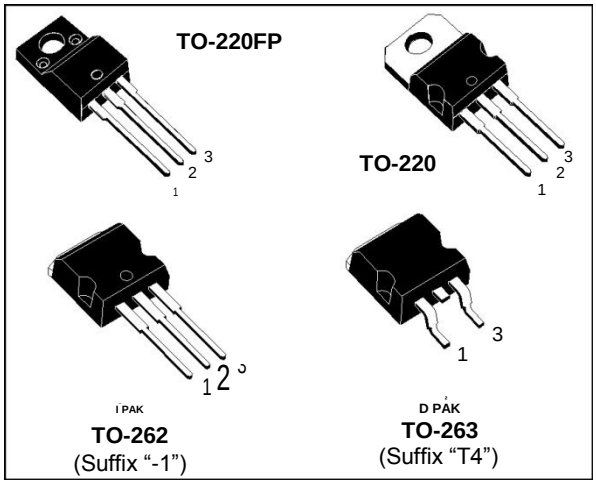

DESCRIPTION

This Power MOSFET is the latest development of ST-Microelectronis unique "Single Feature Size™" strip-based process. The resulting transistor shows ex-tremely high packing density for low on-resistance, rugged avalanche characteristics and less critical alignment steps therefore a remarkable manufactur-ing reproducibility.

INTERNAL SCHEMATIC DIAGRAM

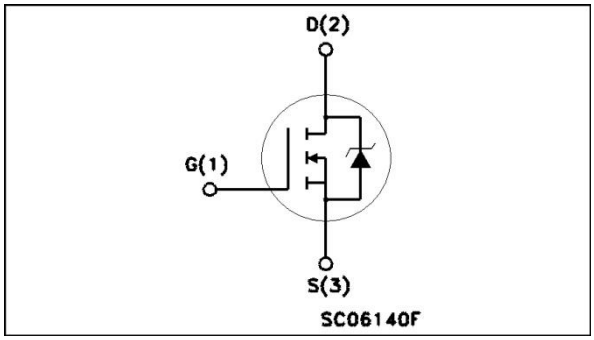

APPLICATIONS

- HIGH CURRENT, HIGH SWITCHING SPEED
- MOTOR CONTROL, AUDIO AMPLIFIERS
- DC-DC & DC-AC CONVERTERS
- AUTOMOTIVE

ABSOLUTE MAXIMUM RATINGS

Symbol	Parameter	Value		Unit
		STP_B55NF06(-1)	STP55NF06FP	
V_{DS}	Drain-source Voltage (V_{GS} = 0)			V
V_{DGR}	Drain-gate Voltage (R_{GS} = 20 kΩ)	60		V
V_{GS}	Gate- source Voltage	± 20		V
I_D	Drain Current (continuous) at T_C = 25°C	50	50(*)	A
I_D	Drain Current (continuous) at T_C = 100°C	35	35(*)	A
I_{DM}(•)	Drain Current (pulsed)	200	200(*)	A
P_{tot}	Total Dissipation at T_C = 25°C	110	30	W
	Derating Factor	0.73	0.2	W/°C
dv/dt (1)	Peak Diode Recovery voltage slope	7		V/ns
E_{AS} (2)	Single Pulse Avalanche Energy	350		mJ
T_{stg}	Storage Temperature	-55 to 175		°C
T_j	Operating Junction Temperature			

(•) Pulse width limited by safe operating area

(*)Refer to soa for the max allowable current value on FP-type due to Rth value

(1) I_{SD} ≤50A, di/dt ≤400A/µs, V_{DD} ≤ $V_{(BR)DSS}$, T_j ≤ T_{JMAX}

(2) Starting T_j = 25 °C, I_D = 25A, V_{DD}= 30V

APPENDIX IV

International
IOR Rectifier

Data Sheet No. PD60147 rev.U

IR2110(-1-2)(S)PbF/IR2113(-1-2)(S)PbF

HIGH AND LOW SIDE DRIVER

Features

- Floating channel designed for bootstrap operation
  Fully operational to +500V or +600V
  Tolerant to negative transient voltage
  dV/dt immune
- Gate drive supply range from 10 to 20V
- Undervoltage lockout for both channels
- 3.3V logic compatible
  Separate logic supply range from 3.3V to 20V
  Logic and power ground ±5V offset
- CMOS Schmitt-triggered inputs with pull-down
- Cycle by cycle edge-triggered shutdown logic
- Matched propagation delay for both channels
- Outputs in phase with inputs

Product Summary

V_{OFFSET}	(IR2110)	500V max.
	(IR2113)	600V max.
I_O+/-		2A / 2A
V_{OUT}		10 - 20V
$t_{on/off}$ (typ.)		120 & 94 ns
Delay Matching	(IR2110)	10 ns max.
	(IR2113)	20ns max.

Packages

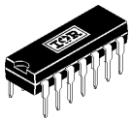

14-Lead PDIP
IR2110/IR2113

16-Lead SOIC
IR2110S/IR2113S

Description

The IR2110/IR2113 are high voltage, high speed power MOSFET and IGBT drivers with independent high and low side referenced output channels. Proprietary HVIC and latch immune CMOS technologies enable ruggedized monolithic construction. Logic inputs are compatible with standard CMOS or LSTTL output, down to 3.3V logic. The output drivers feature a high pulse current buffer stage designed for minimum driver cross-conduction. Propagation delays are matched to simplify use in high frequency applications. The floating channel can be used to drive an N-channel power MOSFET or IGBT in the high side configuration which operates up to 500 or 600 volts.

Typical Connection

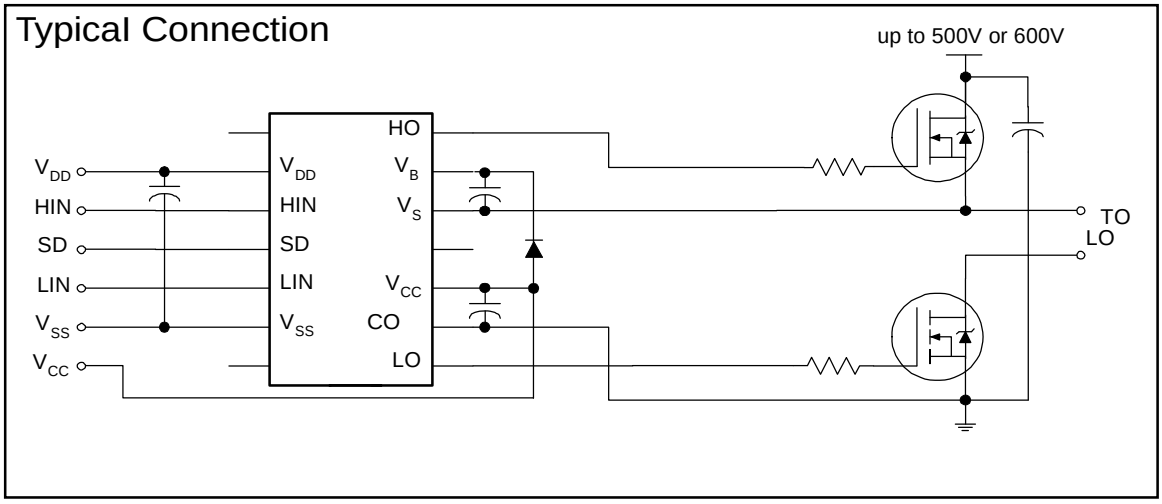

APPENDIX V

SOLAR PUMPING WITH VARIABLE EXCITATION

In this section the effect of varying field excitation on the performance of the DC motor in the solar pumping system without MPPT converter (Fig. A.V.1) is discussed. It is shown that maximum power can be obtained by controlling excitation i.e. field current (I_f) even without MPPT converter. Theoretical background and simulation results are provided for the same.

Three cases of solar pumping system are considered:

a) With fixed (rated) I_f ; without MPPT converter.
b) With Fixed (rated) I_f ; with MPPT converter.
c) With variable I_f ; without MPPT converter.

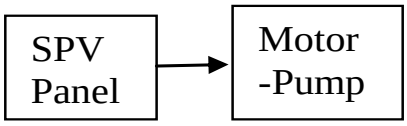

Fig.A.V.1 Solar pumping system without MPPT converter.

A.V. 1 THEORETICAL BACKGROUND

It was shown in section 3.3 that the load equation for solar pumping system with 4 m head can expressed in terms of electrical quantities as shown in equation (3.16). Here that equation is taken and written in terms of E_b using the basic relation between V_a, I_a and E_b given in equation (3.10) yielding equation (A.V.1).

$$4.8\times10^{-6}\, V_a^2/K_b^2 - 0.00019\, V_a/K_b - 6.72\times10^{-6}\, V_a\, I_a/K_b^2 + 2.35\times10^{-6}\, I_a^2/K_b$$
$$- 0.00013\, I_a/K_b - K_b I_a + 0.092 = 0 \qquad \text{(A.V.1)}$$

When I_f is changed, E_b also will vary as E_b is related to I_f. Three different I_f values, 50%, 100% and 200% of the rated value are considered. For each I_f, the corresponding values of E_b and hence the load equation is obtained. Assuming different voltages V_a, values of I_a are obtained by calculation (Table A.V.1) giving load characteristics like

"V_a vs. I_{a1}", "V_a vs. I_{a2}" and "V_a vs. I_{a3}". Then these load curves are superimposed on V_p - I_p characteristics of PV panel (Fig.3.6) as shown in Fig A.V.2.

Table A.V.1 Load equations for different excitations.

V_a	I_{a1} For $0.5I_f$	I_{a2} For I_f	I_{a3} For $2I_f$
4	3.5	2.4	1.2
6	5.2	3.25	1.4
8	7	4.3	1.7
10	9	5.5	2
12	11	6.9	2.5
14			3.0
16			3.6
18			4.2

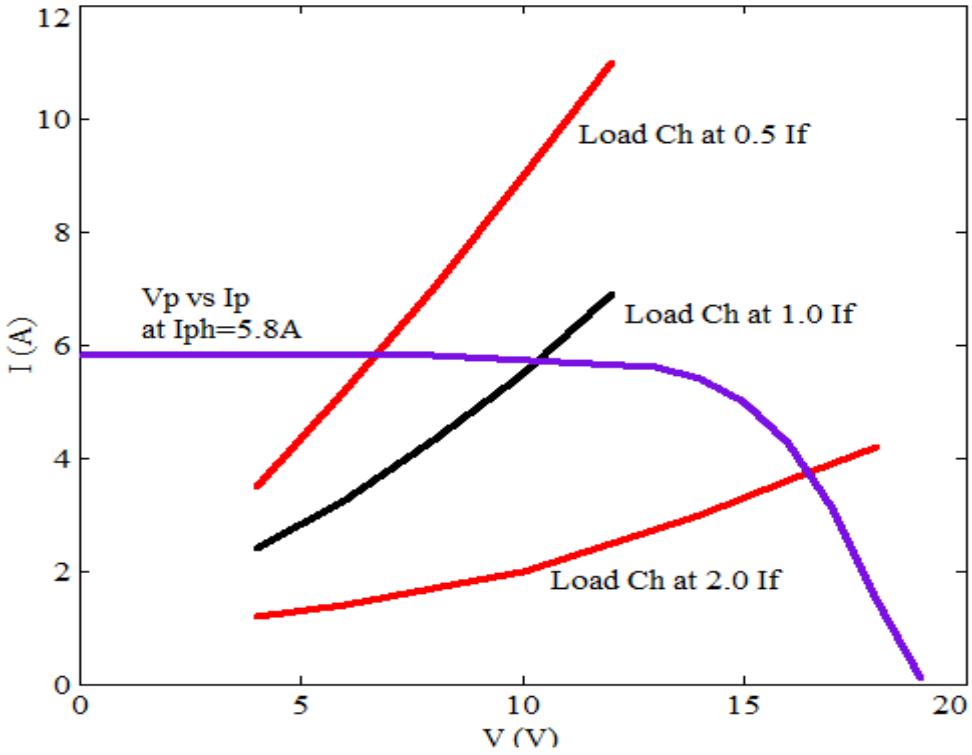

Fig.A.V.2 "Motor-pump load characteristics (varying field)" superimposed on "V-I curve of PV panel".

It is observed from Fig. A.V.2 that load curve for each I_f intersects the V-I curve of the PV panel at different points. This means by changing excitation of motor, the operating point also gets shifted. By suitably adjusting I_f, the operating point can be made to coincide with maximum power thus enhancing the output power almost the same way as done in the system with MPPT converter. This in itself unfolds as a means of realising maximum power even without MPPT converter. This results in increase in speed of pump and hence the water output. It can also be observed that more excitation is required at low radiation. Increased excitation at lower radiation gives higher torque.

A.V.2 SIMULATION

Simulation tests are conducted for both the cases i.e., the system with fixed I_f, with MPPT converter and the system with varying I_f, without MPPT converter (Table A.V.1 & A.V.2). It is observed that by varying I_f, the maximum power can be obtained similar to as is obtained by using MPPT converter. The same type of behaviour is observed regarding the pump speed also. The plot of the speeds corresponding to different cases (Fig.A.V.3) indicates that speed of pump is less when the excitation is fixed and MPPT converter is not employed. The pump speed becomes high in the pump without MPPT converter by varying the excitation. The increase in speed is on par with that obtained by employing MPPT converter.

Table A.V.2 Effect of varying DC motor flux on pump performance.

Inso-lation	"PV Panel – Motor" (Without Converter –Changing I_f)					"PV Panel – Converter- Motor" (With Converter – Fixed I_f) For Max Power					
I_{ph} (A)	**I_a (A)**	**V_{pv} (V)**	**I_f (of rated)**	**ω (rad/s)**	**T (Nm)**	**V_a (V)**	**I_a (A)**	**V_{pv} (V)**	**I_{pv} (A)**	**ω (rad/s)**	**T (Nm)**
4	4	3.75	0.9	62	0.1	7.3	5.9	15	3.2	**143**	0.16
	4	4.5	**1.0**	**83.5**	0.11						
	4	5.25	1.1	99.5	0.12						
	4	5.95	1.2	113	0.13						
	4	6.7	1.3	124.5	0.14						
	4	8.17	**1.5**	**144.2**	0.16						
5	5	5.35	0.9	103	0.12	8.3	6.8	13.5	4.5	**160.8**	0.18
	5	6.05	**1.0**	**119**	0.13						
	5	6.8	1.1	132	0.15						
	5	7.55	1.2	144	0.16						
	5	8.3	1.3	155	0.17						
	5	9.1	**1.4**	**165**	0.19						
6	6	6.55	0.9	130	0.14	8.3	6.8	13.5	4.5	**160.8**	0.18
	6	7.3	**1.0**	**144**	0.16						
	6	8.1	1.1	157	0.18						
	6	8.5	**1.15**	**163.5**	0.19						
7	7	7.64	0.9	150	0.17	8.85	7.4	11.9	6.1	**173.7**	0.2
	7	8.46	**1.0**	**165.5**	0.19						
	7	8.87	**1.05**	**172**	0.2						
	7	9.31	1.1	178.5	0.21						
8	8	8.65	0.9	169	0.19	8.85	7.4	11.9	6.1	**173.7**	0.2
	8	9.5	**1.0**	**184**	0.22						
	7.75	10.2	1.1	193	0.23						
9	8.64	9.28	0.9	180	0.21	9.3	7.8	10.1	7.8	**179.8**	0.21
	8.2	9.75	**1.0**	**187.5**	0.22						
	7.8	10.2	1.1	193.5	0.23						

Table A.V.3 Comparison of "System with converter" and "Direct system with fixed & varying flux".

I_{ph} (A)	With MPPT converter	Without MPPT converter		
		Fixed (rated) Excitation	Variable Excitation	
	ω (rad/s)	ω (rad/s)	ω (rad/s)	I_f (of rated)
4	143	83.5	144.2	1.5
5	160.8	119	165	1.4
6	160.8	144	163.5	1.15
7	173.7	165.5	172	1.05
8	173.7	184	184	1.0
9	179.8	187.5	187.5	1.0

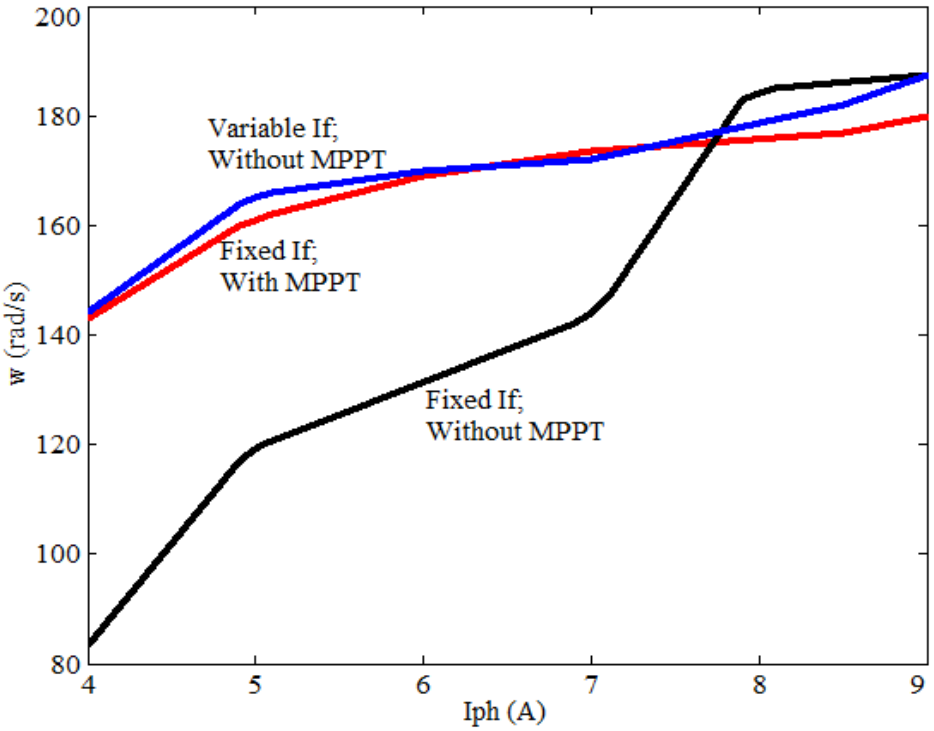

Fig A.V.3 Comparison: System with MPPT converter and Direct system with fixed & varying Flux.

A.V.3 HOW TO VARY EXCITATION?

Now the question that arises is the approach to change the excitation because the motor considered here is PMDC brushed motor. At the very outset, in the presently available PMDC brushed motor, it is not possible to vary the excitation. What is required is a PMDC motor with the possibility of varying the excitation.

Just to give an idea of the internal configuration, the images of the presently employed PMDC brushed motor are given below. Fig.A.V.4 presents the different components of the motor like the end cap, stator, armature and the impellor block. Fig. A.V.5 shows only the stator separately. The two permanent magnets are prominently visible. It can also be observed that in the space between the two poles, there are small permanent magnets. These small magnets are the additional ones placed by the author in an attempt to vary the excitation. However the attempt did not yield the expected results. Fig. A.V.6 shows again the stator but with an attempt of inserting an electromagnet in between the two main permanent poles. Even this attempt also did not yield the expected results. The problem needs to be tackled at the fundamental level, posing a challenge of developing a new motor configuration with modified design of the magnetic circuit.

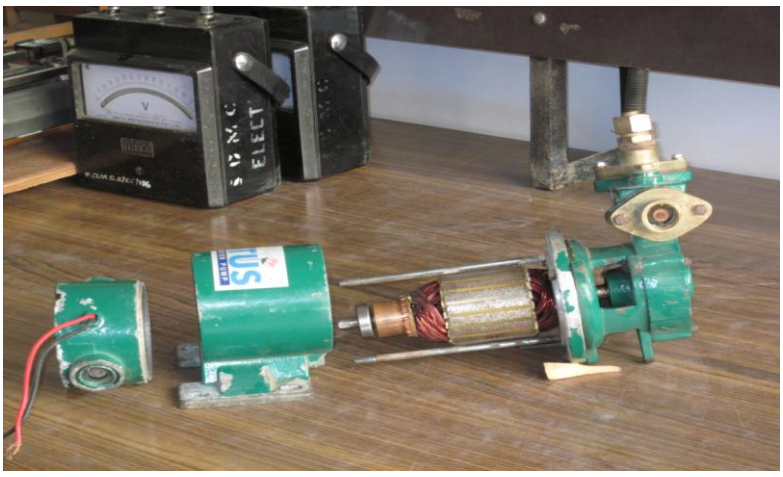

Fig. A.V.4 Different components of PMDC brushed motor.

Fig. A.V.5 Stator of PMDC motor showing the poles.

Fig. A.V.6 Stator of PMDC motor showing field coil.

REFERENCES

- Abdelmalek, M., Abdelhamid, M., Nossair Z., Dahane K., and Said, H. (2007). "Test and Analysis of a Photovoltaic DC-Motor Pumping System." *Proc., Mediterranean Winter Conference* , ICTON-MW'07, 1-7.
- Abidin, F. Z. and Bulent, Y. (2004). "New Approaches on the Optimization of Directly Coupled PV pumping Systems." *Solar Energy*, 77, 81-93.
- Alghuwainum S. M. "Speed Control of a PV Powered DC Motor Driving a Self Excited 3-Phase Induction Generator for Maximum Utilization Efficiency" IEEE Transactions; 11(4), Dec 1996, 768-773.
- Alghuwainem, S.M. (1994). "Matching of a DC motor to a photovoltaic generator using a step-up converter with a current-locked loop." *IEEE Transactions on Energy Conversion*, 9(1), 192–198.
- Anderson, P.G.O. (2000). "The role, reliability and limitations of solar photo-voltaic systems in Botswana." *Proc., Ninth International Conference on Harmonics and Quality of Power*, 3, 973-982.
- Anis, W.R. and Metawally, H.M.B. (1994). "Dynamic Performance of a Directly Coupled PV Pumping System." *Solar Energy*, 53(40), 369-377.
- Appelbaum, J. (1989). "The Operation of Loads Powered by Separate Sources or by a Common Source of Solar Cells." *IEEE Transactions on Energy Conversions*, 4(3), 351-357.
- Appelbaum, J. and Sarma, M. S. (1989). "The Operation of Permanent Magnet DC Motors Powered by a Common Source of Solar Cells." *IEEE Transactions on Energy Conversions*, 4(4), 635-642.
- Armando, B., Stefano, B., Vincenzo, L. and Cristina, C. (2009). "Simplified Model of a Photovoltaic Module." *Proc., of Applied Electronics Conference*, 47-51.
- Arrouf, M. and Ghabrour, S. (2007). "Modelling and simulation of a pumping system fed by photovoltaic generator within the Matlab/Simulink programming environment." *Desalination*, 209 (1-3), 23-30.
- Bhargava, B. (1994). "Solar Photovoltaic Programme." *Electrical India*, Sept, 15-18.

- Bogdan, S. B. and Ziyad, M. S. (1994). "Optimum photovoltaic Array Size for a Hybrid Wind/PV System." *IEEE Transactions on Energy Conversion*, 9(3), 482-488.
- Bogdam, M.W. and Xiangli, L. (2002). "Fuzzy System Based Maximum Power Point Tracking." *Proc., IEEE 28th Annual Conference of the Industrial Electronics Society, IECON 02*, 4, 3280-3284.
- Calavia, M., Perié, J.M., Sanz, J.F. and Sallán, J. (2010). "Comparison of MPPT strategies for solar modules." *Proc., International Conference on Renewable Energies and Power Quality*.
- Casey Roshau, Subbaraya Yuvarajan and Doug Schulz (2009). "Modelling And Hardware Implementation Of V_{mppt} for A PV Panel with a Reference Cell." *Proc., IEEE Photovoltaic Specialists Conference*, PVSC, 1033-1037.
- CEA (2014) www.cea.org
- CERC (2013). www.cercind.gov.in/2013/annual_report.
- Chandrasekaran, N. and Thyagarajah, K. (2011). "Modelling and MATLAB simulation of pumping system using PMDC motor powered by solar system." *European Journal of Scientific Research*, 59(1), 6-13.
- Chowdhury, B.H., Ula, S. and Stokes, K. (1993). "Photovoltaic-powered water pumping-design, and implementation: case studies in Wyoming." *IEEE Transactions on Energy Conversion*, 8(4), 646 - 652.
- Clin Lashway (1988). "Photovoltaic System Testing Techniques and Results." *IEEE Transactions on Energy Conversion*, 3(3), 503-505.
- Clinton Slabbert and Michel Malengret (1998). "Grid Connected Solar Water Pump for Rural Areas." *Proc., International Symposium on Industrial Electronics*, 31-34
- Cristinel Ababei, Subbaraya Yuvarajan and Douglas, L. S. (2010). "Toward integrated PV panels and power electronics using printing technologies." *Solar Energy*, 84(7), 1111-1123.
- Davies, J.L. and Malengret, M. (1992). "Application of Induction Motor for Solar Water Pumping." Proc., IEEE 3rd AFRICON Conference, 209-212.

- Deven, J.B., Revankar, R. and Gadanthi, U.S. (2006). "Cost Effectiveness and Energy Efficiency of Individual Tanks over an OHT in a Multistoried Building." *Project Thesis, Bachelor of Engineering (Civil), Visvesvaraya Technological University*, Belgaum, India.
- Dunlop, J.P. (1988). "Analysis and design optimization of photovoltaic water pumping systems." *Proc., Twentieth IEEE Photovoltaic Specialists Conference,*2, 1182-1187.
- Eduardo, I. Ortiz-Rivera (2008). "Maximum Power Point Tracking using the Optimal Duty Ratio for DC-DC Converters and Load Matching in Photovoltaic Applications." *Proc., IEEE 23rd Annual Applied Power Electronics Conference & Exposition*, 987-991.
- Enslin, J.H.R. and Snyman, D. B. (1991). "Combined Low Cost High Efficient Inverter, Peak Power Tracker and Regulator for PV application." *IEEE Transactions on Power Electronics*, 6(1), 73-82.
- Eugenio, F., Gian, C. C. and Pier, U. C. (1991). "Architectural and Design Issues on Optimal Management of Photovoltaic Pumping Systems." *IEEE Transactions on Industrial Electronics*; 38(5), 385-392.
- Fam, W. Z. and Balachander M. K. (1988). "Dynamic Performance of a DC Shunt Motor Connected to Photovoltaic Array." *IEEE Transactions on Energy Conversion*,3(3), 613-617.
- Francisco, M. G. L. (2005). "Model of Photovoltaic Module in Matlab." *Proc., 2nd Electrical Engineering Congress (II CIBELEC 2005).*
- Ghoneim, A.A. (2006). "Design optimization of photovoltaic powered water pumping systems." *Energy Conversion & Management*, 47, 1449-1463.
- Gilbert, M. Masters (2004). "Renewable and Efficient Electric Power Systems." *John Wiley & Sons, Inc., Publication*.
- Hadj, A. Arab, Benghanem, M. and Chenlo, F. (2006). "Motor Pump System Modelization." *Renewable Energy*, 31, 905-913.
- Hairul Nissah Zainudin and Saad Mekhilef (2010). "Comparison Study of Maximum Power Point Tracker Techniques for PV Systems." *Proc. of International Middle East Power Systems Conference*, Egypt, 750-755.

- Hamid Metwally and Wagdy Anis (1996). "Dynamic Performance of Directly Coupled Photovoltaic Water Pumping System Using DC Shunt Motor." *Energy Conversion Management*, 37(9), 1407-1416.
- Hamid, M. B. and Wagdy Anis (1997). "Performance analysis of PV pumping systems using switched reluctance motor drives." *Energy Conversion and Management*, 38(1), 1-11.
- Hamidat, A. and Benyoucef, B. (2008). "Mathematic models of photovoltaic motor-pump systems." *Renewable Energy*, 33 (5), 933-942.
- Hohm, D. P. and Ropp, M. E. (2003). "Comparative Study of Maximum Power Point Tracking Algorithms." *Progress in Photovoltaic Research and Applications*, 11, 47-62.
- Hussein, K.H. and Zhao, G. (1995). "Maximum Photovoltaic Power Tracking: An Algorithm for Rapidly Changing Atmospheric Conditions." *IEE Proceedings of Generation, Transmission, Distribution*,142 (1), 59-64.
- IEA (International Energy Agency) Key World Energy Statistics 2013.
- Jantsch, M., Real, M., Haberlin, H., Whitaker, C., Kurokawa, K., Blasser, G., Kremer, P. and Verhoeve, C.W.G. (1997). "Measurement of PV Maximum Power Point Tracking Performance." *Netherlands Energy Research Foundation* ECN.
- Kagarakis, C.A. and Avaritsiotis, J.N. (1989). "Assessment of solar photovoltaic systems at the level of rural electrification." *Proc., Electrotechnical Conference MELECON '89,* 'Integrating Research, Industry and Education in Energy and Communication Engineering', Mediterranean, 31–33.
- Katan, R.E., Agelidis, V.G. and Nayar, C.V. (1996). "Performance analysis of a solar water pumping system." *Proc., International Conference on Power Electronics, Drives and Energy Systems for Industrial Growth*, 1, 81-87.
- Kim, J. M., Kim, Y. C., Kim, S. S., Yi, J. S. and Won, C. Y. (1997). "A Study on the Maximum Power Tracking of Photovoltaic Power Generation System using a Neural Network Controller." *Sungkyunkwan University Journal*, Korea, 132-139.
- Kim, Y., Jo, H. and Kim, D. (1996). "A New Peak Power Tracker for Cost Effective Photovoltaic Power Systems." *IEEE Proceedings*, 1996, 3(1), 1673-1678.

- Kiranmayi, R., Vijaya Kumar Reddy, K. and Vijaya Kumar, M. (2008). "Modelling and a MPPT Method for Solar Cells." *Journal of Engineering and Applied Sciences,* (Medwll Journals), 3(1), 128-133.
- Kirk Stokes and John Bigger (1993). "Reliability, Cost, and Performance of PV Powered Water Pumping Systems: A Survey for Electric Utilities." *IEEE Transactions on Energy Conversion*, 8(3), 506-512.
- Kolhe, M.; Joshi, J.C. and Kothari, D.P. (2004). "Performance analysis of a directly coupled photovoltaic water-pumping system." *IEEE Transactions on Energy Conversion* , 19(3), 613 - 618.
- Kou, Q., Klein, S. A. and Beckman, W. A. (1998). "A Method for Estimating the Long Term Performance of Direct Coupled PV Pumping Systems." *Solar Energy*, 64(1), 33-40.
- Liebenberg, R., Enslin, JHR. and Van der Merve FS. (1993). "High Efficiency Long Life Actuator for PV Water Pumping Application." *Proc., European Conference on Power Electronics and Applications*, 5, 495-500.
- Lujara, N.K., Van Wyk, J.D. and Materu, P.N. (1999). "Loss models of photovoltaic water pumping systems." Proc., IEEE Conference AFRICON, 2, 965-970.
- Lyon van der Merve and Gawie Merve (1998). "Universal Converter for DC PV Water Pumping System." *Proc., IEEE International Symposium on Industrial Electronics*, 1, 218-223.
- Mahmoud, M. (1990). "Experience Results and Techno Economic Feasibility of Using Photovoltaic generators instead of Diesel Motors for Water Pumping from Rural Desert Wells in Jordan." *IEE Proceedings*, 137(C, 6), 391-394.
- Mohammad, A.S.M., Dehbonei, H. and Fuchs, E.F. (2002). "Theoretical and experimental analyses of photovoltaic systems with voltage and current-based maximum power-point tracking." *IEEE Transactions on Energy Conversion,* 17(4), 514–522.
- Meirios, M., Melanie, J. and Eddy K. (1991). "Performance Evaluation of ac and dc Direct Coupled Photovoltaic Water Pumping." *Energy Conversion and Management*, 31(6), 521-527.

- Mohamed Mostafa Saied (1998). "Matching of DC Motors to Photovoltaic Generators for Maximum Daily Gross Mechanical Energy." *IEEE Transactions on Energy Conversion*, 3(3), 465-471.
- Moussi, A. , Terki, A. and Asher, G. (2005). "Hysteresis current control of a permanent magnet brushless DC motor PV pumping system." *Proc., International Solar Energy Conference*, 523-528.
- Mukherjee, M. K. (1997). "Solar Photovoltaic Energy Conversion."; *IE(I) Journal (EL)*, 78, 1-5.
- Muljadi, E. (1997). "PV water pumping with a peak-power tracker using a simple six-step square-wave inverter." *IEEE Transactions on Industry Applications*, 33(3), 714-721.
- Mummadi Veerachari and Narri Yadiah (2000). "ANN based peak power tracking for PV supplied DC motors." *Solar Energy*, 69(4), 343-350.
- Nayar, C.V., Vasu, E. and Phillips, S. J. (1993). "Optimized Solar Water Pumping System Based on an Induction Motor Driven centrifugal Pump." *Proc., IEEE TENCON*, Beijing, 388-393.
- Neway Argaw (1994). "Optimization of Photovoltaic Water Pumps coupled with an Interfacing pulse width Modulated DC/AC Inverter Power Conditioning Device." *IEEE Conference Record of World Conference on Photovoltaic Energy Conversion*, 1,1165-1168.
- Nikhil, P. G. and Subhakar, D. (2011). "An Improved Simulation Model for Photovoltaic Cell." *Proc., IEEE International Conference on Electrical & Control Engineering (ICECE)*, 1978-1982.
- Odeh, I., Yohanis, Y.G. and Norton, B. (2006). "Influence of pumping head, insolation and PV array size on PV water pumping system performance." *Solar Energy*, 80(1), 51-64.
- Rashid, M. H. (2004). "Power Electronics: Circuits, Devices & applications", 3rd Edition, PHI - Pearson Publication.
- Renewable Energy sources: www.renewable-energysources.com (US DOE - Annual Energy Outlook 2014).

- Reshef, B., Suehrcke, H. and Appelbaum, J. (1995). "Analysis of a photovoltaic water pumping system." *Proc., Eighteenth Convention of Electrical and Electronics Engineers in Israel,* 1.5.3/1 - 1.5.3/5.
- Salameh, Z.M. and Dagher, F. (1990). "The effect of electrical array reconfiguration on the performance of a PV-powered volumetric water pump." *IEEE Transactions on Energy Conversion,* 5(4), 653-658.
- Sangal, S. K., Ranjan, V. and Sosan, R. K. (1998). "Photovoltaic Water Pumping-Indian Experience." *Proc., IEEE 20th Specialists Conference*, 2,1188-1193.
- Short, T.D. and Mueller, M.A. (2002). "Solar powered water pumps: problems, pitfalls and potential." *Proc., International Conference on Power Electronics, Machines and Drives,* 280–285.
- Silveira, L.C.J., Pereira, A.H., Moreira, A.B., Schmidlin, C.R. Jr., Carvalho, T.N. and Neto, T.N.C. (2004). "Study of technical and financial viability of PV powered water-pumping systems in the Federal University of Ceara." *Proc., IEEE/PES Transmission and Distribution Conference and Exposition, Latin America*, 366–370.
- Singh, B. N., Singh, B. P., Chandra, A. and Al Haddad, K. (1996). "Optimized Performance of Solar Powered Variable Speed Induction Motor Drive." *Proc., International Conference on Power Electronics, Drives and Energy Systems for Industrial Growth*, 1, 58-65.
- Singer, S. and Applebaum, J. (1993). "Starting Characteristics of Direct Current Motors Powered by Solar Cells." *IEEE Transactions on Energy Conversion*, 8(1), 47-52.
- Subha Raghavan, Bharadwaj, A. and Ganesh, N. (2010). "Harnessing Solar Energy: Options for India." *Report, Centre for Science, Technology and Policy*, India, 74-75.
- Surendra, T.S. and Subbaraman S.V.V. (2002). "Solar PV water pumping comes of age in India." Proc. IEEE Photovoltaic Specialists Conference, 1485–1488.
- Swamy, C.L.P., Singh, B., Singh, B.P. and Murthy, S.S. (1996). "Experimental investigations on a permanent magnet brushless DC motor fed by PV array for

water pumping system." Proc., Intersociety Energy Conversion Engineering Conference, 3, 1663-1668.

- Swigers, W. and Enslin, J.H.R. (1998). "An integrated maximum power point tracker for photovoltaic panels." *Proc., IEEE International Symposium on Industrial Electronics*, ISIE'98.
- Tafticht, T., Agbossou, K., Doumbia, M.L. and Cheriti, A. (2008). "An improved maximum power point tracking method for photovoltaic systems." *Renewable Energy*, 33(7), 1608-1616.
- Taufik, Akihiro Oi, Makbul Anwari and Mohammad Taufik (2009). "Modeling and Simulation of Photovoltaic Water Pumping System." *Proc., IEEE Computer Society Third Asia International Conference on Modelling & Simulation*, 497-502.
- Toshihiko Noguchi, Shigenori Togashi and Ryo Nakamoto (2000). "Short Pulse Based Adaptive Maximum Power Point Tracking for Photovoltaic Power Generation System." *Proc., IEEE International Symposium on Industrial Electronics*, 1, 157-162.
- Van Der Merwe, L. and Van Der Merwe G.J. (1998). "Maximum power point tracking-implementation strategies for PV power systems." *Proc., IEEE International Symposium on Industrial Electronics*,1, 214-217.
- Varin Vongmanee (2002). "The Vector Control Inverter for a PV Motor Drive System Implemented by a Single Chip DSP Controller ADMC331." *Proc., IEEE Asia Pacific Conference on Circuits and Systems*, Indonesia, 1, 447-451.
- Varin Vongmanee (2004). "The Photovoltaic Pumping System Using a Variable Speed Single Phase Induction Motor Drive Controlled by Field Oriented Principle." *Proc., IEEE Asia Pacific Conference on Circuits and Systems*, 1185-1188.
- Veerachary Mummadi (2000). "Steady State and Dynamic Performance Analysis of PV Supplied DC motors fed from intermediate power converters.", *Solar Energy Materials and Solar Cells*, 61, 365-381.
- Vilela, O.C., Fraidenraich, N. and Tiba, C. (2003). "Photovoltaic Pumping Systems Driven by Tracking Collectors-Experiments and Simulation." *Solar Energy*,74, 45-52.

- Viorel Badescu (2003). "Dynamic Model of a Complex system including PV Cells, Electric Battery, Electrical Motor and Water Pump." *Energy*, 28, 1165-1181.
- Vongmanee, V., Monyakul, V. and Youngyuan, U. (2002). "Vector control of induction motor drive system supplied by photovoltaic arrays." *Proc., IEEE International Conference on Communications, Circuits and Systems*, 2, 1753-1756.
- Wernher Swiegers and Enslin J.H..R. (1998). "An Integrated Maximum Power Point Tracker for Photovoltaic Panels." *Proc., IEEE International Symposium on Industrial Electronics*, 1, 40-44.